PROTEOLYTIC PROFILING WITH IMAGING AGENTS FOR RATIONAL DESIGN OF TARGET-ACTIVATED PEPTIDE PRODRUGS

by

Cara Hartz Nelson

A dissertation submitted in partial fulfillment
of the requirements for the degree of
Doctor of Philosophy
(Pharmaceutical Sciences)
in The University of Michigan
2012

Doctoral Committee:

Professor Kyung-Dall Lee, Co-Chair
Professor Gordon L. Amidon, Co-Chair
Professor Anna K. Mapp
Associate Professor Duxin Sun

2012

In loving memory of my mother

ACKNOWLEDGEMENTS

I'd like to thank my advisors Dr. Kyung-Dall Lee and Dr. Gordon Amidon. I appreciate all the advice I've gotten from KD over the years and our discussions of current events in lab meetings. I'd like to thank Gordon for the ability to give an executive summary of my research and for sharing all his knowledge on regulatory laws. I'd also like to thank Dr. Chester Provoda for all the editing he's done for me and for him letting me constantly bother him about research techniques in the beginning. I'd like to thank the College of Pharmacy staff for making my time here go smoothly.

My labmates were instrumental in helping me get through graduate school, especially Dr. Emily Rabinsky, Dr. Chasity Andrews, Dr. Zachary Walls, Dr. Hairat Sabit, Stefanie Goodell, and Dr. Yasuhiro Tsume. I always enjoyed our conversations about school, work, and life. I'd like to thank Zach for his critiques of my work and his career advice. I'd like to thank Chasity and Emily for always being there to talk to, even when I just needed a coffee and a break from the lab.

While I consider all of the graduate students here my friends, I would especially like to acknowledge my classmates, Jason Baik, Chinmay Maheshwari, Lindsey White, Juhee Lee, Dr. Nan Zheng, and Dr. Shu-Pei Wu, who have been so supportive throughout graduate school. They have made life so much easier to deal with by sharing their troubles and listening to mine. I'm really going to miss my coffee breaks and lunches with Jason. I'd also like to thank Maria, Maya, and Lilly for being my roommates at

conferences; they made them so much more enjoyable.

Finally, I'd like to thank my family. I love my parents, Ed and Laurie, for always believing in me and supporting me. Even though my mother is no longer with us, I know she is proud of what I have accomplished. I want to express my gratitude to my sister, Chrissy, for always being there more me. I want to thank my in-laws for their encouragement. Finally, I want to thank my husband, Nathan, for being there for me in every way, even when that means moving across the country.

TABLE OF CONTENTS

DEDICATION ii

ACKNOWLEDGEMENTS iii

LIST OF FIGURES xi

LIST OF TABLES xiv

LIST OF ABBREVIATIONS xv

ABSTRACT xvii

CHAPTER 1 Enzyme-activated prodrugs as a strategy to improve drug delivery 1

1.1 Introduction 1

1.2 Prodrugs to improve oral absorption 2

1.2.1 Amino acid and peptide-prodrugs of antiviral compounds 2

1.3 Targeted prodrugs for tumor-specific delivery 5

1.3.1 Protease-activated prodrugs in cancer therapy 7

1.4 Imaging prodrug activation 12

1.4.1 Magnetic resonance imaging 13

1.4.2 Fluorescence imaging 14

1.5 Conclusions 17

1.6 References 24

CHAPTER 2 Puromycin-sensitive aminopeptidase: An antiviral prodrug activating enzyme 41

2.1 Summary 41

2.2 Introduction 42

2.3 Methods 44

2.3.1 Chemicals and reagents 44

2.3.2 Generation of recombinant APP-S 44

2.3.3 Hydrolysis assays 46

2.4 Results 48

2.4.1 Recombinant APP-S hydrolysis investigations 48

2.4.2 Activation pathways for Val-Ser-cHPMPC and its metabolites 49

2.4.3 Kinetic constants for APP-S hydrolysis of p-nitroanilide compounds. 50

2.4.4 APP-S hydrolysis of AMC and ACC compounds 50

2.5 Discussion 51

2.6 References 63

CHAPTER 3 Enzyme-Activated Magnetic Resonance Imaging Contrast Agent 67

3.1 Summary 67

3.2 Introduction 68

3.3 Methods 73

3.3.1 Conjugation of Asn to DTPA 73

3.3.2 Conjugation of NWAE to DTPA 74

3.3.3 Conjugation of Lys-OMe to DTPA 75

3.3.4 Determination of free gadolinium 76

3.3.5 Relaxivities of contrast agents in NMR 76

3.3.6 Relaxivities of contrast agents in MRI 77

3.3.7 Subcloning of legumain 77

3.3.8 Recombinant legumain expression and purification 78

3.3.9 Legumain hydrolysis of Z-AAN-AMC 79

3.3.10 Legumain hydrolysis of neurotensin and NWAE 79

3.3.11 Enzymatic hydrolysis of Gd-DTPA-NWAE 80

3.3.12 HEK-293 cells overexpressing legumain 80

3.3.13 Hydrolysis of Z-AAN-AMC by HEK-LEG cells. 81

3.4 Results 81

3.4.1 Synthesis and characterization of procontrast agents 81

3.4.2 Production and characterization recombinant legumain 82

3.4.3 Legumain incubated with procontrast agent 83

3.4.4 Legumain activity in whole cells 83

3.4.5 Synthesis and characterization of an alternative procontrast agent 83

3.5 Discussion 84

3.6 References 94

CHAPTER 4 Determination of differential peptide hydrolysis in whole cells using fluorescence 96

4.1 Summary 96

4.2 Introduction 96

4.3 Methods 98

4.3.1 Materials 98

4.3.2 Synthesis of ACC compounds 99

4.3.3 Cell culture 99

4.3.4 Transfection of HEK-293 cells 99

4.3.5 Whole cell hydrolysis of AMC and ACC conjugates 100

4.3.6 Hydrolysis of AMC conjugates in mouse serum 100

4.3.7 mRNA expression data 101

4.3.8 Statistical analysis 101

4.4 Results 101

4.4.1 Single amino acid conjugates of AMC in transfected cells 101

4.4.2 Hydrolysis of peptide-AMC conjugates in transfected cells 101

4.4.3 Hydrolysis of single amino acid conjugates by three cell lines 102

4.4.4 Differential hydrolysis of peptide-AMC conjugates by BT-549 cells. 103

4.4.5 Hydrolysis of ACC conjugates 103

4.4.6 Serum and liver stability of AMC conjugates 104

4.4.7 Protease expression levels in breast cancer cells 104

4.5 Discussion 104

4.6 References 118

CHAPTER 5 Selective Hydrolysis of Doxorubicin Prodrugs 123

5.1 Summary 123

5.2 Introduction 123

5.3 Methods 125

5.3.1 Materials 125

5.3.2 Synthesis of doxorubicin prodrugs 125

5.3.3 HPLC analysis 126

5.3.4 pH stability of prodrugs 126

5.3.5 Cell culture 126

5.3.6 Transfection of HEK-293 cells 127

5.3.7 Hydrolysis of prodrugs 127

5.3.8 Whole-cell hydrolysis of L-Lys-L-Ala-AMC 128

5.3.9 Cell viability 128

5.3.10 Microscopy 129

5.3.11 Statistical analysis 129

5.4 Results 129

5.4.1 Synthesis and pH stability 129

5.4.2 Hydrolysis of L-Lys-L-Ala-Doxorubicin by lysed cells 130

5.4.3 Hydrolysis of Dox prodrugs by whole cells..... 130

5.4.4 Hydrolysis of L-Lys-L-Ala-Dox by transfected cells 131

5.4.5 Hydrolysis of L-Lys-L-Ala-AMC by transfected cells..... 131

5.4.6 Cytotoxicity of prodrugs..... 131

5.4.7 Microscopy..... 132

5.5 Discussion..... 132

5.6 References 145

CHAPTER 6 Conclusions 150

6.1 Significance 150

6.2 Future Directions..... 155

6.3 References 160

APPENDIX…….165

LIST OF FIGURES

Figure 1.1 Bioactivation of the ester prodrug oseltamivir 18

Figure 1.2 Absorption and activation of valacyclovir. 19

Figure 1.3 Bioactivation of valacyclovir. 20

Figure 1.4 Chemical structures of cidofovir, cyclic cidofovir, and L-Val-L-Ser-cHPMPC 21

Figure 1.5 Labeling of a cysteine protease by an activity-based probe 22

Figure 1.6 Structure and absorbance spectra of AMC and AMC amino acid conjugate. 23

Figure 2.1 Chemical structures of cidofovir (1) and Val-Ser-cHPMPC (2). 55

Figure 2.2 Superdex-200 purification of APP-S from Caco-2 cell homogenates..... 56

Figure 2.3 Chemical structures of Ala-AMC, Ala-ACC, and Ala-pNA..... 57

Figure 2.4 Purified recombinant APP-S. 58

Figure 2.5 Michaelis-Menten plot of Val-Ser-cHPMPC hydrolysis by APP-S..... 59

Figure 2.6 Chemical structures of the observed metabolites obtained during the hydrolysis of Val-Ser-cHPMPC by recombinant APP-S..... 60

Figure 3.1 Proposed bioactivation of Gd-DTPA-NWAE 87

Figure 3.2 Synthesis Scheme for Gd-DTPA-Asn and Gd-Asn-DTPA-Asn 88

Figure 3.3 Synthesis scheme for Gd-DTPA-NWAE and Gd-NWAE-DTPA-NWAE 89

Figure 3.4 The relaxivity ratios for Gd-DTPA amino acid and tetrapeptide analogues. . 90

Figure 3.5 Purified recombinant mouse legumain is autocatalytically activated in acidic

conditions. 91

Figure 3.6 Structure of Gd-Lys-OMe-DTPA-Lys-OMe 92

Figure 4.1 Chemical structures of AMC and ACC. 109

Figure 4.2 Single amino acids are not ideal candidates for targetd prodrug promoieties. 110

Figure 4.3 Dipeptide promoieties are sufficient for differential hydrolysis in transfected HEK-293 cells. 111

Figure 4.4 Membrane permeabilization by Triton X-100 changes the rate of hydrolysis by transfected HEK-293 cells 112

Figure 4.5 Differential hydrolysis can be achieved with single amino acid substrates. 113

Figure 4.6 Di- and tripeptide promoieties resulted in greater differential hydrolysis. .. 114

Figure 4.7 The promoiety confers differential hydrolysis despite changing the leaving group. 115

Figure 4.8 There is significant X-prolyl peptidase activity in mouse serum. 116

Figure 4.9 mRNA expression levels of select proteases in MCF7 and BT-549 cells.... 117

Figure 5.1 Synthesis scheme for L-Lys-L-Ala-Doxorubicin 137

Figure 5.2 L-Lys-L-Ala-Dox is hydrolyzed significantly faster by detergent-permeabilized BT-549 cells. 138

Figure 5.3 BT-549 cells hydrolyze L-Lys-L-Ala-Dox to L-Ala-Dox significantly faster than MRC-5 or MCF7 cells. 139

Figure 5.4 Bestatin inhibits whole-cell hydrolysis of L-Lys-L-Ala-Dox. 140

Figure 5.5 L-Lys-L-Ala-Dox and L-Lys-L-Ala-AMC are hydrolyzed faster by ANPEP-transfected HEK-293 cells. 141

Figure 5.6 Prodrugs of doxorubicin retain some cytotoxicity. 142

Figure 5.7 Doxorubicin prodrugs accumulate outside the nucleus. 143

Figure 6.1 Structures of doxorubicin (Dox) and Daunorubicin (DNR) 158

Figure 6.2 Activation of Gly-Pro-Aminoluciferin 159

Figure A.1 pH has minimal effect on proteolytic profiles of cell lysates……...172

Figure A.2 Serum starvation has the opposite effect on extent of Ala-AMC hydrolysis in MCF7 and HEK-LEG cells……..173

Figure A.3 Cells from different tissue sources have different proteolytic profiles at physiologic pH…….174

LIST OF TABLES

Table 2.1 Kinetics of Val-Ser-cHPMPC hydrolysis by recombinant APP-S. 61

Table 2.2 Initial velocity of hydrolysis of AMC and ACC substrates by recombinant APP-S..... 62

Table 3.1 Relaxivities (R1) of Gd-DTPA analogues 93

Table 5.1 IC_{50} values of doxorubicin and dox prodrugs in MRC-5, MCF7, and BT-549 cells 144

LIST OF ABBREVIATIONS

ACC	7-amino-4-carbamoylmethylcoumarin
AMC	7-amino-4-methylcoumarin
ANPEP	Gene name for alanyl aminopeptidase
AOMK	Acyloxymethylketone
APN/CD13	Alanyl aminopeptidase/aminopeptidase N
APP-S	Puromycin-sensitive aminopeptidase
BPHL	Biphenyl-hydrolase-like protein/valcyclovirase
cHPMPC	Cyclic cidofovir
DMF	Dimethylformamide
Dox	Doxorubicin
DPP	Dipeptidyl dipeptidase
DTPA	Diethylentriamine pentaacetic acid
ECM	Extracellular matrix
Gd^{3+}	Gadolinium
GnRH	Gonadotropin-releasing hormone
HPMPC	Cidofovir (methyl (*S*)-2-((*S*)-2amino-3-methyl-butyrylamino)-3-[(*S*)-5-(4-amino-2-oxo-2*H*-pyrimidin-1-ylmethyl)-2-oxido-1,4,2-dioxaphosphinan-2—yloxy]propanoate)
MeOH	Methanol

MMP	Matrix metalloproteinase
MRI	Magnetic resonance imaging
MS	Mass spectroscopy
NMR	Nuclear magnetic resonance
NPEPPS	Gene name for puromycin-sensitive aminopeptidase
NWAE	Asparagine-tryptophan-alanine-glutamic acid peptide
PBS	Phosphate-buffered saline
PepTI	Peptide transporter 1
pNA	*para*-nitroaniline
PSA	Prostate-specific antigen
R1	Relaxivity
T1	Spin-lattice time
TEA	Triethylamine
TEAA	Triethylacetic acid
V_0	Initial velocity of hydrolysis
Z	Benzyloxycarbonyl protecting group

ABSTRACT

Peptide prodrugs can be used to alter pharmacokinetic properties of drugs such improved oral bioavailability and site-specific delivery. This thesis focuses on peptide prodrug activating enzymes and selection of peptide promoieties to achieve targeted activation. The peptide prodrug L-Val-L-Ser-cyclic cidofovir (Val-Ser-cHPMPC) was previously shown to improve the oral bioavailability of the poorly absorbed antiviral cHPMPC. However, this prodrug must be efficiently and predictably hydrolyzed *in vivo* to the parent compound cHPMPC to exhibit antiviral activity. Herein, we describe the identification and characterization of puromycin-sensitive aminopeptidase (APP-S) as the primary activator of Val-Ser-cHMPC. For orally absorbed prodrugs, it is often desirable to achieve immediate activation upon absorption. Conversely, to achieve site-specific delivery it is desirable to select a promoiety that is preferentially cleaved by a protease that is overexpressed or uniquely expressed in diseased tissue. One such protease that is overexpressed in tumors is the cysteine endopeptidase legumain. To measure protease activity in a minimally invasive manner, we synthesized a peptide conjugate of the MRI contrast agent Gd-DTPA. The peptide effectively blocked the ninth coordination site of gadolinium, which resulted in a slower relaxitivity (R1) than the parent compound Gd-DTPA or the proposed single amino acid metabolite, which should result in enhanced signal intensity *in vivo*. However, the Gd-DTPA-tetrapeptide analogue was not significantly hydrolyzed by purified recombinant legumain. The purified legumain was

shown to be active using the model substrate Z-Ala-Ala-Asn-AMC, but there was minimal hydrolysis of the model compound when incubated with HEK-293 cells overexpressing legumain. This difference in enzymatic activity between the purified protease and protease expressed in whole cells suggested a whole-cell system would be more physiologically relevant for peptide promoiety screening. We selected amino acid and peptide conjugates of the fluorescent compounds AMC and ACC to screen whole-cells and were able to identify several promoieties that were hydrolyzed significantly faster by BT-549 breast cancer cells compared to MCF7 or MRC-5 cells. One of these dipeptide promoieties, L-Lys-L-Ala, was selected to make a doxorubicin prodrug. There was differential activation of L-Lys-L-Ala-Dox by BT-549 cells, suggesting that our peptide promoiety screening system can be applied to rational prodrug design.

CHAPTER 1

Enzyme-activated prodrugs as a strategy to improve drug delivery

1.1 Introduction

The term prodrug was first introduced by Adrien Albert in the 1950's (*1*) as a compound that is pharmacologically inactive or significantly less active until it is enzymatically or chemically converted to an active drug *in vivo*. Prior to Albert, Paul Ehrlich proposed the concept of a "magic bullet" in which he reasoned that if one could find a compound that is selective for a disease-causing organism, then a toxin could be attached to said compound for selective delivery (*2, 3*). According to a 2004 review by Ettmayer et al., prodrugs are almost 7% of marketed medicines in Germany (*2*) and approximately 10% of marketed drugs worldwide (*4*). The prodrug strategy is often considered only late in drug development, when other approaches have failed to improve the pharmaceutical properties such as solubility, permeability, toxicity or chemical or enzymatic stability In fact, many prodrugs on the market were not intentionally designed as prodrugs and were only recognized as such later on. Examples of this include prontosil, heroin, and isoniazid, which was not discovered to be a prodrug until 40 years after Roche first introduced isoniazid (*4*). Prodrugs represent an exciting opportunity to not only improve pharmacokinetic properties of a compound, but to also extend the life cycle of a drug, often with reduced development costs (*4*). This thesis will focus on one aspect of prodrug development, namely the hydrolases responsible for conversion of

prodrug to parent compound and their identification before, during, and after prodrug development.

1.2 Prodrugs to improve oral absorption

As mentioned previously, prodrugs have been used to improve a variety of pharmaceutical properties including solubility, chemical or enzymatic stability, permeability, and toxicity. As oral drug delivery is the preferred route for most drugs, the prodrug approach can be especially useful in improving oral absorption. One way to accomplish this is to improve the lipophilicity of the compound by masking hydrophilic hydroxyl, carboxyl, phosphate or other charged groups by forming esters (*5*). Oseltamivir (Tamiflu; Genentech (Roche Group)) shown in Figure 1.1 is a good example of an ethyl ester prodrug that was developed to improve bioavailability from 5% for the free carboxylate to nearly 80% for the more lipophilic prodrug (*6*). Following absorption, oseltamivir is extensively metabolized to the active compound oseltamivir carboxylate by hepatic esterases (*6*).

1.2.1 Amino acid and peptide-prodrugs of antiviral compounds

1.2.1.1 Valacyclovir and valganciclovir

The poor oral bioavailability of other compounds such as acyclovir and ganciclovir has been improved by a slightly different approach. Rather than improving the lipophilicity of the compound for passive diffusion, the drugs were given nutrient-like properties to allow them to be absorbed by carried-mediated transport. Valacyclovir and valganciclovir are L-valyl ester prodrugs of acyclovir and ganciclovir (*7-11*). In the case of valacyclovir, the oral absorption was improved 3- to 5-fold compared to the parent compound, acyclovir (*8, 9, 12*). The improved oral bioavailability of valacyclovir over

acyclovir has been shown to be due to carrier-mediated transport by the human peptide transporter 1 (PEPT1) (*7, 13-15*). The absorption and activation of valacyclovir are diagrammed in Figure 1.2. Human PEPT1 is a high capacity, low affinity oligopeptide transporter abundantly expressed in the small intestine with broad substrate specificity and stereoselectivity for L-amino acid residues (*16-18*). Following intestinal absorption, both valacyclovir and valganciclovir are rapidly converted to acyclovir and ganciclovir, respectively, by the esterase biphenyl hydrolase-like protein (BPHL) (*19*). This is important because acyclovir requires phosphorylation to be activated and the valyl ester must be removed for the phosphorylation to occur (*4*), as seen in Figure 1.3. Thus, an amino acid or peptide prodrug strategy relies on the rapid and predictable conversion of the prodrug to the parent compound.

1.2.1.2 Cidofovir and cyclic cidofovir

The antiviral compound cidofovir (HPMPC) is an approved intravenous treatment of cytomegalovirus (CMV) infections in immunocompromised individuals, such as those infected with HIV, however, its use is limited because of nephrotoxicity associated with treatment (*20, 21*). The similarly potent antiviral prodrug cyclic cidofovir (cHPMPC) was developed to reduce the nephrotoxicity resulting from cidofovir treatment (*22*). Cidofovir and cyclic cidofovir are also effective against other DNA viruses such as herpesviruses, adenoviruses, polyomaviruses, and orthopoxviruses (*17, 20, 23-25*). Poor oral bioavailability limits the use of HPMPC and cHPMPC (<5%) (*17, 22*), which can be attributed their negatively charged phosphonic and phosphante groups at physiological pH as seen in Figure 1.4 (*26-28*). The McKenna laboratory has developed several amino acid and dipeptide prodrugs of cHPMPC to mask the charge of cHPMPC at physiological

pH and increase uptake by carrier-mediated transporters such as PEPT1 (*17*, *27*, *29-31*). A serine phosphoester prodrug of cHPMPC, L-Val-L-Ser-cHPMPC (Val-Ser-cHPMC) shown in Figure 1.4 was one of the more successful prodrugs identified by this approach (*27*). Using an *in situ* single pass perfusion method, the permeability of Val-Ser-cHPMPC was more than 20 times greater than cHPMPC (*27*). Furthermore, the oral bioavailability of Val-Ser-cHPMC was 18.1% compared to 2.2% for cHPMPC following direct injection into the gastrointestinal tract of rats (*27*). As mentioned previously, for an amino acid- or peptide-prodrug approach to be successful, the prodrug must be activated to the parent compound in addition to improving the bioavailability. In transport studies in rats, the major species found in plasma was cHPMPC (>90%); thus, Val-Ser-cHPMPC appears to be efficiently activated in rats (*27*). However, this strategy relies on the predictable and efficient conversion of prodrugs in humans; therefore, it would be beneficial to identify the prodrug activating enzyme(s) in humans. It was observed in Caco-2 cell homogenate that valine was cleaved from serine, which led to chemical hydrolysis of the serine residue from cHPMPC, and this process was inhibited by the aminopeptidase inhibitor bestatin (*27*). Also, the co-dosing of bestatin with Val-Ser-cHPMPC increased the plasma level of cHPMPC by more than 3-fold compared to prodrug alone (*27*), which suggests bestatin inhibits enzymes present in the gastrointestinal tract that are hydrolyzing the prodrug prior to absorption. The ability of bestatin to increase the enzymatic stability of Val-Ser-cHPMPC suggested an aminopeptidase was primarily responsible for the hydrolysis of Val-Ser-cHPMPC. The identification of an aminopeptidase responsible for activating Val-Ser-cHPMPC is discussed further in Chapter 2.

1.3 Targeted prodrugs for tumor-specific delivery

The use of prodrugs to enhance site-specific delivery of a compound can be applied to a variety of drugs and targets such as brain, bone, colon, and tumors as previously has been reviewed (*2, 4, 32, 33*). To limit the scope, this thesis will focus on prodrugs to improve tumor-targeting. While many chemotherapeutics on the market are effective at cell killing, they are often limited by a narrow therapeutic window due to cytotoxicity toward normal cells. Doxorubicin (Dox) is a highly potent anthracycline with a broad range of activity. The antitumor activity of Dox has been attributed to its ability to intercalate DNA, bind proteins involved in DNA replication and induce cell death via p53-dependent and independent pathways (*34, 35*). Despite its widespread use, there are many side effects that continue to plague patients treated with Dox, the most troubling being cardiotoxicity (*34*). The cardiotoxicity induced by Dox is thought to be independent of its nuclear DNA-binding, but rather as a result of Dox binding cardiolipin, free-radical formation, and mitochondrial damage, though the exact mechanism is not known (*35*). Another chemotherapeutic, paclitaxel, induces programmed cell death via a different mechanism than Dox, but still has a narrow therapeutic index due to myelo-suppression and sensory neuropathy (*35*).

There have been some successes in limiting off-target cytotoxicity by using a rational approach to designing drugs for molecular targets involved in cancer formation and progression, e.g. inhibitors of Abl kinase (*36*) or EGF receptor kinase (*37*). However, the role of these molecular targets in cancer pathogenesis is often not clearly understood, and inhibition of the target may not result in growth-arrest or apoptosis. Alternatively, these targets could be used as molecular addresses to deliver a cytotoxic

compound to the tumor site. This approach has been exemplified by the conjugation of doxorubicin to the peptide CNGRC (*38, 39*) and the conjugation of paclitaxel to the peptide gonadotropin-releasing hormone (GnRH) (*40*). The cyclic peptide CNGRC has been shown to bind aminopeptidase N (APN/CD13), which is highly expressed on tumor vasculature as well as some solid tumors (*38, 41, 42*). This conjugate prolonged the survival of mice bearing MDA-MB-435 carcinoma cells compared to doxorubicin alone (*39*). There is evidence for the presence of GnRH receptors in prostate cancer tissue, ovarian cancer tissue, and malignant breast cancer tissue (*40*). When the GnRH peptide was conjugated to paclitaxel by the spacer chloroacetic acid to the 2'-hydroxyl group of paclitaxel, it decreased MCF7 cell proliferation more than paclitaxel alone (*40*). Both the doxorubicin-CNGRC conjugate and paclitaxel-GnRH were hydrolyzed by intracellular esterases to release the parent compounds (*38, 40*). Although GnRH and its analogues have pharmacological applications (*43*), in the case of paclitaxel-GnRH the GnRH binding was used as a molecular address tag and to possibly aid in transport, while the paclitaxel was used for its pharmacological effect (*40*).

Peptide prodrugs are not only useful in binding molecular targets; they can also be used to control the activation of prodrugs. In this situation, the prodrug strategy could be employed in an alternative manner, wherein the promoiety is cleaved from the parent compound by an enzyme that is overexpressed or uniquely expressed at the target site, which may or may not be correlated with genetic changes (*35*). As proteases account for ~2% of all proteins and play a role in most cellular processes, they are an attractive target for this type of prodrug design (*44*). Additionally, doxorubicin contains a primary amine, which allows the conjugation of amino acid sequences without the use of a linker (*35*).

Unlike the ester linkages described above, the amino-peptidyl bond is considered relatively stable in serum (*35*). This was taken advantage of in the development of *N*-L-leucyldoxorubicin (Leu-Dox) to reduce the cardiotoxicity of doxorubicin (*45-47*). In phase I clinical trials, Leu-Dox was shown to be rapidly, though not completely, converted to free Dox in plasma after i.v. administration (*46, 47*). The cytotoxicity of Leu-Dox is better correlated to free Dox concentrations in tumor tissues and cell cultures, suggesting Leu-Dox is acting as a prodrug rather than being cytotoxic itself (*45-50*). Leu-Dox had a higher maximum tolerated dose than free Dox, resulting in higher free Dox concentrations in tumor tissues in murine models (*50*).

1.3.1 Protease-activated prodrugs in cancer therapy

To expand on the work with Leu-Dox, many groups have attached longer peptide sequences to doxorubicin to allow for more specific activation at the tumor site (*51-64*). There are three main classes of proteases that are targeted by this approach; serine, cysteine, and metalloproteases (*44, 65, 66*). These proteases are involved in bioregulation, matrix remodeling, digestion, and immune response (*44*). Interestingly, these proteases are often secreted by fibroblasts and inflammatory cells rather than the tumor cells themselves (*67*).

1.3.1.1 Matrix metalloproteases

The matrix metalloproteases (MMPs) are some of the most popular targets of peptide prodrug design for chemotherapeutics. Enzymes of the MMP class are involved in the normal matrix remodeling associated with embryo development, wound healing, and activation or deactivation of signal proteins involved in the immune response (*68*). However, the normal functions of MMPs can be altered in tumors. More specifically,

MMP-2 and -9 have been shown to be involved in the degradation of the basement membrane, which leads to tumor cell invasion (*68*), and their expression by tumor cells has been associated with poor clinical outcomes (*69*). This discovery has led to the development of several doxorubicin prodrugs that are specifically activated by MMPs (*51, 58, 60-62, 70*). Both Albright et al. (*51*) and Lee et al. (*62*) found that doxorubicin prodrugs with MMP-cleavable peptides resulted in less systemic toxicity in mouse models compared to Dox, while still suppressing tumor growth, thus increasing the therapeutic index.

1.3.1.2 Prostate-specific antigen

Another popular target in chemotherapeutic prodrug design is the serine protease prostate-specific antigen (PSA) (*52-54, 59, 71-76*). PSA has chymotrypsin-like activity and is present in both normal and tumor tissues, with the highest expression being in breast and prostate (*52*). PSA gained notoriety as a serological marker of prostate cancer, and levels are positively correlated with tumor burden (*52*). While secreted PSA is present in serum and can be used to aid in the diagnosis of prostate cancer, it is relatively inactive in the systemic circulation because it forms a complex with α_1-antichymotrypsin and α_2-macroglublin, protease inhibitors present in plasma (*52*). Therefore, prodrugs designed to be selectively cleaved by PSA would be primarily activated in the tumor microenvironment where the enzyme is highly expressed and active (*52*). Researchers at Merck laboratories conjugated the peptide N-glutaryl-(4-hydroxyprolyl)-Ala-Ser-cyclohexaglycyl-Gln-Ser-Leu-CO_2H to the aminoglycoside of Dox (*52, 54, 75*). This compound (L-377,202) had 20-fold greater activity against PSA-secreting LNCap cells compared to non-PSA-secreting DuPRO cells *in vitro (75)*. Furthermore, L-377,202 was

15 times more effective than Dox at inhibiting human prostate cancer tumors in nude mice, with minimal total body weight loss (*52*). In a small clinical trial, L-377,202 was found to be well tolerated in addition to being cleaved to Leu-Dox and Dox (*54*).

1.3.1.3 Cathepsins

Cathepsins are cysteine proteases that have been shown to play a role in cancer (*67*). Not only are they involved in the degradation of the extracellular matrix (ECM), but they have also been implicated in angiogenesis and growth of primary and metastatic tumors (*67*). Cathepsin B is able to hydrolyze collagen IV, fibronectin and laminin (ECM components) and was identified in breast cancer progression more than 30 years ago (*67*). To take advantage of cathepsin B overexpression in tumors, Dubowchik and Firestone developed a doxorubicin prodrug in which the internalizing antibody (BR96) was attached to doxorubicin with a cathepsin B cleavable linker (*55, 56*). Similarly, Schmid et al. attached the albumin-binding compound EMC (6-maleimidocaproic acid) to doxorubicin via a cathepsin B cleavable hexapeptide (*77*). The albumin-binding Dox prodrug was efficiently cleaved to H-Leu-Ala-Leu-Dox, H-Leu-Dox, and Dox *in vitro* and the antitumor efficacy was similar to that of doxorubicin *in vivo (77)*. Furthermore, there was no change in body weight associated with H-Leu-Ala-Leu-Dox treatment compared to a 9% weight loss in mice treated with Dox, suggesting the prodrug reduces off-target toxicity (*77*).

1.3.1.4 Legumain

Another cysteine protease that was immunohistochemically identified as being overexpressed in tumors is legumain (*63, 64, 78*). Legumain is a lysosomal endoprotease with specificity for Asn or Asp in the P1 position (*79, 80*). While legumain is normally a

lysosomal enzyme, it was found to be in membrane-associated vesicles at the invadopodia of tumor cells and associated with the cell surface (*63*). Legumain was also shown to be only overexpressed in solid tumors and xenografts of cancer cells, not in cultures of immortalized cancer cell lines (*63*). Liu et al. synthesized the prodrug N-(-*t*-Butoxycarbonyl-L-alanyl-L-alanyl-L-aspraginyl-L-leucyl)doxorubicin (legubicin) (*63*). The cytotoxicity of legubicin was <1% of that of doxorubicin against HEK-293 cells not expressing legumain *in vitro* and it was significantly cytotoxic against HEK-293 cells overexpressing legumain (*63*). When tested *in vivo*, legubicin was tumoricidal against a murine model bearing CT26 carcinoma cells with little weight loss or toxicity against non-tumor bearing organs that express legumain such as kidney and liver (*63*). A similar compound, succinyl-L-alanyl-L-alanyl-L-asparginyl-L-leucyl-doxorubicin (LEG-3) was synthesized by Wu et al. (*64*). LEG-3 was virtually non-cytotoxic toward non-legumain-expressing HEK-293 cells and was shown to be cell-impermeant, whereas it was effectively hydrolyzed by legumain-expressing HEK-293 cells and had an EC_{50} similar to that of doxorubicin (*64*). LEG-3 exhibited a higher maximal tolerable dose and a lower LD_{50} than doxorubicin *in vivo* while still being tumoricidal (*64*). Stern et al. also synthesized a legumain-activated prodrug, carbobenzyloxy-alanine-alanine-aspargine-ethylenediamine-etoposide, that was 100% cleaved by the lysates of HEK-293 cells overexpressing legumain and only 33% cleaved by non-legumain expressing HEK-293 cell lysates (*78*). However, this etoposide prodrug was not efficiently cleaved by intact legumain-expressing HEK-293 cells (*78*).

1.3.1.5 Dipeptidyl peptidase IV

The serine peptidase dipeptidyl peptidase IV (DPP IV) has been associated with

several diseases including cancer (*81, 82*). While not consistently overexpressed in all tumor types, DPP IV has been shown to be overexpressed in thyroid cancer, astrocytic tumors, and breast cancer metastases (*81*). Despite this association, there have been very little development of DPP IV-targeted prodrugs for cancer therapy. There is some evidence that DPP IV would be a good target for a prodrug approach as it has already been successfully applied to the antiviral bicyclic furanopyrimidine nucleoside analogue (*83*).

1.3.1.6 Protease profiling to identify new targets

Although there have been several proteases identified as potential targets for prodrug therapy, it is highly likely there are more proteases yet to be identified. The field of genomics has helped advance the knowledge of differential expression in the diseased state using DNA microarrays; however, these assays cannot account for posttranslational protein concentrations or activity (*84*). To aid in the identification of proteases that exhibit increased activity in disease tissue, many laboratories have developed activity-based probes for protease profiling (*44, 84-92*). In general, activity-based probes label active site residues through a chemical reaction that is both specific and dependent upon enzymatic activity (*93*). One of these probes was able to identify a hydroxypyruvate reductase that was labeled by the activity-based probe 6-fold more in obese (ob/ob) mice compared to wild-type mice (*84*). Despite the developments in expanding the reactivity of these activity-based probes, they are still limited in identifying a diverse array of proteases. For targeting disease tissue it is not necessarily essential to identify proteases that are overexpressed, but rather identify the substrates that are preferentially hydrolyzed in the target tissue. Cloutier et al. accomplished this by using a phage display library and

were able to identify pentapeptides that were specifically cleaved by three different prostate cancer cell lines with varying levels of invasiveness (*94*). Schmid et al. screened a fluorogenic positional-scanning tetrapeptide library to identify albumin-binding camptothecin prodrugs that were hydrolyzed by homogenates of human colon tumor xenografts (*95*). However, these prodrugs were not specifically hydrolyzed by colon tumors (*95*). Another approach employed by Trouet et al. screened oligopeptide derivatives of doxorubicin to find a tetrapeptide prodrug, *N*-β-alanyl-L-leucyl-L-alanyl-L-leucyl-doxorubicin, that was selectively hydrolyzed by MCF7 cells over MRC-5 cells (*57, 96, 97*). Each of the previously described profiling approaches had the same drawbacks, they only screened extracellular and/or secreted proteases and the substrates were tetrapeptides or longer. Thus, a screening system that is able to measure the activity of intracellular proteases and uses shorter peptide or amino acid promoieties has the potential to identify new protease targets including aminopeptidases and dipeptidases.

1.4 Imaging prodrug activation

Targeted prodrugs activated by enzymes overexpressed or uniquely expressed by disease tissue such as tumors have not had great success in clinical trials because of the unpredictability of enzyme expression and activity *in vivo* (*98, 99*). To better predict which promoieties might be effective at targeting *in vivo*, it would be useful to have a relatively non-invasive method to measure enzymatic activity. In this manner, promoieties attached to molecular imaging agents can be useful in the development of the protease-activated prodrugs (*100-103*). There are a variety of imaging techniques that have been adapted to observe enzymatic activity both *in vitro* and *in vivo* including optical (fluorescence and bioluminescence), magnetic resonance imaging (MRI), single-

photon emission computed tomography (SPECT), and positron emission tomography (PET) (*101-104*). The use of MRI and fluorescence in monitoring enzymatic activity are described in further detail below.

1.4.1 Magnetic resonance imaging

MRI works by applying a strong magnetic field to the body or tissue, which will cause the proton spins (mainly from H^+ of water) to align along this magnetic field direction (*105*). Energy is then transferred into the system using an electromagnetic wave that corresponds to the Larmor frequency, which is the precession frequency of spins located in a magnetic field, and causes the spins to be deflected away from the Z-direction (*105*). The time required for the excited spins to recover to the Z-direction, which is along the external magnetic field, is called the spin-lattice time or T1 time and can be determined by monitoring the emission of energy (*105*). A shorter T1 time means the spins recover more quickly, thus emitting a stronger signal (*105*). It was discovered in 1971 that malignant tumors had different relaxation times than normal tissue and could thus be identified by MRI (*106*). The T1 time can further be altered by contrast agents that contain paramagnetic ions, which results in a higher relaxivity. Relaxivity (R1) can be defined as 1/T1 when 1 mol of the contrast agent is dissolved in 1 L of water (*105*). Gd^{3+} is one such paramagnetic element that can create strong local magnetic fields to accelerate the spin-lattice relaxation (T1) of water protons. Like other heavy metals, Gd^{3+} is quite toxic in animals with an LD_{50} of 0.5 mmol/kg body weight in rats (*107*). However, when Gd^{3+} is chelated with a compound such as DTPA (diethylenetriamine pentaacetic acid), it still retains its paramagnetic properties and is considerably less toxic, with an LD_{50} of 8 mmol/kg body weight (*107*). Gd^{3+} has nine coordination sites that can

form complexes with electron-donating ligands. DTPA complexes with eight of the nine coordination sites of Gd^{3+} leaving the ninth coordination site open for Gd^{3+} to interact with water protons (*107*). It is this ninth coordination site of the inner sphere that can be manipulated to cloak the signal enhancement properties of gadolinium.

Many of the advances in this area have been made in the laboratory of Thomas Meade (*108-117*). The attachment of a β-galactopyranose to a gadolinium chelating agent effectively reduced the signal enhancement typically seen with MRI contrast agents by blocking the ninth coordination site (*116*). When incubated *in vitro* with β-galactosidase to remove the β-galactopyranose ring, there was a 20% difference in T1 time (*116*). This structure was later improved upon by adding an α-methyl group to increase the rigidity of the compound, resulting in a 3-fold difference in relaxivity between the cleaved and uncleaved compounds (*113*). When measured *in vivo* in a *Xenopus laevis* embryo expressing β-galactosidase in half of its cells, there was a 57% enhancement in signal intensity in the β-galactosidase expressing cells (*113*). Peptides have also been attached to MRI contrast agents to improve the accumulation of these compounds at sites overexpressing matrix metalloproteases (*118, 119*), but, to our knowledge, have not yet been used as a cloaking mechanism. The development of a peptide procontrast agent to monitor enzymatic activity is discussed further in Chapter 3.

1.4.2 Fluorescence imaging

Historically, fluorescence has not received much attention in the area of clinical *in vivo* imaging for several reasons including strong autofluorescence following external illumination and absorption and scattering of photons in tissues which severely limits the thickness of tissue that can be imaged (*120*). While there have been advances in optical

imaging including bioluminescent quantum dots and near-infrared probes (*104, 120, 121*), fluorescence imaging remains a more useful tool in preclinical applications.

1.4.2.1 Activity-based probes

As previous sections have described, there is significant evidence of differences in protease abundance and activity in disease tissue. Fluorescence imaging can aid in the identification of these proteases as well as allow for high-throughput screening of substrate preferences (*90, 92, 104, 122, 123*). Bogyo et al. have developed several activity-based probes to target cysteine proteases (*90, 122, 123*). These activity-based probes (Figure 1.5) contain a fluorophore, a quenching group, a warhead that irreversibly binds to the active site (acyloxymethyl ketone, AOMK), and a peptide sequence linking the fluorophore to the quencher (*90, 122, 123*). The peptide sequence is recognized by the cysteine protease and the quenching group is hydrolyzed from the AOMK, leaving the warhead covalently attached to the active site of the cysteine protease. The peptide sequence and fluorophore remain attached to the warhead, thus producing a fluorescently labeled enzyme for identification (*90, 122, 123*). Furthermore, when the quenching group is cleaved from the probe, the fluorescence can then be detected allowing real-time imaging of protease activity with reduced background signal (*90, 122, 123*). The peptide sequence can be modified to target different cysteine proteases and identify their preferred substrate sequences (*90, 122, 123*). Using this probe with an aspartic acid in the P1 position and altering the amino acids in the P2, P3, and P4 positions, Sexton et al. were able to identify a highly preferred substrate of legumain with limited cross-reactivity toward the similar cysteine protease, cathepsin B (*124*). While the substrate specificity was identified *in vitro*, there is the potential to use this probe *in vivo*, to image

legumain activity in small animal models similarly to that which was done with cathepsins (*125*).

1.4.2.2 AMC (7-amino-4-methylcoumarin)

AMC (7-amino-4-methylcoumarin) with amino acid sequences attached to the primary amine was developed by Zimmerman et al. to detect the activity of several proteases including chymotrypsin, trypsin, and elastase (*126, 127*). The structures of AMC and an AMC amino acid conjugate are shown in Figure 1.6. Prior to this, *para*-nitroanilides (pNAs) were primarily used to image protease activity using changes in absorbance upon cleavage of the amino acid sequence, but these assays were not as sensitive as fluorescence (*127*). For example, Gly-Phe-AMC had a detection limit of 0.5 μg/ml chymotrypsin compared to 10 μg/ml for Gly-Phe-pNA. AMC is a fluorescent molecule that emits light at 460 nm when excited by light with a wavelength of 380 nm and has ~500-fold greater relative fluorescence in its free form compared to when amino acid(s) are conjugated to AMC (*126, 127*). The absorbance/excitation spectrum and emission spectrum of AMC are shifted when an amino acid or peptide is conjugated to AMC as shown in Figure 1.6, thus allowing the hydrolysis to AMC to be monitored fluorescently. Since its development, AMC has been used in the characterization of many proteases (*128-151*). Many of these AMC substrates are now available inexpensively through commercial sources and are generally used with biochemically purified or recombinant proteases. The use of AMC conjugates in proteolytic profiling of whole-cells is explored further in Chapter 4.

1.4.2.3 ACC (7-amino-4-carbamoylmethylcoumarin)

As outlined in previous sections, proteases play important roles in diseases such as

cancer. To more effectively target these proteases, it is useful to have a rapid method to monitor proteolytic acitivity. While some AMC conjugates are commercially available, screening a more complete peptide library requires custom synthesis, which can be tedious. To overcome the synthetic limitations of an AMC library, Harris et al. developed ACC (7-amino-4-carbamoylmethylcoumarin), which allows for solid-phase coupling of Fmoc-amino acids (*89*). ACC-peptide libraries have been used to screen serine proteases, cysteine proteases, and aminopeptidases (*85, 89, 152*). Thus, ACC has the potential to be even more useful than AMC in protease profiling and its effectiveness in determining protease activity in live cells is demonstrated in Chapter 4.

1.5 Conclusions

The development of prodrugs has been advantageous in improving many pharmacokinetic and pharmacodynamic properties such as absorption, biodistribution reduced toxicity, and targeting. When using a prodrug approach, the efficient and predictable hydrolysis to the pharmacologically active compound *in vivo* is important. This necessitates the identification of hydrolases involved in activation. Often these hydrolases are ubiquitously expressed, although there are proteins solely expressed or highly overexpressed in disease tissue such as tumors. These proteins can be used as molecular addresses or activators of targeted prodrugs. Some potential proteases have already been identified, but molecular imaging can aid in protease profiling to identify new proteases and substrates. The primary goal of this research is to develop a physiologically relevant whole-cell screening method to identify amino acid or peptide promoieties that are preferentially activated by target cells compared to control cells and apply the results of the screening to rational prodrug design.

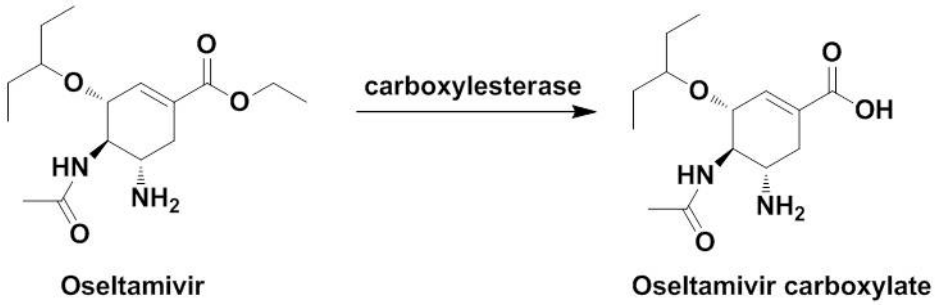

Figure 1.1 Bioactivation of the ester prodrug oseltamivir
Figure adapted from Huttunen et al. (*4*)

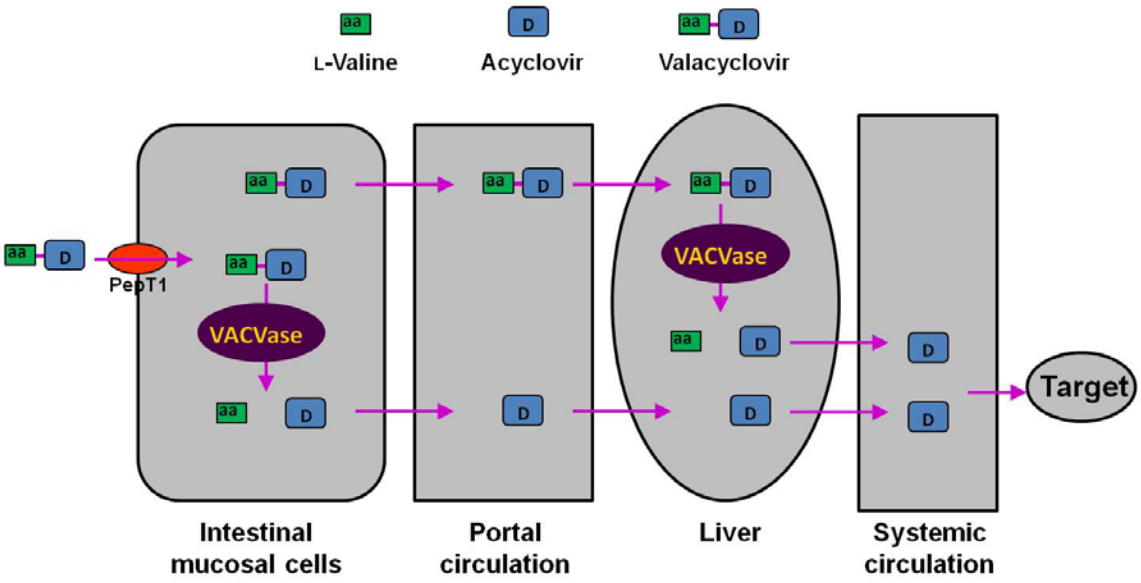

Figure 1.2 Absorption and activation of valacyclovir.
Image modified from Lai et al. (*153*)

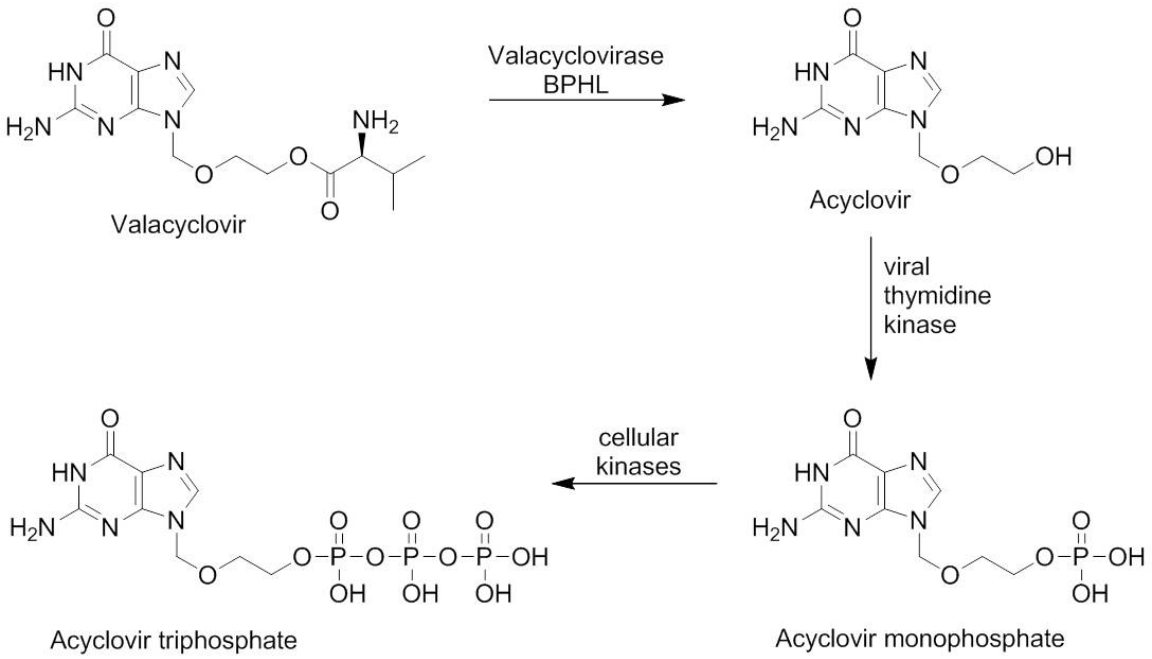

Figure 1.3 Bioactivation of valacyclovir.
Figure adapted from Huttunen et al. (*4*)

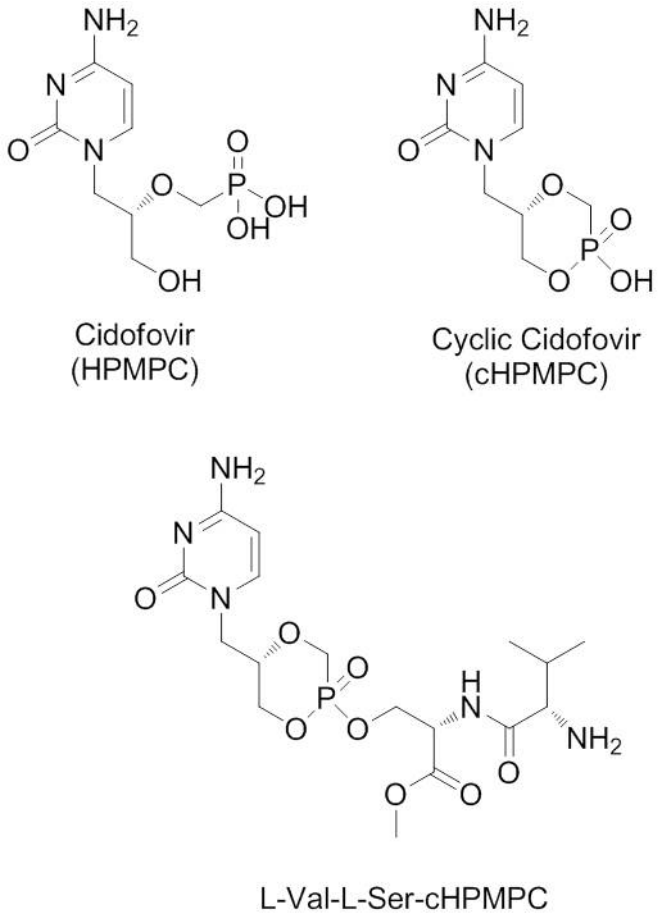

Figure 1.4 Chemical structures of cidofovir, cyclic cidofovir, and L-Val-L-Ser-cHPMPC

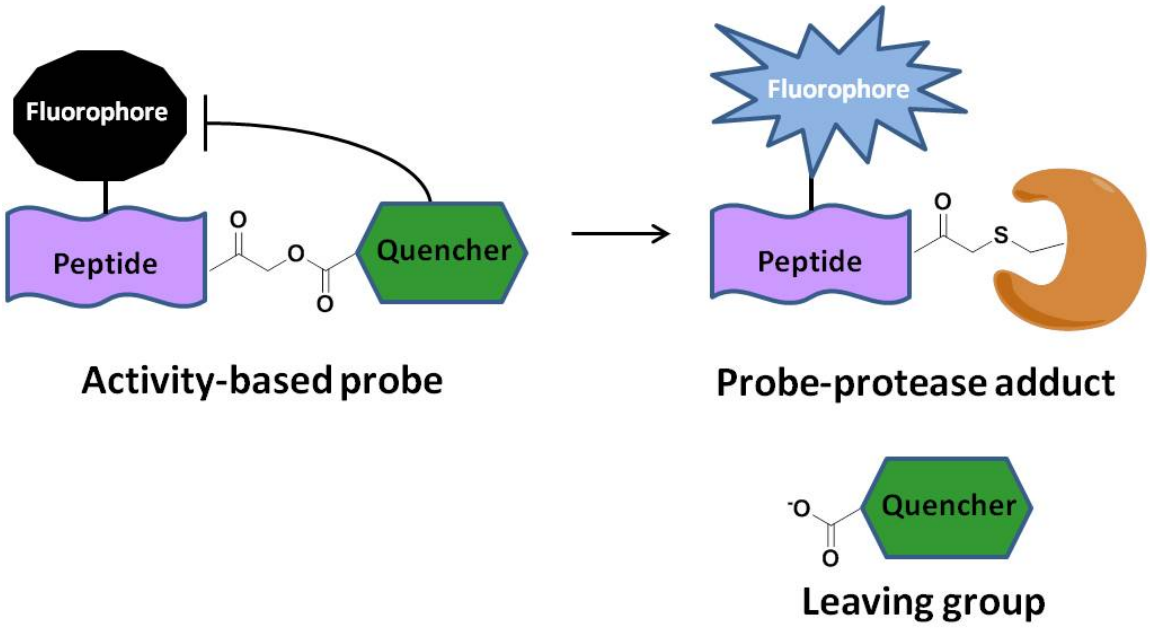

Figure 1.5 Labeling of a cysteine protease by an activity-based probe
The activity based probe consists of a quenching group, a warhead (acyloxymethyl ketone, AOMK), a peptide sequence to be recognize by the protease, and a fluorescent molecule which has an emission wavelength that corresponds to the absorbance wavelength of the quenching group. Upon recognition of the peptide sequence by the cysteine protease, the warhead covalently labels the active site of the protease and the quenching group is removed, resulting in fluorescence emission from the fluorophore. This figure is adapted from Blum et al. (*122*).

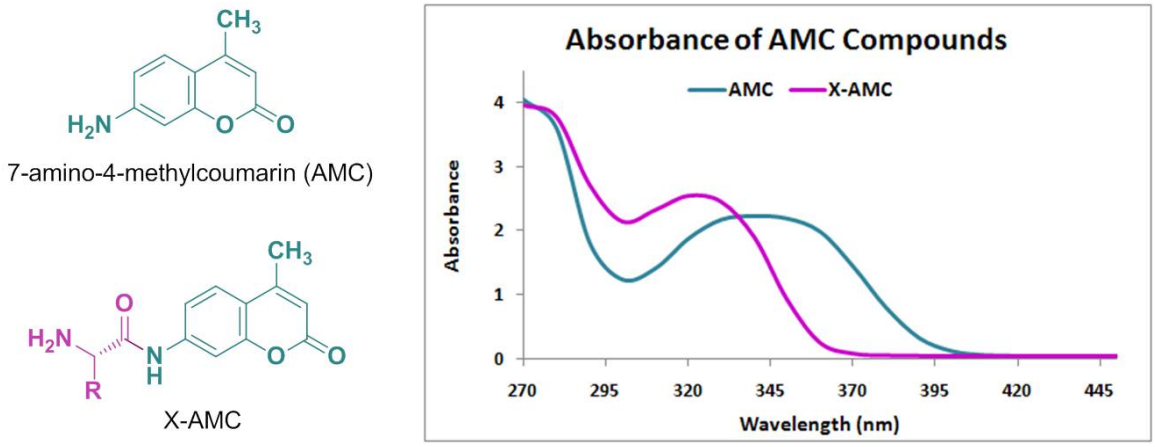

Figure 1.6 Structure and absorbance spectra of AMC and AMC amino acid conjugate.

1.6 References

1. Albert, A. (1958) Chemical aspects of selective toxicity, *Nature 182*, 421-422.

2. Ettmayer, P., Amidon, G. L., Clement, B., and Testa, B. (2004) Lessons Learned from Marketed and Investigational Prodrugs, *Journal of Medicinal Chemistry 47*, 2393-2404.

3. Ehrlich, P. (1910) Die Grundlagen der experimentellen Chemotherapie, *Angewandte Chemie 23*, 2-8.

4. Huttunen, K. M., Raunio, H., and Rautio, J. (2011) Prodrugs - from Serendipity to Rational Design, *Pharmacological Reviews 63*, 750-771.

5. Taylor, M. D. (1996) Improved passive oral drug delivery via prodrugs, *Advanced Drug Delivery Reviews 19*, 131-148.

6. McClellan, K., and Perry, C. M. (2001) Oseltamivir: A Review of its Use in Influenza, *Drugs 61*, 263-283.

7. Beutner, K. R. (1995) Valacyclovir: a review of its antiviral activity, pharmacokinetic properties, and clinical efficacy, *Antiviral Research 28*, 281-290.

8. Smiley, M. L., Murray, A., and de Miranda, P. (1996) Valacyclovir HCl (Valtrex): an acyclovir prodrug with improved pharmacokinetics and better efficacy for treatment of zoster, *Advances in Experimental Medicine and Biology 394*, 33-39.

9. Weller, S., Blum, M. R., Doucette, M., Burnette, T., Cederberg, D. M., de Miranda, P., and Smiley, M. L. (1993) Pharmacokinetics of the acyclovir pro-drug valaciclovir after escalating single- and multiple-dose administration to normal volunteers, *Clinical Pharmacology and Therapeutics 54*, 595-605.

10. Curran, M., and Noble, S. (2001) Valganciclovir, *Drugs 61*, 1145-1150 ; discussion 1151-1142.

11. Pescovitz, M. D., Rabkin, J., Merion, R. M., Paya, C. V., Pirsch, J., Freeman, R. B., O'Grady, J., Robinson, C., To, Z., Wren, K., Banken, L., Buhles, W., and Brown, F. (2000) Valganciclovir results in improved oral absorption of

ganciclovir in liver transplant recipients, *Antimicrob Agents Chemother 44*, 2811-2815.

12. Perry, C. M., and Faulds, D. (1996) Valaciclovir. A review of its antiviral activity, pharmacokinetic properties and therapeutic efficacy in herpesvirus infections, *Drugs 52*, 754-772.

13. Han, H., de Vrueh, R. L., Rhie, J. K., Covitz, K. M., Smith, P. L., Lee, C. P., Oh, D. M., Sadee, W., and Amidon, G. L. (1998) 5'-Amino acid esters of antiviral nucleosides, acyclovir, and AZT are absorbed by the intestinal PEPT1 peptide transporter, *Pharmaceutical Research 15*, 1154-1159.

14. Balimane, P. V., Tamai, I., Guo, A., Nakanishi, T., Kitada, H., Leibach, F. H., Tsuji, A., and Sinko, P. J. (1998) Direct evidence for peptide transporter (PepT1)-mediated uptake of a nonpeptide prodrug, valacyclovir, *Biochemical and Biophysical Research Communications 250*, 246-251.

15. Ganapathy, M. E., Huang, W., Wang, H., Ganapathy, V., and Leibach, F. H. (1998) Valacyclovir: a substrate for the intestinal and renal peptide transporters PEPT1 and PEPT2, *Biochemical and Biophysical Research Communications 246*, 470-475.

16. Faria, T. N., Timoszyk, J. K., Stouch, T. R., Vig, B. S., Landowski, C. P., Amidon, G. L., Weaver, C. D., Wall, D. A., and Smith, R. L. (2003) A Novel High-Throughput PepT1 Transporter Assay Differentiates between Substrates and Antagonists, *Molecular Pharmaceutics 1*, 67-76.

17. McKenna, C. E., Kashemirov, B. A., Eriksson, U., Amidon, G. L., Kish, P. E., Mitchell, S., Kim, J. S., and Hilfinger, J. M. (2005) Cidofovir peptide conjugates as prodrugs, *Journal of Organometallic Chemistry 690*, 2673-2678.

18. Ziegler, T. R., FernÃ¡ndez-EstÃ-variz, C. n., Gu, L. H., Bazargan, N., Umeakunne, K., Wallace, T. M., Diaz, E. E., Rosado, K. E., Pascal, R. R., Galloway, J. R., Wilcox, J. N., and Leader, L. M. (2002) Distribution of the H+/peptide transporter PepT1 in human intestine: up-regulated expression in the colonic mucosa of patients with short-bowel syndrome, *The American Journal of Clinical Nutrition 75*, 922-930.

19. Kim, I., Chu, X. Y., Kim, S., Provoda, C. J., Lee, K. D., and Amidon, G. L. (2003) Identification of a human valacyclovirase: biphenyl hydrolase-like protein as valacyclovir hydrolase, *J Biol.Chem. 278*, 25348-25356.

20. Prichard, M. N., and Kern, E. R. (2011) The search for new therapies for human cytomegalovirus infections, *Virus Research 157*, 212-221.

21. Lalezari, J. P., Stagg, R. J., Kuppermann, B. D., Holland, G. N., Kramer, F., Ives, D. V., Youle, M., Robinson, M. R., Drew, W. L., and Jaffe, H. S. (1997) Intravenous cidofovir for peripheral cytomegalovirus retinitis in patients with AIDS. A randomized, controlled trial, *Ann Intern Med 126*, 257-263.

22. Cundy, K. C., Barditch-Crovo, P., Petty, B. G., Ruby, A., Redpath, M., Jaffe, H. S., and Lietman, P. S. (1999) Clinical Pharmacokinetics of 1-[((S)-2-Hydroxy-2-Oxo-1,4,2-Dioxaphosphorinan-5-yl)methyl]cytosine in Human Immunodeficiency Virus-Infected Patients, *Antimicrobial Agents and Chemotherapy 43*, 271-277.

23. De Clercq, E. (2002) Cidofovir in the treatment of poxvirus infections, *Antiviral Research 55*, 1-13.

24. Keith, K. A., Wan, W. B., Ciesla, S. L., Beadle, J. R., Hostetler, K. Y., and Kern, E. R. (2004) Inhibitory Activity of Alkoxyalkyl and Alkyl Esters of Cidofovir and Cyclic Cidofovir against Orthopoxvirus Replication In Vitro, *Antimicrobial Agents and Chemotherapy 48*, 1869-1871.

25. Williams-Aziz, S. L., Hartline, C. B., Harden, E. A., Daily, S. L., Prichard, M. N., Kushner, N. L., Beadle, J. R., Wan, W. B., Hostetler, K. Y., and Kern, E. R. (2005) Comparative Activities of Lipid Esters of Cidofovir and Cyclic Cidofovir against Replication of Herpesviruses In Vitro, *Antimicrobial Agents and Chemotherapy 49*, 3724-3733.

26. Cundy, K. C., Li, Z. H., Hitchcock, M. J., and Lee, W. A. (1996) Pharmacokinetics of cidofovir in monkeys. Evidence for a prolonged elimination phase representing phosphorylated drug, *Drug Metab Dispos. 24*, 738-744.

27. Eriksson, U., Peterson, L. W., Kashemirov, B. A., Hilfinger, J. M., Drach, J. C., Borysko, K. Z., Breitenbach, J. M., Kim, J. S., Mitchell, S., Kijek, P., and McKenna, C. E. (2008) Serine Peptide Phosphoester Prodrugs of Cyclic Cidofovir: Synthesis, Transport, and Antiviral Activity, *Molecular Pharmaceutics 5*, 598-609.

28. Wachsman, M., Petty, B. G., Cundy, K. C., Jaffe, H. S., Fisher, P. E., Pastelak, A., and Lietman, P. S. (1996) Pharmacokinetics, safety and bioavailability of HPMPC (cidofovir) in human immunodeficiency virus-infected subjects,

Antiviral Res. 29, 153-161.

29. Eriksson, U., Hilfinger, J. M., Kim, J. S., Mitchell, S., Kijek, P., Borysko, K. Z., Breitenbach, J. M., Drach, J. C., Kashemirov, B. A., and McKenna, C. E. (2007) Synthesis and biological activation of an ethylene glycol-linked amino acid conjugate of cyclic cidofovir, *Bioorg.Med Chem.Lett. 17*, 583-586.

30. Eriksson, U., Peterson, L. W., Kim, J.-s., Mitchell, S., Kijek, P., Hilfinger, J. M., Drach, J. C., Kashemirov, B. A., and McKenna, C. E. (2006) Ehylene glycol-linked amino acid conjuagted of cyclic cidofovir: synthesis and biological activity, *Antiviral Research 70*, A58.

31. McKenna, C. E., Kashemirov, B. A., Peterson, L. W., Eriksson, U., Saejung, K., Kim, J.-S., Mitchell, S., Kijek, P., Hilfinger, J. M., and Drach, J. C. (2006) Cidofovir and Foscarnet peptide prodrugs, *Antiviral Research 70*, A37.

32. Han, H. K., and Amidon, G. L. (2000) Targeted prodrug design to optimize drug delivery, *AAPS PharmSci 2*, E6.

33. Stella, V. J., and Himmelstein, K. J. (1980) Prodrugs and site-specific drug delivery, *Journal of Medicinal Chemistry 23*, 1275-1282.

34. Carvalho, C., Santos, R. X., Cardoso, S., Correia, S., Oliveira, P. J., Santos, M. S., and Moreira, P. I. (2009) Doxorubicin: the good, the bad and the ugly effect, *Curr Med Chem 16*, 3267-3285.

35. Huang, P. S., and Oliff, A. (2001) Drug-targeting strategies in cancer therapy, *Curr Opin Genet Dev 11*, 104-110.

36. le Coutre, P., Mologni, L., Cleris, L., Marchesi, E., Buchdunger, E., Giardini, R., Formelli, F., and Gambacorti-Passerini, C. (1999) In Vivo Eradication of Human BCR/ABL-Positive Leukemia Cells With an ABL Kinase Inhibitor, *Journal of the National Cancer Institute 91*, 163-168.

37. Noonberg, S. B., and Benz, C. C. (2000) Tyrosine Kinase Inhibitors Targeted to the Epidermal Growth Factor Receptor Subfamily: Role as Anticancer Agents, *Drugs 59*, 753-767.

38. van Hensbergen, Y., Broxterman, H. J., Elderkamp, Y. W., Lankelma, J., Beers, J.

C., Heijn, M., Boven, E., Hoekman, K., and Pinedo, H. M. (2002) A doxorubicin-CNGRC-peptide conjugate with prodrug properties, *Biochem Pharmacol 63*, 897-908.

39. Arap, W., Pasqualini, R., and Ruoslahti, E. (1998) Cancer treatment by targeted drug delivery to tumor vasculature in a mouse model, *Science 279*, 377-380.

40. Pribylova, M., Dvorakova, M., Hanusova, V., Nemethova, I., Skalova, L., and Vanek, T. (2011) Paclitaxel conjugation with the analog of the gonadotropin-releasing hormone as a targeting moiety, *International Journal of Pharmaceutics 415*, 175-180.

41. Piedfer, M., Dauzonne, D., Tang, R., N'Guyen, J., Billard, C., and Bauvois, B. (2011) Aminopeptidase-N/CD13 is a potential proapoptotic target in human myeloid tumor cells, *The FASEB Journal*.

42. Wickström, M., Larsson, R., Nygren, P., and Gullbo, J. (2011) Aminopeptidase N (CD13) as a target for cancer chemotherapy, *Cancer Science 102*, 501-508.

43. Barbieri, R. L. (1992) Clinical applications of GnRH and its analogues, *Trends in Endocrinology & Metabolism 3*, 30-34.

44. Lim, M. D., and Craik, C. S. (2009) Using specificity to strategically target proteases, *Bioorganic & Medicinal Chemistry 17*, 1094-1100.

45. Bennis, S., Garcia, C., and Robert, J. (1993) Aspects of the cellular pharmacology of N-l-leucyldoxorubicin in human tumor cell lines, *Biochem Pharmacol 45*, 1929-1931.

46. Canal, P., Robert, J., Ramon, M., Baurain, R., Tresca, P., de Forni, M., Marty, M., Pujade-Lauraine, E., Bugat, R., Magis, A., and et al. (1992) Human pharmacokinetics of N-L-leucyl-doxorubicin, a new anthracycline derivative, and its correlation with clinical toxicities, *Clin Pharmacol Ther 51*, 249-259.

47. de Jong, J., Geijssen, G. J., Munniksma, C. N., Vermorken, J. B., and van der Vijgh, W. J. (1992) Plasma pharmacokinetics and pharmacodynamics of a new prodrug N-l-leucyldoxorubicin and its metabolites in a phase I clinical trial, *J Clin Oncol 10*, 1897-1906.

48. Boven, E., Hendriks, H. R., Erkelens, C. A., and Pinedo, H. M. (1992) The anti-tumour effects of the prodrugs N-l-leucyl-doxorubicin and vinblastine-isoleucinate in human ovarian cancer xenografts, *Br J Cancer 66*, 1044-1047.

49. Breistol, K., Hendriks, H. R., Berger, D. P., Langdon, S. P., Fiebig, H. H., and Fodstad, O. (1998) The antitumour activity of the prodrug N-L-leucyl-doxorubicin and its parent compound doxorubicin in human tumour xenografts, *Eur J Cancer 34*, 1602-1606.

50. Breistol, K., Hendriks, H. R., and Fodstad, O. (1999) Superior therapeutic efficacy of N-L-leucyl-doxorubicin versus doxorubicin in human melanoma xenografts correlates with higher tumour concentrations of free drug, *Eur J Cancer 35*, 1143-1149.

51. Albright, C. F., Graciani, N., Han, W., Yue, E., Stein, R., Lai, Z., Diamond, M., Dowling, R., Grimminger, L., Zhang, S. Y., Behrens, D., Musselman, A., Bruckner, R., Zhang, M., Jiang, X., Hu, D., Higley, A., Dimeo, S., Rafalski, M., Mandlekar, S., Car, B., Yeleswaram, S., Stern, A., Copeland, R. A., Combs, A., Seitz, S. P., Trainor, G. L., Taub, R., Huang, P., and Oliff, A. (2005) Matrix metalloproteinase-activated doxorubicin prodrugs inhibit HT1080 xenograft growth better than doxorubicin with less toxicity, *Mol Cancer Ther 4*, 751-760.

52. DeFeo-Jones, D., Garsky, V. M., Wong, B. K., Feng, D. M., Bolyar, T., Haskell, K., Kiefer, D. M., Leander, K., McAvoy, E., Lumma, P., Wai, J., Senderak, E. T., Motzel, S. L., Keenan, K., Van Zwieten, M., Lin, J. H., Freidinger, R., Huff, J., Oliff, A., and Jones, R. E. (2000) A peptide-doxorubicin 'prodrug' activated by prostate-specific antigen selectively kills prostate tumor cells positive for prostate-specific antigen in vivo, *Nat Med 6*, 1248-1252.

53. Denmeade, S. R., Nagy, A., Gao, J., Lilja, H., Schally, A. V., and Isaacs, J. T. (1998) Enzymatic activation of a doxorubicin-peptide prodrug by prostate-specific antigen, *Cancer Res 58*, 2537-2540.

54. DiPaola, R. S., Rinehart, J., Nemunaitis, J., Ebbinghaus, S., Rubin, E., Capanna, T., Ciardella, M., Doyle-Lindrud, S., Goodwin, S., Fontaine, M., Adams, N., Williams, A., Schwartz, M., Winchell, G., Wickersham, K., Deutsch, P., and Yao, S. L. (2002) Characterization of a novel prostate-specific antigen-activated peptide-doxorubicin conjugate in patients with prostate cancer, *J Clin Oncol 20*, 1874-1879.

55. Dubowchik, G. M., and Firestone, R. A. (1998) Cathepsin B-sensitive dipeptide

prodrugs. 1. A model study of structural requirements for efficient release of doxorubicin, *Bioorg Med Chem Lett 8*, 3341-3346.

56. Dubowchik, G. M., Mosure, K., Knipe, J. O., and Firestone, R. A. (1998) Cathepsin B-sensitive dipeptide prodrugs. 2. Models of anticancer drugs paclitaxel (Taxol), mitomycin C and doxorubicin, *Bioorg Med Chem Lett 8*, 3347-3352.

57. Fernandez, A. M., Van Derpoorten, K., Dasnois, L., Lebtahi, K., Dubois, V., Lobl, T. J., Gangwar, S., Oliyai, C., Lewis, E. R., Shochat, D., and Trouet, A. (2001) N-Succinyl-(beta-alanyl-L-leucyl-L-alanyl-L-leucyl)doxorubicin: an extracellularly tumor-activated prodrug devoid of intravenous acute toxicity, *J Med Chem 44*, 3750-3753.

58. Hu, Z., Jiang, X., Albright, C. F., Graciani, N., Yue, E., Zhang, M., Zhang, S. Y., Bruckner, R., Diamond, M., Dowling, R., Rafalski, M., Yeleswaram, S., Trainor, G. L., Seitz, S. P., and Han, W. (2010) Discovery of matrix metalloproteases selective and activated peptide-doxorubicin prodrugs as anti-tumor agents, *Bioorg Med Chem Lett 20*, 853-856.

59. Khan, S. R., and Denmeade, S. R. (2000) In vivo activity of a PSA-activated doxorubicin prodrug against PSA-producing human prostate cancer xenografts, *Prostate 45*, 80-83.

60. Kline, T., Torgov, M. Y., Mendelsohn, B. A., Cerveny, C. G., and Senter, P. D. (2004) Novel antitumor prodrugs designed for activation by matrix metalloproteinases-2 and -9, *Mol Pharm 1*, 9-22.

61. Kratz, F., Drevs, J., Bing, G., Stockmar, C., Scheuermann, K., Lazar, P., and Unger, C. (2001) Development and in vitro efficacy of novel MMP2 and MMP9 specific doxorubicin albumin conjugates, *Bioorganic & Medicinal Chemistry Letters 11*, 2001-2006.

62. Lee, G. Y., Song, J. h., Kim, S. Y., Park, K., and Byun, Y. (2006) Peptide-doxorubicin conjugates specifically degraded by matrix metalloproteinases expressed from tumor, *Drug Development Research 67*, 438-447.

63. Liu, C., Sun, C., Huang, H., Janda, K., and Edgington, T. (2003) Overexpression of legumain in tumors is significant for invasion/metastasis and a candidate enzymatic target for prodrug therapy, *Cancer Res. 63*, 2957-2964.

64. Wu, W., Luo, Y., Sun, C., Liu, Y., Kuo, P., Varga, J., Xiang, R., Reisfeld, R., Janda, K. D., Edgington, T. S., and Liu, C. (2006) Targeting cell-impermeable prodrug activation to tumor microenvironment eradicates multiple drug-resistant neoplasms, *Cancer Res. 66*, 970-980.

65. Atkinson, J. M., Siller, C. S., and Gill, J. H. (2008) Tumour endoproteases: the cutting edge of cancer drug delivery?, *Br J Pharmacol 153*, 1344-1352.

66. Lee, M., Fridman, R., and Mobashery, S. (2004) Extracellular proteases as targets for treatment of cancer metastases, *Chemical Society Reviews 33*, 401-409.

67. Jedeszko, C., and Sloane, B. F. (2004) Cysteine cathepsins in human cancer, *Biological Chemistry 385*, 1017-1027.

68. Fingleton, B. (2006) Matrix metalloproteinases: roles in cancer and metastasis, *Front Biosci 11*, 479-491.

69. Overall, C., and Dean, R. (2006) Degradomics: Systems biology of the protease web. Pleiotropic roles of MMPs in cancer, *Cancer and Metastasis Reviews 25*, 69-75.

70. Young, L., Di Salvo, A., Turnbull, A., Lyle, J., Bibby, M. C., Double, J. A., Kay, G., Loadman, P. M., and Mincher, D. (2003) Design of Tumour-Activated Prodrugs that Harness the 'Dark Side' of MMP-9, *Br J Cancer 88*, S27.

71. DeFeo-Jones, D., Brady, S. F., Feng, D.-M., Wong, B. K., Bolyar, T., Haskell, K., Kiefer, D. M., Leander, K., McAvoy, E., Lumma, P., Pawluczyk, J. M., Wai, J., Motzel, S. L., Keenan, K., Van Zwieten, M., Lin, J. H., Garsky, V. M., Freidinger, R., Oliff, A., and Jones, R. E. (2002) A Prostate-specific Antigen (PSA)-activated Vinblastine Prodrug Selectively Kills PSA-secreting Cells in Vivo, *Molecular Cancer Therapeutics 1*, 451-459.

72. Denmeade, S. R., Jakobsen, C. M., Janssen, S., Khan, S. R., Garrett, E. S., Lilja, H., Christensen, S. B., and Isaacs, J. T. (2003) Prostate-Specific Antigen-Activated Thapsigargin Prodrug as Targeted Therapy for Prostate Cancer, *Journal of the National Cancer Institute 95*, 990-1000.

73. Denmeade, S. R., Sokoll, L. J., Chan, D. W., Khan, S. R., and Isaacs, J. T. (2001) Concentration of enzymatically active prostate-specific antigen (PSA) in the extracellular fluid of primary human prostate cancers and human prostate cancer

xenograft models, *Prostate 48*, 1-6.

74. Elsadek, B., Graeser, R., Esser, N., Schäfer-Obodozie, C., Ajaj, K. A., Unger, C., Warnecke, A., Saleem, T., El-Melegy, N., Madkor, H., and Kratz, F. (2010) Development of a novel prodrug of paclitaxel that is cleaved by prostate-specific antigen: An in vitro and in vivo evaluation study, *European Journal of Cancer 46*, 3434-3444.

75. Garsky, V. M., Lumma, P. K., Feng, D. M., Wai, J., Ramjit, H. G., Sardana, M. K., Oliff, A., Jones, R. E., DeFeo-Jones, D., and Freidinger, R. M. (2001) The synthesis of a prodrug of doxorubicin designed to provide reduced systemic toxicity and greater target efficacy, *J Med Chem 44*, 4216-4224.

76. Wong, B. K., DeFeo-Jones, D., Jones, R. E., Garsky, V. M., Feng, D. M., Oliff, A., Chiba, M., Ellis, J. D., and Lin, J. H. (2001) PSA-specific and non-PSA-specific conversion of a PSA-targeted peptide conjugate of doxorubicin to its active metabolites, *Drug Metab Dispos 29*, 313-318.

77. Schmid, B., Chung, D. E., Warnecke, A., Fichtner, I., and Kratz, F. (2007) Albumin-binding prodrugs of camptothecin and doxorubicin with an Ala-Leu-Ala-Leu-linker that are cleaved by cathepsin B: synthesis and antitumor efficacy, *Bioconjug Chem 18*, 702-716.

78. Stern, L., Perry, R., Ofek, P., Many, A., Shabat, D., and Satchi-Fainaro, R. (2009) A Novel Antitumor Prodrug Platform Designed to Be Cleaved by the Endoprotease Legumain, *Bioconjugate Chemistry 20*, 500-510.

79. Chen, J. M., Dando, P. M., Rawlings, N. D., Brown, M. A., Young, N. E., Stevens, R. A., Hewitt, E., Watts, C., and Barrett, A. J. (1997) Cloning, isolation, and characterization of mammalian legumain, an asparaginyl endopeptidase, *J Biol.Chem. 272*, 8090-8098.

80. Schwarz, G., Brandenburg, J., Reich, M., Burster, T., Driessen, C., and Kalbacher, H. (2002) Characterization of legumain, *Biol Chem 383*, 1813-1816.

81. Kotackova, L., Balaziova, E., and Sedo, A. (2009) Expression pattern of dipeptidyl peptidase IV activity and/or structure homologues in cancer, *Folia Biol (Praha) 55*, 77-84.

82. Thompson, M. A., Ohnuma, K., Abe, M., Morimoto, C., and Dang, N. H. (2007)

CD26/dipeptidyl peptidase IV as a novel therapeutic target for cancer and immune disorders, *Mini Rev Med Chem 7*, 253-273.

83. Diez-Torrubia, A., Balzarini, J., Andrei, G., Snoeck, R., De Meester, I., Camarasa, M. J., and Velazquez, S. (2011) Dipeptidyl peptidase IV dependent water-soluble prodrugs of highly lipophilic bicyclic nucleoside analogues, *J Med Chem 54*, 1927-1942.

84. Barglow, K. T., and Cravatt, B. F. (2004) Discovering Disease-Associated Enzymes by Proteome Reactivity Profiling, *Chemistry & Biology 11*, 1523-1531.

85. Choe, Y., Leonetti, F., Greenbaum, D. C., Lecaille, F., Bogyo, M., Bromme, D., Ellman, J. A., and Craik, C. S. (2006) Substrate Profiling of Cysteine Proteases Using a Combinatorial Peptide Library Identifies Functionally Unique Specificities, *Journal of Biological Chemistry 281*, 12824-12832.

86. Goetz, D. H., Choe, Y., Hansell, E., Chen, Y. T., McDowell, M., Jonsson, C. B., Roush, W. R., McKerrow, J., and Craik, C. S. (2007) Substrate Specificity Profiling and Identification of a New Class of Inhibitor for the Major Protease of the SARS Coronavirusâ€ ,â€¡, *Biochemistry 46*, 8744-8752.

87. Gosalia, D. N., Salisbury, C. M., Ellman, J. A., and Diamond, S. L. (2005) High Throughput Substrate Specificity Profiling of Serine and Cysteine Proteases Using Solution-phase Fluorogenic Peptide Microarrays, *Molecular & Cellular Proteomics 4*, 626-636.

88. Gosalia, D. N., Salisbury, C. M., Maly, D. J., Ellman, J. A., and Diamond, S. L. (2005) Profiling serine protease substrate specificity with solution phase fluorogenic peptide microarrays, *PROTEOMICS 5*, 1292-1298.

89. Harris, J. L., Backes, B. J., Leonetti, F., Mahrus, S., Ellman, J. A., and Craik, C. S. (2000) Rapid and general profiling of protease specificity by using combinatorial fluorogenic substrate libraries, *Proc Natl Acad Sci U S A 97*, 7754-7759.

90. Kato, D., Boatright, K. M., Berger, A. B., Nazif, T., Blum, G., Ryan, C., Chehade, K. A., Salvesen, G. S., and Bogyo, M. (2005) Activity-based probes that target diverse cysteine protease families, *Nat.Chem.Biol. 1*, 33-38.

91. Pan, Z., Jeffery, D. A., Chehade, K., Beltman, J., Clark, J. M., Grothaus, P.,

Bogyo, M., and Baruch, A. (2006) Development of activity-based probes for trypsin-family serine proteases, *Bioorg.Med Chem.Lett. 16*, 2882-2885.

92. Sadaghiani, A. M., Verhelst, S. H., and Bogyo, M. (2007) Tagging and detection strategies for activity-based proteomics, *Curr Opin.Chem.Biol. 11*, 20-28.

93. Fonovic, M., and Bogyo, M. (2007) Activity based probes for proteases: applications to biomarker discovery, molecular imaging and drug screening, *Curr Pharm.Des 13*, 253-261.

94. Cloutier, S. M., Kundig, C., Gygi, C. M., Jichlinski, P., Leisinger, H. J., and Deperthes, D. (2004) Profiling of proteolytic activities secreted by cancer cells using phage display substrate technology, *Tumour Biol 25*, 24-30.

95. Schmid, B. r., Warnecke, A., Fichtner, I., Jung, M., and Kratz, F. (2007) Development of Albumin-Binding Camptothecin Prodrugs Using a Peptide Positional Scanning Library, *Bioconjugate Chemistry 18*, 1786-1799.

96. Trouet, A., Passioukov, A., Van derpoorten, K., Fernandez, A. M., Abarca-Quinones, J., Baurain, R., Lobl, T. J., Oliyai, C., Shochat, D., and Dubois, V. (2001) Extracellularly tumor-activated prodrugs for the selective chemotherapy of cancer: application to doxorubicin and preliminary in vitro and in vivo studies, *Cancer Res 61*, 2843-2846.

97. Ravel, D., Dubois, V., Quinonero, J., Meyer-Losic, F., Delord, J., Rochaix, P., Nicolazzi, C., Ribes, F., Mazerolles, C., Assouly, E., Vialatte, K., Hor, I., Kearsey, J., and Trouet, A. (2008) Preclinical toxicity, toxicokinetics, and antitumoral efficacy studies of DTS-201, a tumor-selective peptidic prodrug of doxorubicin, *Clin Cancer Res 14*, 1258-1265.

98. Bagshawe, K. D. (1993) Antibody-Directed Enzyme Prodrug Therapy (ADEPT), *Advances in Pharmacology Volume 24*, 99-121.

99. Connors, T. A., and Knox, R. J. (1995) Prodrugs in cancer chemotherapy, *Stem Cells 13*, 501-511.

100. Gabriel, D., Zuluaga, M. F., and Lange, N. (2011) On the cutting edge: protease-sensitive prodrugs for the delivery of photoactive compounds, *Photochemical & Photobiological Sciences 10*, 689-703.

101. Gabriel, D., Zuluaga, M. F., van den Bergh, H., Gurny, R., and Lange, N. (2011) It is all about proteases: from drug delivery to in vivo imaging and photomedicine, *Curr Med Chem 18*, 1785-1805.

102. Tong, X., Chen, X., and Li, C. (2011) Imaging beyond the diagnosis: image-guided enzyme/prodrug cancer therapy, *Acta Biochimica et Biophysica Sinica 43*, 4-12.

103. Yang, Y., Hong, H., Zhang, Y., and Cai, W. (2009) Molecular Imaging of Proteases in Cancer, *Cancer Growth Metastasis 2*, 13-27.

104. Baruch, A., Jeffery, D. A., and Bogyo, M. (2004) Enzyme activity--it's all about image, *Trends Cell Biol. 14*, 29-35.

105. Weishaupt, D., Koechli, V. D., and Marincek, B. (2003) *How does MRI work? an introduction to the physics and function of magnetic resonance imaging*, Springer, Berlin.

106. Damadian, R. (1971) Tumor detection by nuclear magnetic resonance, *Science 171*, 1151-1153.

107. Gries, H. (2002) Extracellular MRI Contrast Agents Based on Gadolinium, *Topics in Current Chemistry 221*, 2-24.

108. Duimstra, J. A., Femia, F. J., and Meade, T. J. (2005) A gadolinium chelate for detection of beta-glucuronidase: a self-immolative approach, *J Am Chem.Soc 127*, 12847-12855.

109. Frullano, L., Tejerina, B., and Meade, T. J. (2006) Synthesis and characterization of a doxorubicin-Gd(III) contrast agent conjugate: a new approach toward prodrug-procontrast complexes, *Inorg.Chem. 45*, 8489-8491.

110. Lee, J., Zylka, M. J., Anderson, D. J., Burdette, J. E., Woodruff, T. K., and Meade, T. J. (2005) A steroid-conjugated contrast agent for magnetic resonance imaging of cell signaling, *J Am Chem.Soc 127*, 13164-13166.

111. Li, W. H., Fraser, S. E., and Meade, T. J. (1999) A Calcium-Sensitive Magnetic Resonance Imaging Contrast Agent, *Journal of the American Chemical Society 121*, 1413-1414.

112. Li, W. H., Parigi, G., Fragai, M., Luchinat, C., and Meade, T. J. (2002) Mechanistic studies of a calcium-dependent MRI contrast agent, *Inorg.Chem. 41*, 4018-4024.

113. Louie, A. Y., Huber, M. M., Ahrens, E. T., Rothbacher, U., Moats, R., Jacobs, R. E., Fraser, S. E., and Meade, T. J. (2000) In vivo visualization of gene expression using magnetic resonance imaging, *Nat.Biotechnol. 18*, 321-325.

114. Major, J. L., Parigi, G., Luchinat, C., and Meade, T. J. (2007) The synthesis and in vitro testing of a zinc-activated MRI contrast agent, *Proc.Natl.Acad.Sci.U.S.A 104*, 13881-13886.

115. Meade, T. J., Taylor, A. K., and Bull, S. R. (2003) New magnetic resonance contrast agents as biochemical reporters, *Curr Opin.Neurobiol. 13*, 597-602.

116. Moats, R. A., Fraser, S. E., and Meade, T. J. (1997) A "Smart" Magnetic Resonance Imaging Agent That Reports on Specific Enzymatic Activity, *Angew.Chem.Int.Ed.Engl. 36*, 726-728.

117. Modo, M., Cash, D., Mellodew, K., Williams, S. C., Fraser, S. E., Meade, T. J., Price, J., and Hodges, H. (2002) Tracking transplanted stem cell migration using bifunctional, contrast agent-enhanced, magnetic resonance imaging, *Neuroimage. 17*, 803-811.

118. Lancelot, E., Amirbekian, V., Brigger, I., Raynaud, J. S., Ballet, S., David, C., Rousseaux, O., Le Greneur, S., Port, M., Lijnen, H. R., Bruneval, P., Michel, J. B., Ouimet, T., Roques, B., Amirbekian, S., Hyafil, F., Vucic, E., Aguinaldo, J. G., Corot, C., and Fayad, Z. A. (2008) Evaluation of matrix metalloproteinases in atherosclerosis using a novel noninvasive imaging approach, *Arterioscler Thromb Vasc Biol 28*, 425-432.

119. Lebel, R., Jastrzebska, B., Therriault, H., Cournoyer, M. M., McIntyre, J. O., Escher, E., Neugebauer, W., Paquette, B., and Lepage, M. (2008) Novel solubility-switchable MRI agent allows the noninvasive detection of matrix metalloproteinase-2 activity in vivo in a mouse model, *Magn Reson Med 60*, 1056-1065.

120. So, M. K., Xu, C., Loening, A. M., Gambhir, S. S., and Rao, J. (2006) Self-illuminating quantum dot conjugates for in vivo imaging, *Nat Biotechnol 24*, 339-343.

121. Rao, J., Dragulescu-Andrasi, A., and Yao, H. (2007) Fluorescence imaging in vivo: recent advances, *Current Opinion in Biotechnology 18*, 17-25.

122. Blum, G., Mullins, S. R., Keren, K., Fonovic, M., Jedeszko, C., Rice, M. J., Sloane, B. F., and Bogyo, M. (2005) Dynamic imaging of protease activity with fluorescently quenched activity-based probes, *Nat.Chem.Biol. 1*, 203-209.

123. Blum, G., von, D. G., Merchant, M. J., Blau, H. M., and Bogyo, M. (2007) Noninvasive optical imaging of cysteine protease activity using fluorescently quenched activity-based probes, *Nat.Chem.Biol. 3*, 668-677.

124. Sexton, K. B., Witte, M. D., Blum, G., and Bogyo, M. (2007) Design of cell-permeable, fluorescent activity-based probes for the lysosomal cysteine protease asparaginyl endopeptidase (AEP)/legumain, *Bioorg.Med Chem.Lett. 17*, 649-653.

125. Joyce, J. A., Baruch, A., Chehade, K., Meyer-Morse, N., Giraudo, E., Tsai, F.-Y., Greenbaum, D. C., Hager, J. H., Bogyo, M., and Hanahan, D. (2004) Cathepsin cysteine proteases are effectors of invasive growth and angiogenesis during multistage tumorigenesis, *Cancer Cell 5*, 443-453.

126. Zimmerman, M., Ashe, B., Yurewicz, E. C., and Patel, G. (1977) Sensitive assays for trypsin, elastase, and chymotrypsin using new fluorogenic substrates, *Anal Biochem 78*, 47-51.

127. Zimmerman, M., Yurewicz, E., and Patel, G. (1976) A new fluorogenic substrate for chymotrypsin, *Analytical Biochemistry 70*, 258-262.

128. Bar, J., Weber, A., Hoffmann, T., Stork, J., Wermann, M., Wagner, L., Aust, S., Gerhartz, B., and Demuth, H. U. (2003) Characterisation of human dipeptidyl peptidase IV expressed in Pichia pastoris. A structural and mechanistic comparison between the recombinant human and the purified porcine enzyme, *Biol Chem 384*, 1553-1563.

129. Bromme, D., Rossi, A. B., Smeekens, S. P., Anderson, D. C., and Payan, D. G. (1996) Human bleomycin hydrolase: molecular cloning, sequencing, functional expression, and enzymatic characterization, *Biochemistry 35*, 6706-6714.

130. Diaz-Perales, A., Quesada, V., Peinado, J. R., Ugalde, A. P., Alvarez, J., Suarez, M. F., Gomis-Ruth, F. X., and Lopez-OtÃn, C. (2005) Identification and Characterization of Human Archaemetzincin-1 and -2, Two Novel Members of a

Family of Metalloproteases Widely Distributed in Archaea, *Journal of Biological Chemistry 280*, 30367-30375.

131. Ezaki, J., Takeda-Ezaki, M., Oda, K., and Kominami, E. (2000) Characterization of endopeptidase activity of tripeptidyl peptidase-I/CLN2 protein which is deficient in classical late infantile neuronal ceroid lipofuscinosis, *Biochem Biophys Res Commun 268*, 904-908.

132. Flores, M., Aristoy, M. C., and Toldra, F. (1993) HPLC purification and characterization of porcine muscle aminopeptidase B, *Biochimie 75*, 861-867.

133. Geiss-Friedlander, R., Parmentier, N., Moller, U., Urlaub, H., Van den Eynde, B. J., and Melchior, F. (2009) The Cytoplasmic Peptidase DPP9 Is Rate-limiting for Degradation of Proline-containing Peptides, *Journal of Biological Chemistry 284:*, 27211-27219.

134. Gibson, A. M., Biggins, J. A., Lauffart, B., Mantle, D., and McDermott, J. R. (1991) Human brain leucyl aminopeptidase: Isolation, characterization and specificity against some neuropeptides, *Neuropeptides 19*, 163-168.

135. Hattori, A., Kitatani, K., Matsumoto, H., Miyazawa, S., Rogi, T., Tsuruoka, N., Mizutani, S., Natori, Y., and Tsujimoto, M. (2000) Characterization of recombinant human adipocyte-derived leucine aminopeptidase expressed in Chinese hamster ovary cells, *J Biochem 128*, 755-762.

136. Hattori, A., Matsumoto, H., Mizutani, S., and Tsujimoto, M. (1999) Molecular Cloning of Adipocyte-Derived Leucine Aminopeptidase Highly Related to Placental Leucine Aminopeptidase/Oxytocinase, *J Biochem 125*, 931-938.

137. Maes, M. B., Lambeir, A. M., Gilany, K., Senten, K., Van der Veken, P., Leiting, B., Augustyns, K., Scharpe, S., and De Meester, I. (2005) Kinetic investigation of human dipeptidyl peptidase II (DPPII)-mediated hydrolysis of dipeptide derivatives and its identification as quiescent cell proline dipeptidase (QPP)/dipeptidyl peptidase 7 (DPP7), *Biochem J 386*, 315-324.

138. Mantle, D. (1991) Characterization of dipeptidyl and tripeptidyl aminopeptidases in human kidney soluble fraction, *Clinica Chimica Acta 196*, 135-142.

139. Mantle, D., Hardy, M. F., Lauffart, B., McDermott, J. R., Smith, A. I., and Pennington, R. J. (1983) Purification and characterization of the major

aminopeptidase from human skeletal muscle, *Biochem J 211*, 567-573.

140. Mantle, D., Lauffart, B., and Gibson, A. (1991) Purification and characterization of leucyl aminopeptidase and pyroglutamyl aminopeptidase from human skeletal muscle, *Clin Chim Acta 197*, 35-45.

141. Matsumoto, H., Rogi, T., Yamashiro, K., Kodama, S., Tsuruoka, N., Hattori, A., Takio, K., Mizutani, S., and Tsujimoto, M. (2000) Characterization of a recombinant soluble form of human placental leucine aminopeptidase/oxytocinase expressed in Chinese hamster ovary cells, *Eur J Biochem 267*, 46-52.

142. Oyama, H., Fujisawa, T., Suzuki, T., Dunn, B. M., Wlodawer, A., and Oda, K. (2005) Catalytic residues and substrate specificity of recombinant human tripeptidyl peptidase I (CLN2), *J Biochem 138*, 127-134.

143. Schneck, J. L., Villa, J. P., McDevitt, P., McQueney, M. S., Thrall, S. H., and Meek, T. D. (2008) Chemical Mechanism of a Cysteine Protease, Cathepsin C, As Revealed by Integration of both Steady-State and Pre-Steady-State Solvent Kinetic Isotope Effects, *Biochemistry 47*, 8697-8710.

144. Sentandreu, M. A., and Toldra, F. (1998) Biochemical Properties of Dipeptidyl Peptidase III Purified from Porcine Skeletal Muscle, *Journal of Agricultural and Food Chemistry 46*, 3977-3984.

145. Sentandreu, M. A., and Toldra, F. (2000) Purification and Biochemical Properties of Dipeptidyl Peptidase I from Porcine Skeletal Muscle, *Journal of Agricultural and Food Chemistry 48*, 5014-5022.

146. Sharma, K. K., and Ortwerth, B. J. (1986) Isolation and characterization of a new aminopeptidase from bovine lens, *J Biol Chem 261*, 4295-4301.

147. Tanioka, T., Hattori, A., Masuda, S., Nomura, Y., Nakayama, H., Mizutani, S., and Tsujimoto, M. (2003) Human Leukocyte-derived Arginine Aminopeptidase, *Journal of Biological Chemistry 278*, 32275-32283.

148. Thompson, M. W., Beasley, K. A., Schmidt, M. D., and Seipelt, R. L. (2009) Arginyl aminopeptidase-like 1 (RNPEPL1) is an alternatively processed aminopeptidase with specificity for methionine, glutamine, and citrulline residues, *Protein Pept Lett 16*, 1256-1266.

149. Tian, Y., Sohar, I., Taylor, J. W., and Lobel, P. (2006) Determination of the substrate specificity of tripeptidyl-peptidase I using combinatorial peptide libraries and development of improved fluorogenic substrates, *J Biol Chem 281*, 6559-6572.

150. Tran, T. V., Ellis, K. A., Kam, C. M., Hudig, D., and Powers, J. C. (2002) Dipeptidyl peptidase I: importance of progranzyme activation sequences, other dipeptide sequences, and the N-terminal amino group of synthetic substrates for enzyme activity, *Arch.Biochem.Biophys. 403*, 160-170.

151. Yang, G., Kirkpatrick, R. B., Ho, T., Zhang, G.-F., Liang, P.-H., Johanson, K. O., Casper, D. J., Doyle, M. L., Marino, J. P., Thompson, S. K., Chen, W., Tew, D. G., and Meek, T. D. (2001) Steady-State Kinetic Characterization of Substrates and Metal-Ion Specificities of the Full-Length and N-Terminally Truncated Recombinant Human Methionine Aminopeptidases (Type 2), *Biochemistry 40*, 10645-10654.

152. Drag, M., Bogyo, M., Ellman, J. A., and Salvesen, G. S. (2010) Aminopeptidase Fingerprints, an Integrated Approach for Identification of Good Substrates and Optimal Inhibitors, *Journal of Biological Chemistry 285*, 3310-3318.

153. Lai, L., Xu, Z., Zhou, J., Lee, K.-D., and Amidon, G. L. (2008) Molecular Basis of Prodrug Activation by Human Valacyclovirase, an Î±-Amino Acid Ester Hydrolase, *Journal of Biological Chemistry 283*, 9318-9327.

CHAPTER 2

Puromycin-sensitive aminopeptidase: An antiviral prodrug activating enzyme

2.1 Summary

The broad-spectrum antiviral agent Cidofovir (HPMPC) is currently administered intravenously to treat AIDS-related human cytomegalovirus retinitis. While Cidofovir has the potential to be used in the treatment of other herpes and DNA viruses, its use is hampered by the inherent low bioavailability of the compound. Val-Ser-cyclic HPMPC (Val-Ser-cHPMPC) is a promising peptide prodrug that has been previously shown to improve oral bioavailability of the parent compound in rodent models (*1*). The conjugation of Val-Ser to cyclic cidofovir makes it a substrate for the intestinal peptide transporter PEPT1, but renders it pharmacologically inactive. Thus, this prodrug strategy requires reliable and predictable *in vivo* activation. Puromycin-sensitive aminopeptidase (APP-S) was partially purified from Caco-2 cellular homogenates and identified as a potential prodrug-activating enzyme for Val-Ser-cHPMPC (*2*). A recombinant APP-S was generated and its substrate specificity was investigated using amino acid conjugates of *para*-nitroaniline (pNA), 7-amino-4-methylcoumarin (AMC), and 7-amino-4-carbamoylmethylcoumarin (ACC). The k_{cat} values for Ala-pNA and Ala-AMC were 18-fold and 48-fold faster than the values for Val-pNA and Val-AMC, respectively, suggesting APP-S prefers some amino acids over others. Furthermore, the drastically different k_{cat} values for Val-pNA, Val-AMC, and Val-Ser-cHPMPC suggests that the

leaving group may play an important role in determining the rate of hydrolysis. In addition to its ability to hydrolyze a variety of substrates, the *in vitro* hydrolysis of Val-Ser-cHPMPC and the inhibition of hydrolysis by the aminopeptidase inhibitor bestatin in Caco-2 homogenates suggest that APP-S is an important enzyme for activating Val-Ser-cHPMPC *in vivo*. Taken together, our data suggest that APP-S makes an attractive target for activation of orally absorbed amino acid or peptide prodrugs.

2.2 Introduction

The development of prodrugs to improve bioavailability has become an increasingly common strategy. For example, the valyl ester prodrugs of acyclovir (valacyclovir) and ganciclovir (valganciclovir) have been used to dramatically increase the oral absorption compared to their parent compounds; 3- to 5-fold in the case of valacyclovir (*3-7*). Cidofovir (Vistide®, HPMPC, **1**, Figure 2.1) is an antiviral agent that is clinically used for treatment of the AIDS-related herpes virus infection, cytomegalovirus retinitis. It is a broad-spectrum antiviral agent with therapeutic potential in the treatment of other herpes and DNA viruses, including polyoma-, papilloma-, adeno-, and poxvirus infections (*8, 9*). Cidofovir is of particular interest due to its potential use as therapy in the event of an outbreak of smallpox (*10*). Currently, a major drawback of using cidofovir in a large-scale emergency situation is its need for intravenous administration. This has led to the development of several cyclic cidofovir (cHPMPC) prodrugs incorporating dipeptides (*1, 11-14*). One of the lead prodrugs, Val-Ser-cHPMPC (**2**, Figure 2.1), shows significantly enhanced intestinal uptake (18.1% versus 2.2% for cHPMPC) in an *in situ* rat perfusion model (*1, 13*).

The term prodrug describes chemicals with little or no pharmacological activity

that undergo biotransformation to yield a therapeutically active metabolite (*15*). This biotransformation may be chemically or enzymatically mediated. Reliable and predictable *in vivo* activation is a critical aspect of the prodrug strategy; therefore, identification of the mechanisms of their *in vivo* activation is important from a prodrug design perspective. Our laboratory has previously identified human valacyclovirase (BPHL) as one of the enzymes responsible for activation of valacyclovir and valganciclovir (*16*). Interestingly, the majority (≥ 90%) of Val-Ser-cHPMPC was found to be converted to cHPMPC during *in situ* rat perfusion experiments (*1*). Since Val-Ser-cHPMPC undergoes substantial *in vivo* activation in the rat intestine, we are interested in investigating plausible human activation pathway(s) for Val-Ser-cHPMPC. Puromycin-sensitive aminopeptidase (APP-S) was partially purified from Caco-2 cell homogenates in our laboratory and identified as a potential activator of Val-Ser-cHPMPC (Figure 2.2) (*2*). To further confirm this finding, we produced a recombinant APP-S (GenBank accession no. CAA68964) to determine the kinetic constants of Val-Ser-cHPMPC hydrolysis as well as the APP-S prodrug activating pathway. The broad tissue distribution of APP-S and other neutral aminopeptidases, as well as their homology and expression in a variety of species (*17-20*) makes them attractive targets for activation of orally absorbed prodrugs. To aid in the design of prodrugs to be activated by these compounds, we studied the hydrolysis kinetics of other amino acids and leaving groups such as *para*-nitroaniline (pNA), 7-amino-4-methylcoumarin (AMC), and 7-amino-4-carbamoylmethylcoumarin (ACC) shown in Figure 2.3.

2.3 Methods

2.3.1 Chemicals and reagents

Val-Ser-cHPMPC was synthesized as previously described (*1*). Amino acid conjugates of *para*-nitroaniline (pNA) and 7-amino-4-methylcoumarin (AMC) were purchased from Bachem. Cell culture reagents and 4-12% Bis-Tris polyacrylamide gels were obtained from Invitrogen/Gibco. Bestatin, trifluoroacetic acid (TFA) and *N*-(3-dimethylaminopropyl)-*N*′-ethylcarbodiimide (EDC) were purchased from Sigma-Aldrich. Other chemicals were either ACS reagent grade, analytical or HPLC grade and purchased from Thermo Fisher Scientific, Inc. unless otherwise noted.

2.3.1.1 Synthesis of ACC compounds

ACC (7-amino-4-carbamoylmethylcoumarin) was synthesized and conjugated to Rink amide AM resin according to the method of Maly et al.(*21*) The single amino acid conjugates of valine and alanine were made using the coupling conditions described previously (*21*). Compound identities and purity were confirmed by TOF mass spec (ES^+) and ^1H NMR.

2.3.2 Generation of recombinant APP-S

2.3.2.1 Subcloning of APP-S cDNA

Human APP-S cDNA (IMAGE clone ID 6059589) in the mammalian expression vector pCMV-SPORT6 (Open Biosystems) was subcloned into the pET-28a vector (Novagen) for expression of the N-terminally His-tagged construct in *Escherichia coli*. Briefly, the APP-S cDNA was excised from pCMV-SPORT6 and ligated into pET28a after digesting both with the restriction enzymes EcoRI and XhoI (New England Biolabs) and purifying by electrophoresis in a 1% agarose gel. The ~2.8 kb band corresponding to

APP-S and the ~5.4 kb band corresponding to pET-28a were purified from the agarose using a QIAEX II gel extraction kit (QIAGEN) and ligated using T4 DNA ligase (New England Biolabs). To shift the inserted cDNA to the correct reading frame, one nucleotide was inserted upstream of the APP-S cDNA using the primers 5'-GGCCTCGCCGCG AATGCCGGAGAAGAGG -3' and 5'-CTCTTCTCCGGCATTCG CGGCGAGGCC -3' (Integrated DNA Technologies) and QuikChange Site Directed Mutagenesis kit (Stratagene). The His-APP-S/pET-28a construct was then transformed into *E. coli* strain BL21-RIPL (Stratagene) followed by dideoxy sequencing (University of Michigan DNA Sequencing Core) to confirm the nucleotide sequence of the recombinant His-APP-S.

2.3.2.2 Recombinant APP-S expression and purification

His-APP-S protein expression was induced according to the method of Sengupta et al. (*22*) with modifications. Briefly, BL21-RIPL cells containing His-APP-S/pET-28a were grown to stationary phase in LB broth at 37 °C, and then expanded until cultures reached an optical density of 0.8-1.0 at 570 nm, at which point His-APP-S expression was induced with 1 mM isopropyl β-D-thiogalactopyranoside (IPTG) at 18 °C for 18-20 hr. Following centrifugation at 6,000 × *g* for 10 min at 4 °C, the cell pellet was resuspended in 50 mM sodium phosphate, 300 mM sodium chloride, and 20 mM imidazole, pH 8 (wash buffer) containing 1 mg/ml lysozyme (Sigma-Aldrich), followed by three cycles of freeze-thaw. After a 10 min incubation at 37 °C, the homogenate was pulsed for 30 seconds with a probe sonicator (Model KT40, Kontes) followed by centrifugation at 20,000 × *g* for 40 min. His-APP-S was purified from the supernatant using Ni-NTA agarose (QIAGEN), followed by washing with 100 bed volumes (~ 250

ml) wash buffer. The recombinant APP-S was eluted with 100 U (~15 µg) thrombin (GE Healthcare) in 1 ml PBS pH 7.4 for 18 hours at 25 °C with gentle agitation, which also served to remove the His-tag. The thrombin and APP-S were separated from the Ni-NTA agarose by spinning at 1,500 × g for 5 min and the supernatant transferred to a clean tube, after which the Ni-NTA agarose was washed 3 × 1 ml with PBS, pH 7.4 and all four supernatants were combined. Thrombin was removed by incubating with 400 µl p-aminobenzamidine agarose (Sigma-Aldrich; binding capacity 4-8 mg thrombin) for 2 hours at 25 °C, followed by pelleting of the p-aminobenzamidine agarose at 1,500 × *g*. Protein concentration was determined using the Pierce BCA assay (Thermo Fisher Scientific). Gel images were acquired and quantified uising a Molecular Dynamics Typhoon 9200 imager and ImageQuant software (GE Healthcare). Purified APP-S was aliquoted and stored at -80 °C.

2.3.3 Hydrolysis assays

2.3.3.1 Prodrug hydrolysis by recombinant APP-S

2.3.3.1.1 HPLC assay of metabolites

Recombinant APP-S (30 µg/ml) was preincubated with and without the inhibitor bestatin (Fluka, 20 µg/ml) in 10 mM HEPES, 100 mM NaCl (pH 7.4) for 5 minutes at 37°C. Prodrug was added at final concentrations ranging from 0.125 to 1 mM to initiate the enzymatic reaction. Aliquots of 40 µl were removed at predetermined time points (0-15 min) and quenched by the addition of 80 µl of 10% ice-cold TFA. The quenched samples were spun through 96-well 0.45 µm polyvinylidene difluoride (PVDF) membranes (Unifilter, Whatman) at 1,800 × *g* in a Jouan MR 22i tabletop centrifuge to remove the precipitates before HPLC analysis. The HPLC system (Waters) consisted of a

reverse-phase column (XTerra RP18, 5 µm, 4.6 x 250 mm), a 515 pump, a 996 Photodiode Array UV detector and a 717 Plus Autosampler. The remaining prodrug and the production of parent drug were analyzed using a mobile phase consisting of an acetonitrile (0.1% TFA) gradient (2-52%) mobile phase with a flow rate of 1 ml/min and detection at 274 nm. The specific activity was expressed as nmol min^{-1} mg^{-1} of protein based on the disappearance of the prodrug.

2.3.3.1.2 LC-MS identification of the metabolites

Further identification of the APP-S hydrolysis products was achieved on a Finnigan LCQ Deca XP Max mass spectrometer in positive mode with a Finnigan Surveyor PDA Plus detector and MS Pump Plus, all controlled using Xcalibur software. The samples (20 µl injection volume) were resolved in a Varian Microsorb-MV C-18 column (100-5, 250 × 4.6 mm) with UV detection at 274 nm. The eluate was diverted immediately before the mass spectrometer, such that only half of the flow was injected into the MS. The mobile phases consisted of 0.1 N ammonium acetate buffer, pH 5.5 containing either 0% acetonitrile (A) or 17.5% acetonitrile (B), run at 1 ml/min. Mobile phase gradients consisted of 100% A/ 0% B for 5 min, 50% A/ 50% B at 6 min (or 25% A/ 75% B at 7 min for prodrug alone samples), 20% A/ 80% B from 15 to 20 min.

2.3.3.2 APP-S hydrolysis of para-nitroanilide compounds

The ability of APP-S to hydrolyze various amino acids was tested using the chromogenic substrates L-valine *para*-nitroanilide (Val-pNA) and L-alanine *para*-nitroanilide (Ala-pNA) (Bachem). Recombinant APP-S was pre-incubated in PBS, pH 7.4 with and without 20 µg/ml bestatin in a final volume of 300 µl. The reaction was started by adding 0.05 – 1.6 mM substrate dissolved in dimethyl sulfoxide (DMSO) and

carried out at 37 °C. The production of p-nitroaniline was measured spectrophotometrically at 405 nm every 30 sec for 15 min. The concentration of p-nitroaniline was determined using the Beer-Lambert equation (ε_{405} = 9500 L mol^{-1} cm^{-1}). K_m and V_{max} were calculated for each substrate using GraphPad Prism 4.

2.3.3.3 APP-S hydrolysis of AMC and ACC compounds

Recombinant APP-S was diluted in 10 mM Hepes, 100 mM sodium chloride (pH 7.4) to a concentration of 1 ng/µl. The protein was distributed to a black-walled 96-well plate in 100 µl aliquots and pre-incubated at 37°C for 5 min. AMC and ACC conjugates were then added at a final concentration of 100 µM to determine V_0 or 6.25 to 100 µM to determine kinetic constants. Hydrolysis was monitored by measuring fluorescence ($400_{ex}/580_{em}$ nm) every 2 min for 1 hr in a Biotek Synergy plate reader heated to 37°C. Using AMC standards, the fluorescence was used to calculate the amount of compound hydrolyzed to AMC or ACC, which was plotted against time. The slope of the linear portion of the best fit line was equal to the initial velocity (V_0). To determine the kinetic constants, the initial velocities were plotted against the initial concentration of the compound in GraphPad Prism 4.0. Using non-linear regreassion, the Michaelis-Menton equation was fit to the data to calculate K_m and V_{MAX}. The catalytic constant (k_{cat}) was then determined using the following equations:

[E] = (Amount of enzyme/ volume of sample)/molecular weight of enzyme

$k_{cat} = V_{MAX}/ [E]$

2.4 Results

2.4.1 Recombinant APP-S hydrolysis investigations

To confirm that APP-S is an activating enzyme of Val-Ser-cHPMPC, the APP-S

cDNA (Open Biosystems) was subcloned into the bacterial expression vector pET-28a (Novagen). Recombinant His-tagged APP-S was purified to > 98% purity (Figure 2.4) using Ni-NTA agarose (QIAGEN) and thrombin cleavage to remove the His-tag. The purified recombinant APP-S migrated as two bands in SDS-PAGE when eluted from Ni-NTA by thrombin digestion (Figure 2.4), but as a single band when eluted with imidazole (data not shown). Both thrombin-eluted bands were identified as APP-S by peptide mass analysis at the University of Michigan Proteome Core, and the presence of a potential thrombin-cleavable sequence, in addition to the expected pET-28a vector thrombin cleavage site, was subsequently identified at amino acid 15 in APP-S's N-terminus, consistent with the ~1.5 kDa MW difference observed in these gels. To determine the K_m and V_{max} of APP-S for Val-Ser-cHPMPC, APP-S was incubated with a range of substrate concentrations with aliquots withdrawn at predetermined time points. Using HPLC to determine the concentration of Val-Ser-cHPMPC at various time points, V_0 was calculated using the disappearance of prodrug. The data from four independent experiments were plotted (Figure 2.5) and analyzed by non-linear regression (GraphPad Prism 4, GraphPad Software, Inc) to determine V_{max} and K_m. APP-S was shown to hydrolyze Val-Ser-cHPMPC with a V_{max} of 1873 ± 400 nmol min^{-1} mg^{-1} protein and a K_m of 0.85 ± 0.33 mM. As expected, this hydrolysis was almost completely inhibited by addition of bestatin. APP-S was not able to appreciably hydrolyze D-Val-D-Ser-cHPMPC beyond that which was detected in buffer alone; similar to what was observed with Caco-2 homogenates (data not shown).

2.4.2 Activation pathways for Val-Ser-cHPMPC and its metabolites

Using LC-MS analysis it was observed that in the presence of the recombinant

APP-S, the peptide bond in Val-Ser-cHPMPC was cleaved to remove the N-terminal amino acid (L-valine, Figure 2.6) to generate the intermediate, Ser-cHPMPC, (**3**). When Val-Ser-cHPMPC was incubated in buffer alone or with APP-S in the presence of the inhibitor bestatin the peak corresponding to compound **3** was not present. Besides the above-mentioned activating products, a minor species (≤ 15%) with a mass of 480 (positive ion mode) was also observed (**4**). This mass corresponds to the intact dipeptide conjugate attached to the parent compound and not the cyclic version of cidofovir.

2.4.3 Kinetic constants for APP-S hydrolysis of p-nitroanilide compounds

The activity of purified recombinant APP-S was then analyzed using the model substrates L-alanine *p*-nitroanilide (Ala-pNA) and L-valine *p*-nitroanilide (Val-pNA) in the presence and absence of the inhibitor bestatin. Val-pNA was shown to have a lower K_m than Ala-pNA (0.28 ± 0.19 mM vs 0.51 ± 0.14 mM, respectively) and a greater than 18-fold lower V_{max} (289 ± 85.1 nmol/min·mg protein vs 5365 ± 610.0 nmol min^{-1} mg^{-1} protein, respectively) as shown in Table 2.1. APP-S hydrolysis of the model substrates was completely inhibited by the addition of bestatin.

The k_{cat} for Val-pNA was approximately 18-fold lower ($p < 0.06$) than the k_{cat} for Ala-pNA and approximately three-fold lower than the k_{cat} for Val-Ser-cHPMPC. The k_{cat}/K_m values for Val-Ser-cHPMPC cleavage by APP-S (0.22×10^6 M^{-1} min^{-1}) are comparable to those obtained for the para-nitroanilide derivatives of L-alanine and L-valine as well as by others (*22*).

2.4.4 APP-S hydrolysis of AMC and ACC compounds

The K_m and k_{cat} values for Ala-AMC and Val-AMC hydrolysis by APP-S were determined (Table 2.1). Similar to the p-nitroanilide compounds, Val-AMC had a lower

K_m value than Ala-AMC (0.038 mM and 0.29 mM, respectively) and Ala-AMC had a faster k_{cat} than Val-AMC (201 min^{-1} and 4.2 min^{-1}, respectively). While the preference of APP-S for Ala substrates compared to Val substrates remained, the k_{cat}/K_m values for the AMC substrates were 2- to 3-fold lower for the AMC substrates compared to the pNA substrates.

The initial velocities of hydrolysis of several single amino acid substrates by APP-S were determined (Table 2.2). Val-AMC and Val-ACC had similar V_0 values as well as Ala-AMC and Ala-ACC. Ala substrates were still hydrolyzed faster than Val substrates; however the hydrolysis of Leu-, Met-, and Phe-AMC were significantly faster.

2.5 Discussion

By stepwise purification from the human intestinal cell line Caco-2 and MS/MS analysis we previously demonstrated that puromycin-sensitive aminopeptidase (APP-S) is involved in activation of the antiviral prodrug Val-Ser-cHPMPC (*2*). While previous data do not exclude the possibility that other proteases may be involved, the observation that bestatin, a known inhibitor of APP-S (*17, 22*), is able to inhibit enzymatic hydrolysis of Val-Ser-cHPMPC in Caco-2 cell homogenates further suggests that APP-S is important in the *in vivo* activation of the prodrug (*1*). Moreover, it has been reported that APP-S prefers basic and hydrophobic amino acids and has relatively low affinity for acidic residues (*17, 23*), consistent with our observation that the valine residue is efficiently cleaved from Val-Ser-cHPMPC. Finally, APP-S has been shown to hydrolyze a variety of amino acid substrates, with the exception of: (i) those that have acidic side chains, (ii) D-amino acid isomers, or (iii) N-terminally blocked amino acids (*17, 23*). Consistent with these observations, the recombinant APP-S was unable to hydrolyze the

D-amino acid version of **2**, D-Val-D-Ser-cHMPC (data not shown). Similarly, there was no significant hydrolysis of D-Val-D-Ser-cHPMPC in Caco-2 homogenate as compared to buffer alone (*2*).

The recombinant APP-S was able to efficiently hydrolyze Val-Ser-cHPMPC *in vitro*, reinforcing our hypothesis concerning APP-S's role in Val-Ser-cHPMPC activation *in vivo*. Similar to that observed in Caco-2 cell homogenates (*1*), bestatin was able to inhibit APP-S hydrolysis of Val-Ser-cHPMPC. The approximately 18-fold lower k_{cat} for Val-pNA as compared to Ala-pNA further demonstrated that some amino acids are preferred over others. This was further confirmed by the almost 50-fold faster k_{cat} of Ala-AMC compared to Val-AMC. Furthermore, the three-fold and almost 50-fold higher k_{cat} for Val-Ser-cHPMPC as compared to Val-pNA and Val-AMC, respectively, suggests that the leaving group may play an important role in determining the rate of hydrolysis. Interestingly, the K_m value for the hydrolysis of Val-Ser-cHPMPC by APP-S is in the sub-millimolar range, suggesting that under *in vivo* conditions the conversion of Val-Ser-cHPMPC is likely to occur well below saturating substrate concentrations. The k_{cat}/K_m value for Val-Ser-cHPMPC cleavage by APP-S (0.22×10^6 min^{-1} M^{-1}) is comparable to those obtained for the *para*-nitroanilide derivatives of L-alanine and L-valine as well as by others (*22*), suggesting that the prodrug hydrolysis is likely to occur with a reasonable efficiency even in the presence of other substrates. The preference of APP-S for certain amino acids seems to remain regardless of leaving group as Met-, Leu-, and Ala-AMC were hydrolyzed significantly faster than Val- or Pro-AMC, as was reported for *p*-nitroanilide substrates by Sengupta et al. (*22*).

LC-MS analysis revealed that the peptide bond in Val-Ser-cHPMPC was cleaved

to remove the N-terminal valine to generate the Ser-cHPMPC intermediate (**3**) when incubated with APP-S, but not in buffer alone or in the presence of APP-S and bestatin. This intermediate also disappeared with prolonged incubation in the presence of the Caco-2 homogenates while the peak associated with cHPMPC (cyclic cidofovir, **1**) correspondingly increased (*2*). One likely mechanism for this relative instability of Ser-cHPMPC is nucleophilic attack on the phosphodiester linkage by the primary amine of serine that is produced after the removal of valine by APP-S. Indeed, Lazarus et al. have previously proposed and demonstrated such a mechanism to explain the intramolecular hydrolysis of amine-containing phosphoryl esters (*24, 25*). Based on these findings, and the fact that the major species found in rat plasma after a modified *in situ* single pass perfusion is indeed cHPMPC (*1*), we suspected that the activation of Val-Ser-cHPMPC occurs through both enzymatic and chemical pathways. It is worth noting that cyclic cidofovir itself undergoes a biotransformation to generate cidofovir when exposed to endogenous cyclic cytidine 3′,5′-monophosphate (cCMP) phosphodiesterase (*26, 27*), and can therefore be regarded as a prodrug of cidofovir. In addition, cyclic cidofovir has been reported to be less nephrotoxic than cidofovir, while also exhibiting potent antiviral activity (*26*). Nevertheless, cyclic cidofovir itself shows low oral bioavailability (*28*), indicating the need to mask the residual phosphonate negative charge present at physiological pH, which the reported Val-Ser-cHPMPC prodrug has been designed to do.

APP-S has been extensively studied and has been implicated in a number of physiological processes, including normal cellular turnover (*29-31*), cell cycle regulation (*17*), processing of antigenic peptides for display on MHC class I (*32*), and degradation of neuropeptides and brain function (*19, 33*). However, to our knowledge, this is the first

reported finding that APP-S is able to hydrolyze an antiviral prodrug. The broad tissue distribution of APP-S and other neutral aminopeptidases, as well as their homology and expression in a variety of species (*17-20*) can be advantageous to ensure complete and rapid prodrug activation, as was previously noted for Val-Ser-cHPMPC *in situ* (*1*). Additionally, APP-S has been shown to have a broad substrate specificity with preference for hydrophobic and basic amino acids, (*22, 23, 34-36*) making it an attractive target for future design of orally absorbed prodrugs.

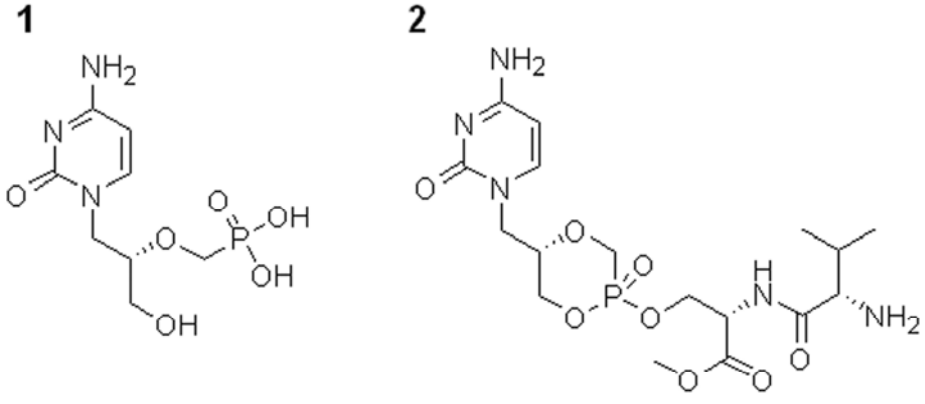

Figure 2.1 Chemical structures of cidofovir (1) and Val-Ser-cHPMPC (2).

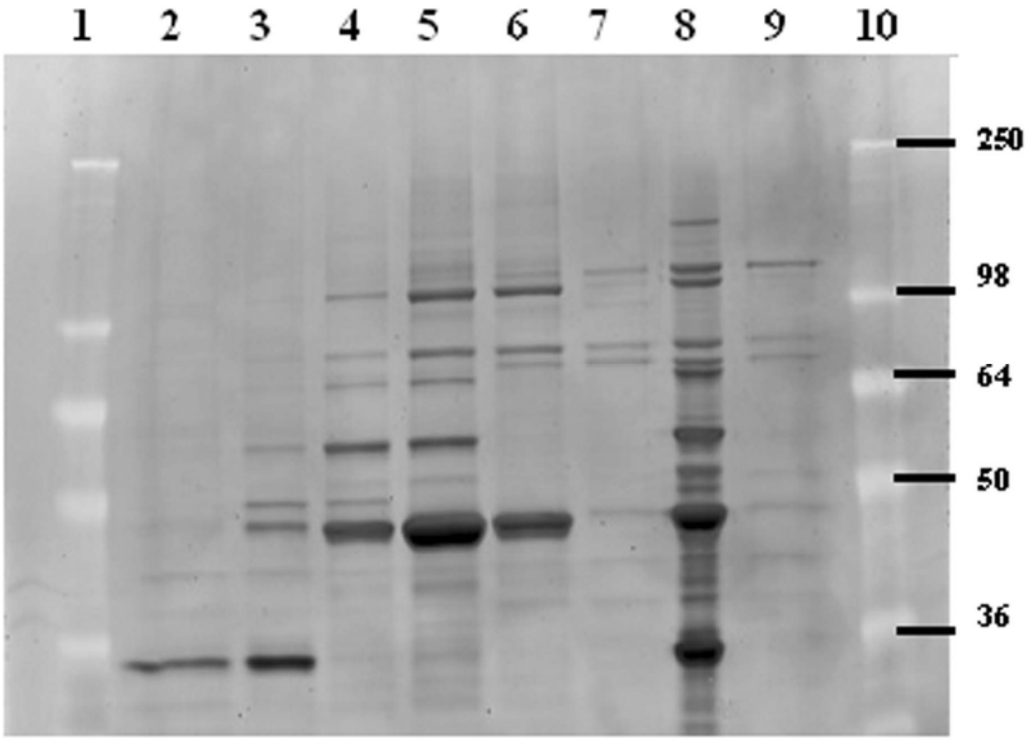

Figure 2.2 Superdex-200 purification of APP-S from Caco-2 cell homogenates. Active and non-active fractions from the Superdex-200 purification were analyzed by 10% SDS-PAGE, here stained with SYPRO Red. Lanes 4-6 contain active fractions hydrolyzing Val-Ser-cHPMPC, while lanes 2, 3, 7 and 9 are non-active fractions. Lane 8 corresponds to the pooled active MonoQ fractions that were initially applied to the Superdex-200 column. Lanes 1 and 10 are size markers with molecular mass expressed in kDa. The band visible at ~ 100 kDa in lane 4-6 and 8 was exclusively present in the active fractions and its identity was determined by tandem mass spectrometry and database searches to be puromycin-sensitive aminopeptidase (APP-S).

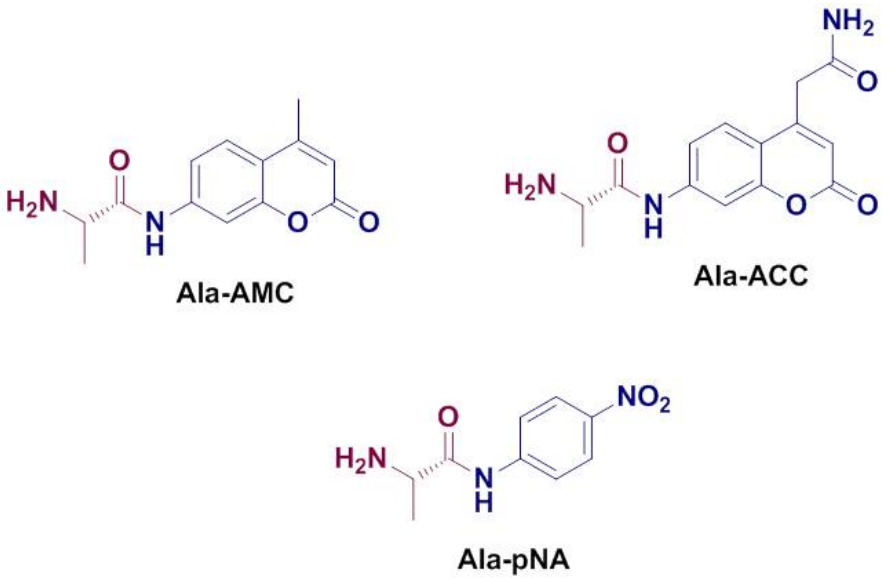

Figure 2.3 Chemical structures of Ala-AMC, Ala-ACC, and Ala-pNA

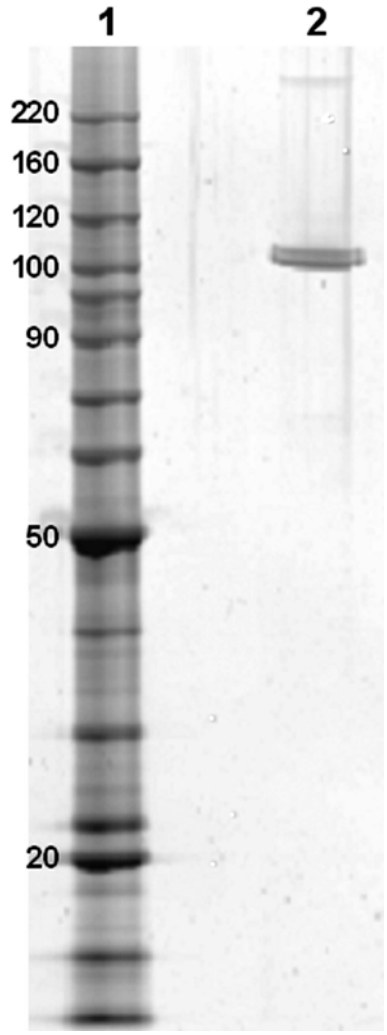

Figure 2.4 Purified recombinant APP-S.
Recombinant human APP-S was expressed in BL21-RIPL cells and purified using a Ni-NTA affinity column. APP-S was eluted via cleavage by thrombin between the His-tag and the recombinant APP-S. Following quantification of total protein using the BCA assay (Pierce), 80 ng of APP-S was run in a 4-12% Bis-Tris gel (Invitrogen) and stained with Krypton Protein Stain (Pierce Biotechnology, Inc.). Lane 1 contains BenchMark Protein Ladder (Invitrogen) and lane 2 contains the purified recombinant APP-S. APP-S was purified to > 97% purity as determined by ImageQuant Analysis (Molecular Dynamics).

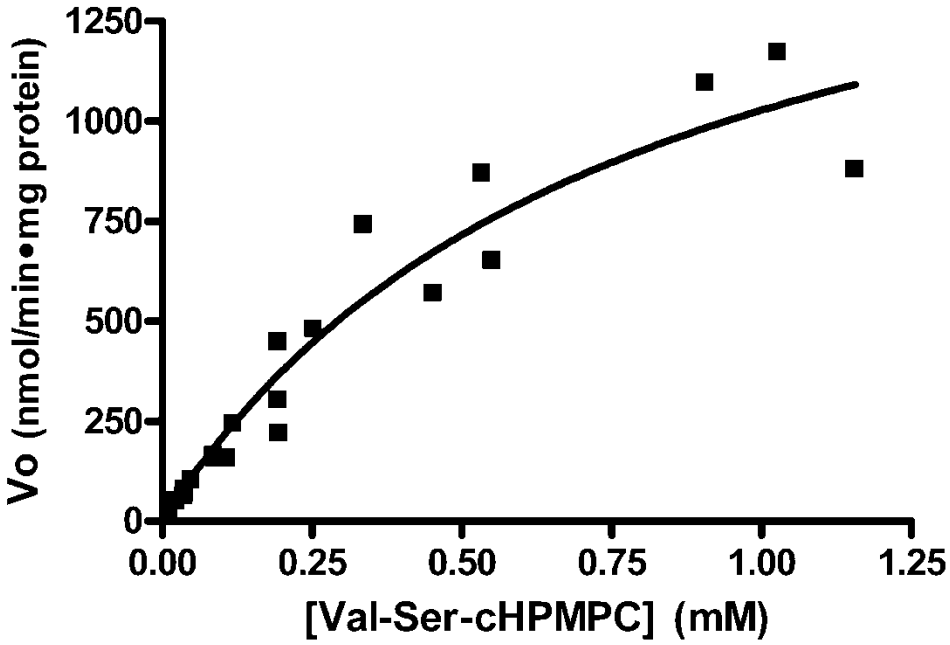

Figure 2.5 Michaelis-Menten plot of Val-Ser-cHPMPC hydrolysis by APP-S. Recombinant APP-S (30 μg/ml) was incubated in 10 mM HEPES, 100 mM NaCl, pH 7.4 at 37 ºC with 0.125 to 1 mM Val-Ser-cHPMPC. Aliquots of 40 μl were removed at predetermined time points (0-15 min) and quenched by the addition of 80 μl of 10% ice-cold TFA. The samples were analyzed by HPLC with a 2-52% acetonitrile gradient mobile phase at 1 ml/min and detection at 274 nm. The concentration detected at 0 min was used as the initial concentration in the plot above to control for variability between sample sets. The V_0 was calculated and the plot was generated using GraphPad Prism 4.0.

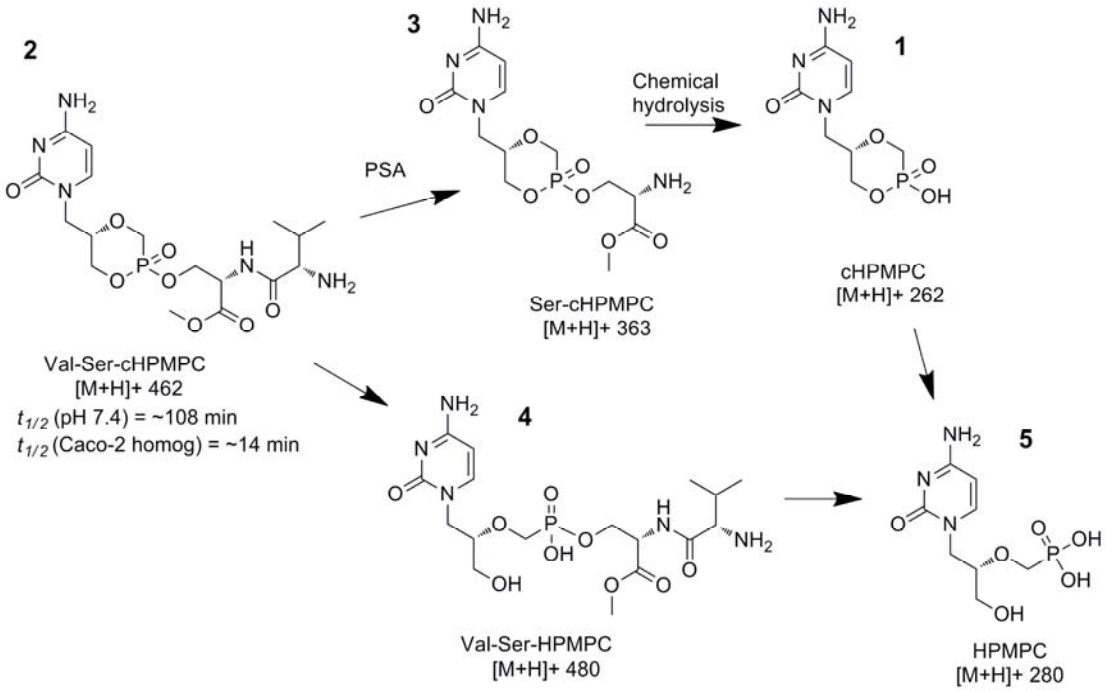

Figure 2.6 Chemical structures of the observed metabolites obtained during the hydrolysis of Val-Ser-cHPMPC by recombinant APP-S.
Samples from APP-S hydrolysis of Val-Ser-cHPMPC were analyzed by LC/MS. It was found that the peak corresponding to **3** was present in the samples hydrolyzed by APP-S, but not present in the negative control samples (prodrug in buffer alone or with APP-S and bestatin). Enzymatic (APP-S) as well as chemical hydrolysis is involved in the overall prodrug activation process.

Table 2.1 Kinetics of Val-Ser-cHPMPC hydrolysis by recombinant APP-S. Recombinant APP-S was incubated with Ala-pNA, Val-pNA or Val-Ser-cHPMPC at 37°C in the presence or absence of the inhibitor bestatin. Hydrolysis of the *p*-nitroanilide compounds was monitored spectrophotometrically at 405 nm every 30 sec for 15 min. Hydrolysis of Val-Ser-cHPMPC was determined by monitoring the disappearance of the prodrug peak by HPLC (detection at 274 nm) at $t = 0$, 1, 2, 3, 5, 10, and 15 min. K_m and V_{max} were calculated using GraphPad Prism 4.0.

Substrate	K_m (mM)	V_{max} (nmol min^{-1} mg^{-1} protein)	k_{cat} (min^{-1})[a]	k_{cat}/K_m (min^{-1} M^{-1})
Ala-AMC	0.29 ± 0.09	2008 ± 475	201	6.9×10^5
Ala-pNA	0.51 ± 0.14	5365 ± 610	1071	2.1×10^6
Val-AMC	0.038 ± 0.007	42 ± 3	4.2	1.1×10^5
Val-pNA	0.28 ± 0.19	289 ± 85	58	0.21×10^6
Val-Ser-cHPMPC	0.85 ± .33	1873 ± 400	187	0.22×10^6

[a] k_{cat} values are calculated from V_{max} values with the assumption that all enzyme molecules are catalytically active.

Table 2.2 Initial velocity of hydrolysis of AMC and ACC substrates by recombinant APP-S.

Recombinant APP-S was incubated with 100 μM AMC or ACC substrates at 37°C. Hydrolysis was monitored by fluorescence emission at 508 nm (excitation at 400 nm) every 2 min for 1 hr. Data were analyzed by One-way ANOVA with a Bonferroni post test using GraphPad Prism 4.0 and values were considered significantly different if $p < 0.05$.

Substrate	V_o (nmol/min•mg protein)
D-Ala-AMC	0.93 ± 0.06^a
Val-AMC	12 ± 1.5^a
Val-ACC	20 ± 1.7^a
Pro-AMC	21 ± 1.5^a
Ala-ACC	235 ± 7.1^b
Ala-AMC	271 ± 7.1^b
Tyr-AMC	263 ± 12^b
Leu-AMC	335 ± 13^c
Met-AMC	488 ± 51^d
Phe-AMC	611 ± 24^e

*Values with different letters are significantly different from each other ($p < 0.05$).

2.6 References

1. Eriksson, U., Peterson, L. W., Kashemirov, B. A., Hilfinger, J. M., Drach, J. C., Borysko, K. Z., Breitenbach, J. M., Kim, J. S., Mitchell, S., Kijek, P., and McKenna, C. E. (2008) Serine Peptide Phosphoester Prodrugs of Cyclic Cidofovir: Synthesis, Transport, and Antiviral Activity, *Molecular Pharmaceutics 5*, 598-609.

2. Tehler, U., Nelson, C. H., Peterson, L. W., Provoda, C. J., Hilfinger, J. M., Lee, K.-D., McKenna, C. E., and Amidon, G. L. (2010) Puromycin-sensitive aminopeptidase: An antiviral prodrug activating enzyme, *Antiviral Research 85*, 482-489.

3. Curran, M., and Noble, S. (2001) Valganciclovir, *Drugs 61*, 1145-1150 ; discussion 1151-1142.

4. Perry, C. M., and Faulds, D. (1996) Valaciclovir. A review of its antiviral activity, pharmacokinetic properties and therapeutic efficacy in herpesvirus infections, *Drugs 52*, 754-772.

5. Pescovitz, M. D., Rabkin, J., Merion, R. M., Paya, C. V., Pirsch, J., Freeman, R. B., O'Grady, J., Robinson, C., To, Z., Wren, K., Banken, L., Buhles, W., and Brown, F. (2000) Valganciclovir results in improved oral absorption of ganciclovir in liver transplant recipients, *Antimicrob. Agents Chemother. 44*, 2811-2815.

6. Smiley, M. L., Murray, A., and de Miranda, P. (1996) Valacyclovir HCl (Valtrex): an acyclovir prodrug with improved pharmacokinetics and better efficacy for treatment of zoster, *Adv. Exp. Med. Biol. 394*, 33-39.

7. Weller, S., Blum, M. R., Doucette, M., Burnette, T., Cederberg, D. M., de Miranda, P., and Smiley, M. L. (1993) Pharmacokinetics of the acyclovir pro-drug valaciclovir after escalating single- and multiple-dose administration to normal volunteers, *Clinical Pharmacology and Therapeutics 54*, 595-605.

8. De Clercq, E. (1997) In search of a selective antiviral chemotherapy, *Clinical Microbiology Reviews 10*, 674-693.

9. De Clercq, E., and Holy, A. (2005) Case history: Acyclic nucleoside phosphonates: a key class of antiviral drugs, *Nature Reviews. Drug Discovery 4*, 928-940.

10. De Clercq, E. (2002) Cidofovir in the treatment of poxvirus infections, *Antiviral Res. 55*, 1-13.

11. Eriksson, U., Hilfinger, J. M., Kim, J. S., Mitchell, S., Kijek, P., Borysko, K. Z., Breitenbach, J. M., Drach, J. C., Kashemirov, B. A., and McKenna, C. E. (2007) Synthesis and biological activation of an ethylene glycol-linked amino acid conjugate of cyclic cidofovir, *Bioorg. Med. Chem. Lett. 17*, 583-586.

12. Eriksson, U., Peterson, L. W., Kim, J.-s., Mitchell, S., Kijek, P., Hilfinger, J. M., Drach, J. C., Kashemirov, B. A., and McKenna, C. E. (2006) Ehylene glycol-linked amino acid conjuagted of cyclic cidofovir: synthesis and biological activity, *Antiviral Res. 70*, A58.

13. McKenna, C. E., Kashemirov, B. A., Eriksson, U., Amidon, G. L., Kish, P. E., Mitchell, S., Kim, J. S., and Hilfinger, J. M. (2005) Cidofovir peptide conjugates as prodrugs, *J. Organomet. Chem. 690*, 2673-2678.

14. McKenna, C. E., Kashemirov, B. A., Peterson, L. W., Eriksson, U., Saejung, K., Kim, J.-S., Mitchell, S., Kijek, P., Hilfinger, J. M., and Drach, J. C. (2006) Cidofovir and Foscarnet peptide prodrugs, *Antiviral Res. 70*, A37.

15. Albert, A. (1958) Chemical aspects of selective toxicity, *Nature 182*, 421-422.

16. Kim, I., Chu, X. Y., Kim, S., Provoda, C. J., Lee, K. D., and Amidon, G. L. (2003) Identification of a human valacyclovirase: biphenyl hydrolase-like protein as valacyclovir hydrolase, *J. Biol. Chem 278*, 25348-25356.

17. Constam, D. B., Tobler, A. R., Rensing-Ehl, A., Kemler, I., Hersh, L. B., and Fontana, A. (1995) Puromycin-sensitive aminopeptidase. Sequence analysis, expression, and functional characterization, *J. Biol. Chem 270*, 26931-26939.

18. McLellan, S., Dyer, S. H., Rodriguez, G., and Hersh, L. B. (1988) Studies on the tissue distribution of the puromycin-sensitive enkephalin-degrading aminopeptidases, *J. Neurochem. 51*, 1552-1559.

19. Schulz, C., Perezgasga, L., and Fuller, M. T. (2001) Genetic analysis of dPsa, the Drosophila orthologue of puromycin-sensitive aminopeptidase, suggests redundancy of aminopeptidases, *Dev. Genes Evol. 211*, 581-588.

20. Tobler, A. R., Constam, D. B., Schmitt-Graff, A., Malipiero, U., Schlapbach, R., and Fontana, A. (1997) Cloning of the human puromycin-sensitive aminopeptidase and evidence for expression in neurons, *J. Neurochem. 68*, 889-897.

21. Maly, D. J., Leonetti, F., Backes, B. J., Dauber, D. S., Harris, J. L., Craik, C. S., and Ellman, J. A. (2002) Expedient solid-phase synthesis of fluorogenic protease substrates using the 7-amino-4-carbamoylmethylcoumarin (ACC) fluorophore, *J Org Chem 67*, 910-915.

22. Sengupta, S., Horowitz, P. M., Karsten, S. L., Jackson, G. R., Geschwind, D. H., Fu, Y., Berry, R. W., and Binder, L. I. (2006) Degradation of Tau Protein by Puromycin-Sensitive Aminopeptidase in Vitro, *Biochemistry (Mosc). 45*, 15111-15119.

23. Wagner, G. W., Tavianini, M. A., Herrmann, K. M., and Dixon, J. E. (1981) Purification and characterization of an enkephalin aminopeptidase from rat brain, *Biochemistry (Mosc). 20*, 3884-3890.

24. Lazarus, R. A., Benkovic, P. A., and Benkovic, S. J. (1980) Mechanism of hydrolysis of phosphorylethanolamine diesters. Intramolecular nucleophilic amine participation, *Journal of the Chemical Society*, 373-379.

25. Lazarus, R. A., and Benkovic, S. J. (1979) Mechanism of hydrolysis of phosphorylethanolamine triesters. Multiple catalytic effects of an intramolecular amino group, *J. Am. Chem. Soc. 101*, 4300-4312.

26. Bischofberger, N., Hitchcock, M. J. M., Chen, M. S., Barkhimer, D. B., Cundy, K. C., Kent, K. M., Lacy, S. A., Lee, W. A., Li, Z.-H., and et al. (1994) 1-[((S)-2-Hydroxy-2-oxo-1,4,2-dioxaphosphorinan-5-yl)methyl]cytosine, an intracellular prodrug for (S)-1-(3-hydroxy-2-phosphonylmethoxypropyl)cytosine with improved therapeutic index in vivo, *Antimicrob. Agents Chemother. 38*, 2387-2391.

27. Mendel, D. B., Cihlar, T., Moon, K., and Chen, M. S. (1997) Conversion of 1-[((S)-2-hydroxy-2-oxo-1,4,2-dioxaphosphorinan-5-yl)methyl]cytosine to cidofovir by an intracellular cyclic CMP phosphodiesterase, *Antimicrob. Agents Chemother. 41*, 641-646.

28. Cundy, K. C., Li, Z. H., Hitchcock, M. J., and Lee, W. A. (1996) Pharmacokinetics of cidofovir in monkeys. Evidence for a prolonged elimination

phase representing phosphorylated drug, *Drug Metab. Dispos. 24*, 738-744.

29. Bhutani, N., Venkatraman, P., and Goldberg, A. L. (2007) Puromycin-sensitive aminopeptidase is the major peptidase responsible for digesting polyglutamine sequences released by proteasomes during protein degradation, *EMBO J. 26*, 1385-1396.

30. Botbol, V., and Scornik, O. A. (1983) Peptide intermediates in the degradation of cellular proteins. Bestatin permits their accumulation in mouse liver in vivo, *J. Biol. Chem 258*, 1942-1949.

31. Goldberg, A. L., and Rock, K. L. (1992) Proteolysis, proteasomes and antigen presentation, *Nature 357*, 375-379.

32. Stoltze, L., Schirle, M., Schwarz, G., Schroter, C., Thompson, M. W., Hersh, L. B., Kalbacher, H., Stevanovic, S., Rammensee, H. G., and Schild, H. (2000) Two new proteases in the MHC class I processing pathway, *Nature Immunology 1*, 413-418.

33. Osada, T., Ikegami, S., Takiguchi-Hayashi, K., Yamazaki, Y., Katoh-Fukui, Y., Higashinakagawa, T., Sakaki, Y., and Takeuchi, T. (1999) Increased anxiety and impaired pain response in puromycin-sensitive aminopeptidase gene-deficient mice obtained by a mouse gene-trap method, *J. Neurosci. 19*, 6068-6078.

34. Hui, K. S., Wang, Y. J., and Lajtha, A. (1983) Purification and characterization of an enkephalin aminopeptidase from rat brain membranes, *Biochemistry (Mosc). 22*, 1062-1067.

35. Johnson, G. D., and Hersh, L. B. (1990) Studies on the subsite specificity of the rat brain puromycin-sensitive aminopeptidase, *Arch. Biochem. Biophys. 276*, 305-309.

36. Schnebli, H. P., Phillipps, M. A., and Barclay, R. K. (1979) Isolation and characterization of an enkephalin-degrading aminopeptidase from rat brain, *Biochim. Biophys. Acta 569*, 89-98.

CHAPTER 3

Enzyme-Activated Magnetic Resonance Imaging Contrast Agent

3.1 Summary

There has been increasing attention on targeting of drugs. One way to target drugs is to make prodrugs activated by enzymes expressed at the target site. To monitor this activation *in vivo*, it would be useful to have an imaging agent that is activated in a similar manner. The magnetic resonance imaging (MRI) contrast agent Gd-DTPA (gadolinium diethylenetriamine pentaacetic acid) is a good candidate for this approach as the ninth coordination site of Gd^{3+} can potentially be blocked by a peptide to cloak the signal enhancing qualities of Gd^{3+}. Several analogues of Gd-DTPA were synthesized including Gd-DTPA-NWAE, Gd-NWAE-DTPA-NWAE, Gd-DTPA-Asn, and Gd-Asn-DTPA-Asn. T1 times were measured by NMR and MRI to determine the relaxivity of each compound. Recombinant mouse legumain was expressed and purified from Sf9 insect cells as well as overexpressed in HEK-293 cells. The activity of recombinant legumain was characterized using model substrates such as Z-AAN-AMC and neurotensin. Legumain was incubated with Gd-DTPA-NWAE in an attempt to activate the procontrast agent. The relaxivities of Gd-DTPA-Asn and Gd-Asn-DTPA-Asn were slower than that of the parent compound, but still faster than the relaxivities of the tetrapeptide-DTPA conjugates by 1.5-2.5-fold. Recombinant mouse legumain from Sf9 insect cells was catalytically active as evidenced by the hydrolysis of the model

substrates, Z-AAN-AMC and neurotensin. However, there was no detectable hydrolysis of Gd-DTPA-NWAE by legumain possibly due to steric hindrance. Furthermore, HEK-293 cells stably expressing legumain were only able to hydrolyze Z-AAN-AMC to a limited extent, suggesting legumain may not have sufficient activity for prodrug activity *in vivo*. Despite the lack of activation of Gd-DTPA-NWAE, we have shown a peptide procontrast agent to be a feasible concept for monitoring enzymatic activity.

3.2 Introduction

To date, many researchers have focused on developing prodrugs to improve the bioavailability of poorly absorbed drugs. Often these prodrugs are activated prior to reaching systemic circulation and so behave similarly to an i.v. injection of the parent compound. A prodrug would be dosed in its inactive form and would be activated upon enzymatic cleavage prior to reaching the target tissue, as was the case for Val-Ser-cHPMPC discussed in Chapter 2. Drug-induced toxicity is a major side effect of many drugs; the concept of targeting the drug to the site of action has been proposed to get around this issue. To take this idea one step further would be to make a prodrug which is inactive until acted upon by enzyme(s) at the target site. While this does not guarantee absolute specificity, it should result in a higher concentration of active drug at the target site and reduced toxicity to non-target cells. One of the biggest hurdles of this strategy is identifying appropriate enzymes to target, which are either greatly overexpressed or solely expressed at the target tissue. Once an enzyme has been identified and a prodrug has been developed it can be difficult to monitor the efficacy using endpoints alone. Also, in order to determine which patients would benefit most from this kind of prodrug therapy requires knowing the activity of the target enzyme. A proimaging agent, that is

an imaging agent that produces little to no signal until acted upon by the target enzyme, is one way to determine enzyme activity *in vivo* in a noninvasive manner. For example, monitoring the activity of an enzyme that is overexpressed in metastatic tumors is one way to use the proimaging agent as a diagnostic tool, as it is currently very difficult to locate metastatic tumors in the early stages. Furthermore, it can be very difficult to treat metastatic tumors, so an imaging agent that is activated at the tumor site can give very good insight as to what prodrug will be most effective for treatment, or alternatively the imaging agent may deliver the drug itself. Finally, during or after treatment the proimaging agent can be used to monitor the effectiveness of the treatment. It is foreseeable that a proimaging agent can be useful both in the research setting to aid in the design of prodrugs and in the clinical setting as a diagnostic tool and to monitor treatment.

There are many enzymes that potentially could be targeted by this approach for the treatment of a variety of diseases including, but not limited to, cancer, arthritis, inflammation, and cardiovascular disease. For example, in the case of inflammation, leukocytes are recruited to the site. Serine proteases such as cathepsin G, neutrophil elastase, and proteinase 3 are expressed exclusively in mature neutrophils (*1*). It is not necessary for these enzymes to be expressed at high levels in each individual cell because accumulation of neutrophils at the site of inflammation will lead to high enzyme concentrations within the target area. Dipeptidyl peptidase I (DPPI) is a lysosomal cysteine protease believed to be responsible for the activation of the previously listed serine proteases (*2*). By targeting DPPI it may be possible to treat inflammation earlier in the process.

More recently the cysteine endopeptidase legumain has been the target of anticancer prodrugs. Legumain is a lysosomal protease found sparsely in most tissues with the highest expression in kidney followed by liver and spleen (*3-5*). However, when tumor tissues were analyzed immunohistochemically with anti-legumain anti-sera, legumain was found to be highly expressed in a broad range of tumor tissues including prostate carcinoma, breast carcinoma, colon carcinoma, and all tested central nervous system malignancies (*5*). While legumain is normally localized to the lysosome, it also has been shown to be present in membranous vesicles at the invadopodia of tumor cells and associated with the cell surface (*5*). Similar to other lysosomal endopeptidases such as cathepsins B and L, legumain has been shown to be stable in the pH range 4.2-5.5, with stability decreasing sharply above pH 6.0 (*3*). Curiously, when assayed *in vitro* at 25°C, the enzyme was more stable and had maximal activity at pH 6.4 (*3*). Tumor tissue tends to be more acidic than normal tissue; extracellular tumor pH has been shown to be as low as 5.5, but on average ranges from pH 6.9 to 7.2 (*6-8*). Therefore, legumain would be active outside the cell in the acidic microenvironment of the tumor, but highly unstable in most cases. The presence of extracellular legumain in a variety of tumor types led researchers to develop the prodrug legubicin, which consists of the tetrapeptide Ala-Ala-Asn-Leu attached to the amino group of doxorubicin (*5*). Legubicin was cell-impermeant until the Ala-Ala-Asn tripeptide was cleaved extracellularly by legumain (*9*). This is a successful example in which the prodrug showed greater efficacy and reduced toxicity as compared to the parent compound (*5, 9*). In this particular case they were able to visualize doxorubicin localization in cell culture fluorometrically ($470_{ex}/590_{em}$ nm), but not all drug compounds can be imaged directly. Furthermore, the excitation

wavelength for doxorubicin is in the blue-green range, which can cause cell damage and has high background *in vivo* due to scattering and cellular autofluorescence, making it less than ideal for imaging (*10, 11*). Therefore, the creation of enzyme-targeted imaging agents can aid in the monitoring of enzyme-activated prodrugs.

Overexpression of legumain by tumor cells appears to be stress-induced, as it is undetectable in cultured cancer cells under normal conditions and its expression is elevated in serum-starved conditions and in xenografts (5). This highlights the importance of determining enzyme activity *in vivo* for two reasons; the enzyme may be less active or less expressed *in vivo*, and furthermore, not all tumors result in overexpression of legumain, so an accurate determination of activity in patients would be necessary to prescribe treatment. As a solution to this problem, we propose a MRI (magnetic resonance imaging) contrast agent that will be activated in a similar manner to the prodrug legubicin. Activation of the contrast agent can be used to non-invasively monitor enzyme activity using whole-body imaging. Not only will this allow us to monitor activity at the target site, but we will also be able to monitor off-target activation. A similar contrast agent was developed by Moats, et al. (*12*) that targeted the non-mammalian enzyme β-galactosidase. In their system a galactopyranosyl ring was attached to a gadolinium chelating agent. The chelating agent occupies eight of the nine coordination sites of gadolinium (Gd^{3+}) and the galactopyranose ring blocks the ninth coordination site. Cleavage of the galactopyranose ring from the chelating agent by β-galactosidase allows water protons to interact with the ninth coordination site of Gd^{3+} which results in an increased T_1 relaxation time and an increased MR signal. They were able to use this contrast agent to follow the expression of the β-galactosidase gene in

Xenopus laevis embryos (*13*). However, there were three potential caveats to their model system. Because this is not an endogenous enzyme there would be very little off-target activation, thus inherently biasing the results in favor of selectivity. Secondly, because β-galactosidase mRNA was directly injected into the cells the expression levels may have been significantly higher than in the case of an endogenous enzyme. Thirdly microinjection, which was used to deliver the contrast agent to the cells,is generally not a good delivery option for whole-body imaging, which is why we have chosen to target an enzyme that is present extracellularly. Furthermore, the use of a membrane-impermeant proimaging agent should help to prevent off-target activation by intracellular enzymes. In the future, it may be possible to use a delivery system such as liposomes to allow targeting of intracellular enzymes.

Previously our laboratory has developed prodrugs by attaching amino acids which can be cleaved by proteases to activate the drug. To continue along these lines the imaging agents will also have peptides attached to them in the inactive state. Upon reaching the target tissue, overexpressed enzyme(s) such as legumain (*5*) at the site will recognize the peptide sequence and activate the imaging agent as shown in Figure 3.1. The MRI contrast agent gadolinium-diethylenetriamine pentaacetic acid (Gd-DTPA) has been approved for use in humans since 1988 (*14*). We have attached a tetrapeptide to Gd-DTPA to block the ninth coordination site of Gd^{3+}, hence blocking the ability of Gd^{3+} to interact with water and affect signal intensity. This tetrapeptide Gd-DTPA contrast agent has a slower T1 time than the activated single amino acid Gd-DTPA conjugate.

3.3 Methods

3.3.1 Conjugation of Asn to DTPA

Diethylenetriamine pentaacetic acid (DTPA) was purchased from Fluka and Boc-L-asparagine was purchased from Novabiochem. A benzyl protection group was added to the C-terminus followed by the removal of the Boc-protecting group. 100 mg (0.28 mmol) of DTPA was dissolved in 5 ml anhydrous *N*,*N*-dimethylformamide (DMF) and stirred at 0°C. Benzyl asparagine (Asn-Bzl) (52 mg, 0.23 mmol) was dissolved in DMF and slowly added to the DTPA solution followed by the addition of triethylamine (TEA) (320 µl, 2.3 mmol) with continued stirring at 0°C for 30 min under argon gas. The reaction was then quenched with 2 ml water and rotovaporized. Compounds were purified using a Hypersep C18 column (10 g/75 ml, Thermo Scientific, 60108-703) with 0.5% acetonitrile in water (0.1% TFA) and increasing the gradient to 5% acetonitrile (0.1% TFA) over 150 ml, collecting 10 ml fractions. The gradient was then increased to 15% ACN (0.1% TFA) over the next 70 ml, while collecting 10 ml fractions. Fractions were then analyzed by mass spectroscopy in ES^- mode to determine fractions containing the bi-derivative (m/z = 800.4 +14) and the mono-derivative (m/z = 596 +14, +28). Samples were then dried on the rotovaporizer and NMR and MS were performed to confirm purity. There was ~27% yield of the bi-derivative and ~4% yield of the mono-derivative. For the benzyl group de-protection, the compounds were dissolved in anhydrous methanol and palladium, 10% (w/w) on activated carbon with a drop of acetic acid. The reaction was stirred for 30 min at room temperature under hydrogen gas. Purity of the compounds were again confirmed by NMR and MS in ES^- mode; Asn-DTPA-Asn (m/z = 620.3) and Asn-DTPA (m/z = 506.2). To chelate the gadolinium, 10

mM solutions of DTPA-Asn, Asn-DTPA-Asn and gadolinium chloride ($GdCl_3$) in water were made. $GdCl_3$ was slowly added to the solution containing the chelate while simultaneously adding 1 M sodium hydroxide to maintain the pH ~7. Upon addition of all of the $GdCl_3$, the pH was adjusted to 7.3 and the solution was concentrated by rotovaporization and filtered through a 0.22 μm PTFE filter followed by lyophilization for 24 hrs. Mass spectroscopy in ES^- mode was done to confirm the presence of the complex, (m/z = 569, MW +Na).

3.3.2 Conjugation of NWAE to DTPA

The tetrapeptide Asn-Trp-Ala-Glu-OH was custom synthesized by Genscript Corp. The tetrapeptide (NWAE, 20 mg, 0.0286 mmol) was dissolved in 2 ml anhydrous DMF and added to a stirring solution of DTPA (12.3 mg, 0.034 mmol) in anhydrous DMF (dimethylformamide) at 0°C followed by the addition of 120 μL (0.86 mmol) TEA. The reaction was stirred for 2 hr at 0°C under argon gas, then quenched by the addition of water. The reaction mixture was purified on a Hypersep C18 column (10 g/75 ml) from Thermo Scientific (60108-703) starting with 100% water (0.1% TFA) and increasing the gradient to 100% ACN in 10 ml increments. Fractions were then analyzed by mass spectroscopy in ES^- mode to determine fractions containing the mono-derivative (m/z = 567) and the bi-derivative (m/z = 508). Samples were then dried on the rotovaporizer and NMR and MS were performed to confirm purity. To chelate the gadolinium, 1 mM solutions of DTPA-NWAE, NWAE-DTPA-NWAE, and gadolinium chloride ($GdCl_3$) in water were made. $GdCl_3$ was slowly added to the solution containing the chelate while simultaneously adding 1 M sodium hydroxide to maintain the pH >7. Upon addition of all of the $GdCl_3$, the pH was adjusted to 7.3 and the solution was concentrated by

rotovaporization and filtered through a 0.22 μm PTFE filter followed by lyophilization for 24 hrs.

3.3.3 Conjugation of Lys-OMe to DTPA

Carboxybenzyl-lysine with a methyl protection group on the C-terminus (Z-Lys-OMe) was purchased from Bachem. 100 mg (0.28 mmol) of DTPA was dissolved in 5 ml anhydrous DMF and stirred at 0°C. Z-Lys-OMe•HCl (83.4 mg, 0.252 mmol) was dissolved in DMF and slowly added to the DTPA solution followed by the addition of TEA (400 μl, 2.8 mmol) with continuous stirring at 0°C and further stirred for 15 min under argon gas. The reaction was then quenched with 2 ml water and rotovaporized. Compounds were purified using a Hypersep C18 column (10 g/75 ml) with a methanol: 0.1 M triethylacetic acid (TEAA) gradient. Fractions were then analyzed by mass spectroscopy in ES^+ mode to determine fractions containing the bi-derivative (m/z = 946) and the mono-derivative (m/z = 669). The mono-derivative eluted at 40% methanol and 60% TEAA while the bi-derivative eluted at 60-70% methanol and 40-30% TEAA. Samples were then dried on the rotovaporizer and NMR and MS were performed to confirm purity. There was ~60% yield of the bi-derivative and ~10% yield of the mono-derivative. For the carboxybenzyl group de-protection, the Z-Lys-OMe-DTPA-Z-Lys-OMe was dissolved in 5 ml anhydrous methanol and palladium, 10% (w/w) on activated carbon with a drop of acetic acid. The reaction was stirred for 2 hrs at room temperature under hydrogen gas. Purity of the compounds was again confirmed by NMR and MS in ES^+ mode; Lys-OMe-DTPA-Lys-OMe (m/z = 677). To chelate the gadolinium, 10 mM solutions of Lys-OMe-DTPA-Lys-OMe and gadolinium chloride ($GdCl_3$) in water were made. $GdCl_3$ was slowly added to the solution containing the chelate while

simultaneously adding 1 M sodium hydroxide to maintain the pH ~7. Upon addition of all of the $GdCl_3$, the pH was adjusted to 7.3 and the solution was concentrated by rotovaporization and filtered through a 0.22 μm PTFE filter followed by lyophilization for 24 hrs.

3.3.4 Determination of free gadolinium

The method of Barge, et al. (*15*) was used to determine the amount of free gadolinium after complexation. Briefly, a 12 μg/ml solution of xylenol orange (Fluka) was prepared in 50 mM acetate buffer, pH 5.8. To generate a standard curve, 0-50 μM dilutions of the gadolinium atomic absorption standard solution (Sigma-Aldrich) were made in 50 mM acetate buffer, pH 5.8. The absorbance was measured at 433 nm and 573 nm and the ratio A_{573}/A_{433} was plotted versus the concentration of gadolinium. Dilutions of the contrast agents were prepared (0 – 2 mM) and absorbance at 433 nm and 573 nm was measured in the presence of xylenol orange solution and the concentration of free gadolinium was calculated from the standard curve.

3.3.5 Relaxivities of contrast agents in NMR

Gd-DTPA was purchased from Sigma-Aldrich to be used as a positive control and deionized water was used as the negative control. Solutions of 0.1 mM to 5 mM Gd-DTPA analogues in deionized water were prepared. Samples were loaded into coaxial insert NMR tubes with a 60 μL internal capacity. Deuterated chloroform ($CdCl_3$) (Cambridge Isotope Laboratories) was loaded in the outer tube for external locking. T1 relaxation times were measured on a Bruker Avance DRX-500 NMR spectrometer with an 11.75 Tesla field strength magnet and a 1H NMR frequency of 500 MHz by an inversion-recovery sequence with *tau* equal to 1, 5,10, 20, 30, 40, 50, 100, 500, and 1000

ms. T1 was calculated using TopSpin (Bruker Biospin). The relaxation rate is equal to 1/T1 (s^{-1}). The relaxation rates were plotted against the concentration of the contrast agent. The slope of the best-fit line for the data is equal to the relaxivity ($mM^{-1}s^{-1}$) of the contrast agent.

3.3.6 Relaxivities of contrast agents in MRI

Solutions of 0.1 mM to 4 mM DTPA analogues were prepared in deionized water. T1 of these solutions were determined using a small animal MRI (GE 7T). T1 was measured by an inversion recovery fast spin echo imaging sequence using inversion times of 50, 100, 500, 800, 1200, and 2500 ms, an echo time (TE) of 12 ms, and an echo train length of 8 at a repeat time (TR) of 6000 ms. All images were obtained from a single axial slice, 0.5 mm slice thickness. T1 for each solution and deionized water were calculated using the RT Image software. The relaxivity (R1) value was calculated from the slope of the plot of (1/T1, solution – 1/T1, water) versus the equivalent concentration of Gd-DTPA analogues.

3.3.7 Subcloning of legumain

All restriction enzymes were purchased from New England Biolabs. *Mus musculus* legumain cDNA (mLGMN, Accession # BC132515) in pCR4-TOPO was ordered from Open Biosystems. mLGMN cDNA was amplified using the primers 5'-CCTAGTGCTA GCGAC-3' and 5'CCTTGCTAGAGCTCTTGTAGTGACTAAGACA CACTTTGTCC-3' (Integrated DNA Technologies). The PCR product and the vector pET-28a were double digested with the restriction enzymes NheI and SacI and ligated using T4 DNA ligase (New England Biolabs). Digested mLGMN-pET-28a with BlpI and the vector pFastBac (containing a secretion signal peptide, MDPPRPALLALLALPA

LLLLLLAGA RAE) with NotI and filled in the 5'-overhangs with T4 DNA polymerase (New England Biolabs). mLGMN-pET-28a and pFastBac were further digested with NdeI. His-mLGMN and pFastBac were purified in an agarose gel. Following gel extraction using a QIAEX II gel extraction kit (QIAGEN), His-mLGMN and pFastBac were ligated using T4 DNA ligase. DNA sequence in pFastBac was verified by dideoxy sequencing (University of Michigan Sequencing Core).

3.3.8 Recombinant legumain expression and purification

His-mLGMN-pFastBac was transposed into DH10Bac competent cells by heat shock and streaked on LB Agar plates containing 50 μg/ml kanamycin, 7 μg/ml gentamicin, 10 μg/ml tetracycline, 100 μg/ml Bluo-gal, and 40 μg/ml IPTG. The plate was incubated inverted for 24-48 hrs at 37°C. White colonies were selected to inoculate liquid cultures of LB Broth containing 50 μg/ml kanamycin, 10 μg/ml tetracycline, and 10 μg/ml gentamycin and incubated overnight on a shaker (230 rpm) at 37°C. Bacmid DNA was isolated using the protocol as described in the Bac-to-Bac® Baculovirus Expression System manual by Invitrogen. Transfection of Sf9 insect cells with the recombinant bacmid DNA and infection of insect cells with recombinant baculovirus particles were also done according to the same manual. A titer of 1×10^8 pfu/ml was assumed after two rounds of amplification and an MOI of 0.5 pfu/ml was selected. Cells and media were harvested 96 hours after infection for protein purification.

To purify the secreted legumain protein, cells and media were centrifuged at 9100 $\times g$ for 15 min at 4°C. The supernatant was collected and filtered with 0.22 μm cellulose acetate membrane. A filtration cartridge was used to exchange the media with wash buffer (50 mM sodium phosphate, 300 mM sodium chloride, and 20 mM imidazole, pH

8.0). The supernatant was then incubated overnight with Ni-NTA resin, which had previously been equilibrated in wash buffer. The resin was then washed with ~100 column volumes of wash buffer before eluting with 50 mM sodium phosphate, 300 mM sodium chloride, 250 mM imidazole, pH 8.0. The purified protein was then dialyzed in 25 mM Tris and 0.15 M sodium chloride, pH 7.5. Protein concentration was determined using the Pierce BCA assay (Thermo Fisher Scientific). A sample was run in a 4-12% Bis-Tris gel and stained with Krypton™ Protein Stain (Thermo Fisher Scientific) according to manufacturer's protocol to determine the relative purity of the protein. Protein aliquots were stored at -80°C until needed for activity assays.

3.3.9 Legumain hydrolysis of Z-AAN-AMC

Recombinant mouse legumain (50 µg/ml) was auto-activated by incubation in 100 mM NaOAc, 0.1 M NaCl (pH 4.5) at 37°C for 4 hrs. Legumain was then diluted to 1 µg/ml in 50 mM MES, 0.25 M NaCl (pH 5.5) and Z-Ala-Ala-Asn-AMC was added at a final concentration of 12.5 – 100 µM. Fluorescence ($400_{ex}/508_{em}$ nm) was measured every 3 min for 1 hr in a BioTek Synergy HT plate reader with an internal temperature of 37°C. The concentration of free AMC was calculated from fluorescence values and plotted against time. The linear portion of the curve was used to calculate the initial velocity of hydrolysis (nmol/min). GraphPad Prism 4.0 was used to determine the kinetic constants K_m and V_{MAX}.

3.3.10 Legumain hydrolysis of neurotensin and NWAE

Recombinant mouse legumain (50 µg/ml) was auto-activated by incubation in 100 mM NaOAc, 0.1 M NaCl (pH 4.5) at 37°C for 4 hrs. As a negative control, legumain was heat-inactivated (HI-lgmn) at 90°C for 10 min. Legumain and HI-lgmn were then

diluted to 1 μg/ml in 50 mM MES, 0.25 M NaCl (pH 5.5). Then, 50 μM or 100 μM neurotensin peptide (Glp-Leu-Tyr-Glu-Asn-Lys-Pro-Arg-Arg-Pro-Tyr-Ile-Leu) or 1 mM NWAE peptide (Asp-Trp-Ala-Glu-OH) was added. Neurotensin samples were incubated overnight and NWAE peptides were incubated 2 hrsat room temperature overnight and then spun through 96-well 0.45 μm polyvinylidene difluoride (PVDF) membranes (Unifilter, Whatman) at 1,800 × *g* in a Jouan MR 22i tabletop centrifuge cooled to 4°C to remove legumain before HPLC analysis. The HPLC system (Waters) consisted of a reverse-phase column (XTerra RP18, 5 μm, 4.6 x 250 mm), a 515 pump, a 996 Photodiode Array UV detector and a 717 Plus Autosampler. The remaining NWAE peptide, full-length neurotensin, and the production of Glp-Leu-Tyr-Glu-Asn and Lys-Pro-Arg-Arg-Pro-Tyr-Ile-Leu were analyzed using a mobile phase consisting of an acetonitrile (0.1% TFA) gradient (2-52%) mobile phase with a flow rate of 1 ml/min and detection at 274 nm. Peaks were collected and further analyzed by mass spectroscopy in ES^+ mode.

3.3.11 Enzymatic hydrolysis of Gd-DTPA-NWAE

Recombinant mouse legumain (50 μg/ml) was auto-activated as described above (3.3.10). As a negative control, legumain was heat-inactivated (HI-lgmn) at 90°C for 10 min. Legumain or HI-lgmn was then diluted to 1 μg/ml in 50 mM MES, 0.25 M NaCl (pH 5.5), Gd-DTPA-NWAE was added at a final concentration of 1 mM and samples were incubated at room temperature overnight. The T1 times of the samples were measure as described above.

3.3.12 HEK-293 cells overexpressing legumain

HEK-293 cells stably expressing legumain (HEK-LEG) were a generous gift from

Dr. G. David Roodman from the University of Pittsburgh. Cells were maintained in Dulbecco's Modified Eagle Medium (DMEM, Gibco/Invitrogen) containing 10% heat-inactivated fetal bovine serum (HI-FBS) in a 37°C incubator with 5% CO_2 and 90% humidity. Cells were washed and collected in PBS (pH 7.4) and pellets were stored at -20°C until analysis. Protein concentration was determined using the Pierce BCA assay (Thermo Fisher Scientific).

3.3.13 Hydrolysis of Z-AAN-AMC by HEK-LEG cells.

Lysed HEK-293 or HEK-LEG cells (65 mg/ml protein) were incubated with 100 μM Z-AAN-AMC in 50 mM MES, 0.25 M NaCl (pH 5.5) for 2 hrs at 37°C. HEK-LEG cells were seeded at a density of 50000 cells per well in a black wall, clear bottom 96-well plate. Prior to adding 100 μM Z-AAN-AMC, media was replaced with 100 μL of 10 mM Hepes, 100 mM NaCl (pH 7.4) or 50 mM MES, 0.25 M NaCl (pH 5.5). Fluorescence ($400_{ex}/508_{em}$ nm) was measured every 3 min for 2 hrs in a BioTek Synergy HT plate reader with an internal temperature of 37°C. The concentration of free AMC was calculated from fluorescence values and plotted against time.

3.4 Results

3.4.1 Synthesis and characterization of procontrast agents

Gd-DTPA-Asn and Gd-Asn-DTPA-Asn were synthesized and purified according to the scheme shown in Figure 3.2. The tetrapeptide NWAE was conjugated to Gd-DTPA and the mono- and bi-derivatives were purified according to the scheme shown in Figure 3.3. Mass spectrometry confirmed the structures of the DTPA conjugates, which were then complexed with $GdCl_3 \bullet 6H_20$. The free gadolinium concentration was determined to be minimal (<2%) using the xylenol orange assay. T1 times of 0.5 to 5

mM solutions of the contrast agents were measured in NMR and MRI and used to calculate the relaxivities of the compounds, shown in **Error! Reference source not ound.**. Gd-DTPA had the fastest R_1 (4.59 mM^{-1} s^{-1} in NMR and 6.971 mM^{-1} s^{-1} in MRI), while Gd-DTPA-NWAE had the slowest R_1 (0.846 mM^{-1} s^{-1} in NMR and 1.588 mM^{-1} s^{-1} in MRI). The relaxivities of Gd-DTPA-Asn and Gd-Asn-DTPA-Asn were slower than that of Gd-DTPA (1.73 mM^{-1} s^{-1} and 2.75 mM^{-1} s^{-1} in NMR, respectively). While the absolute values for the relaxivities of the compounds in NMR and MRI were not the same, the ratio of relaxivities between the tetrapeptide conjugates and single amino acid metabolites were similar in both, with ratios >1.5 (Figure 3.4) and should be sufficient to observe signal enhancement upon activation *in vivo*.

3.4.2 Production and characterization recombinant legumain

Recombinant mouse legumain with a C-terminal His-tag was subcloned and transfected in Sf9 insect cells to produce secreted His-tagged legumain. His-lgmn was purified to >98% purity using Ni-NTA agarose (Qiagen). The legumain precursor with His-tag had a molecular weight of ~50 kDa, while the autocatalytically activated legumain had a molecular weight of ~35 kDa as shown in Figure 3.5. The activity of the recombinant legumain was analyzed using the model substrate benzoylcarbonyl-L-alanyl-L-alanyl-L-asparagine-4- methylcoumaryl-7-amide (Z-AAN-AMC). Recombinant mouse legumain had a K_m value of 0.04 ± 0.015 mM, a V_{MAX} of 797 ± 136 nmol/min•mg protein, and a k_{cat} value of 44.8 min^{-1}.

To confirm the specificity of recombinant mouse legumain for asparagine in the P1 position, recombinant lgmn was incubated with the peptide neurotensin (Glp-Leu-Tyr-Glu-Asn-Lys-Pro-Arg-Arg-Pro-Tyr-Ile-Leu). HPLC and MS analysis confirmed that

neurotensin was cleaved into two fragments by lgmn, Glp-Leu-Tyr-Glu-Asn (m/z = 649) and Lys-Pro-Arg-Arg-Pro-Tyr-Ile-Leu (m/z = 521, z = 2), while only full-length neurotensin (m/z = 837, z = 2) was detectable when incubated with heat-inactivated legumain (data not shown). NWAE peptide was incubated with legumain or heat-inactivated legumain and analyzed by HPLC. There was no detectable hydrolysis of NWAE in either sample (data not shown).

3.4.3 Legumain incubated with procontrast agent

Gd-DTPA-NWAE was incubated with legumain or heat-inactivated legumain and T1 times were measured by NMR. There were no differences in the T1 times for the contrast agent incubated with legumain or heat-inactivated legumain at the concentrations tested (data not shown). Furthermore, T1 times of the the procontrast agent in the presence of buffer and protein were different than those seen in pure water.

3.4.4 Legumain activity in whole cells

The hydrolysis of Z-AAN-AMC was tested in cell lysates and whole cells of HEK-293 cells stably overexpressing legumain. Though Z-AAN-AMC seemed to be specifically activated by legumain, the extent of hydrolysis was nominal. While, there was ~10-fold greater hydrolysis of Z-AAN-AMC by HEK-LEG cell lysates compared to HEK-293 cell lysates, there was still very little hydrolysis overall (0.035 nmol vs 0.35 nmol in 2hrs). Similarly, HEK-LEG whole cells hydrolyzed Z-AAN-AMC to a greater extent in acidic buffer (1.8%) compared to whole cells in neutral buffer (<0.4%).

3.4.5 Synthesis and characterization of an alternative procontrast agent

After determining Gd-DTPA-NWAE could not be significantly activated by legumain, an alternative procontrast agent was proposed wherein the N-terminal of

asparagine was no longer conjugated to DTPA. One way to accomplish this is through the conjugation of the side chain of lysine to DTPA. Furthermore, this would allow amino acids to be attached to the N- or C-terminal of lysine to target different proteases. The epsilon amine group of lysine was conjugated to DTPA to form Gd-Lys-OMe-DTPA-Lys-OMe as shown in Figure 3.6. The relaxivity of this compound was determined to be 3.7445 mM^{-1} s^{-1} by NMR.

3.5 Discussion

The procontrast agents Gd-DTPA-NWAE, Gd-NWAE-DTPA-NWAE and their proposed metabolites, Gd-DPTA-Asn and Gd-Asn-DTPA-Asn, were successfully synthesized and purified. The relaxivities of these contrast agents as well as the parent compound, Gd-DTPA, were determined by both NMR (11.75T) and MRI (7T) because the relaxivity is specific to the magnetic field strength, with MRI generally being lower strength than NMR. The ratio of the relaxivities between the single amino acid conjugates and tetrapeptide conjugates of Gd-DTPA were greater than 1.5 in NMR and MRI. Louie et al. found that a 3-fold difference in relaxivities of their cleaved and uncleaved contrast agent, EgadMe, resulted in a 57% enhancement in signal intensity *in vivo* (*13*). This suggests that there would be a detectable difference between the tetrapeptide contrast agent and the single amino acid metabolite *in vivo*.

Groups previously working with legumain used biochemically purified legumain from tissue sources or overexpressed the protein in transfected mammalian cells for purification (*3, 4, 16-18*). We successfully expressed full-length mouse preprolegumain with a C-terminal His-tag and an N-terminal secretion signal in Sf9 insect cells. The work of Chen et al. hypothesized that mouse legumain autocatalytically activates after

Asp-27, leaving Gly-28 as the first amino acid of the mature form (*4*). The size difference between the prolegumain and mature legumain suggests that there is also post-translational processing at the C-terminus, as is the case with legumain in other species (*17, 18*). The shift in gel electrophoretic mobility between the preprolegumain and the legumain incubated in acidic buffer, suggests that the recombinant mouse legumain is able to autocatalytically activate.

To further confirm that the recombinant mouse legumain produced by Sf9 insect cells was catalytically active, we determined the kinetic constants for legumain with the model substrate Z-AAN-AMC. The calculated values for recombinant legumain expressed by Sf9 cells were similar to those of legumain from other species (*3, 17, 19*). Recombinantly expressed legumain was also able to hydrolyze the peptide neurotensin, as has been previously reported for pig legumain (*3*). The recombinant legumain was not able to hydrolyze the tetrapeptide NWAE. This was not unexpected, as Dando et al. found that legumain requires a minimum of two amino acids N-terminal of the P1 asparagine for activity and prefers a blocking group on the N-terminus (*16*).

When Gd-DTPA-NWAE was incubated with legumain or heat-inactivated legumain there was no difference in the T1 times measured by NMR. Most likely, Gd-DTPA-NWAE is not being hydrolyzed by legumain to Gd-DTPA-Asn, or the extent of hydrolysis is too insignificant to detect, possibly due to steric hindrance of DTPA in the P2 position or an insufficient number of amino acids N-terminal of Asn. Furthermore, there was minimal hydrolysis of Z-AAN-AMC when incubated with either intact HEK-LEG cells or lysates. Taken together, the evidence suggests that legumain is not the ideal target enzyme for our procontrast agent. Despite promising NMR results with Gd-

DTPA-NWAE, Gd-DTPA-Asn, and Gd-DTPA-Lys-OMe, a procontrast agent targeted to legumain was not pursued further due to insufficient legumain activity. The differences in relaxivities between the tetrapeptide contrast agent and the single amino acid contrast agent are encouraging; thus it would be worthwhile to pursue a peptide procontrast agent with a new enzymatic target and peptide sequence and possibly the use of a linker such as Lys-OMe or propanediamine to overcome issues of steric hindrance.

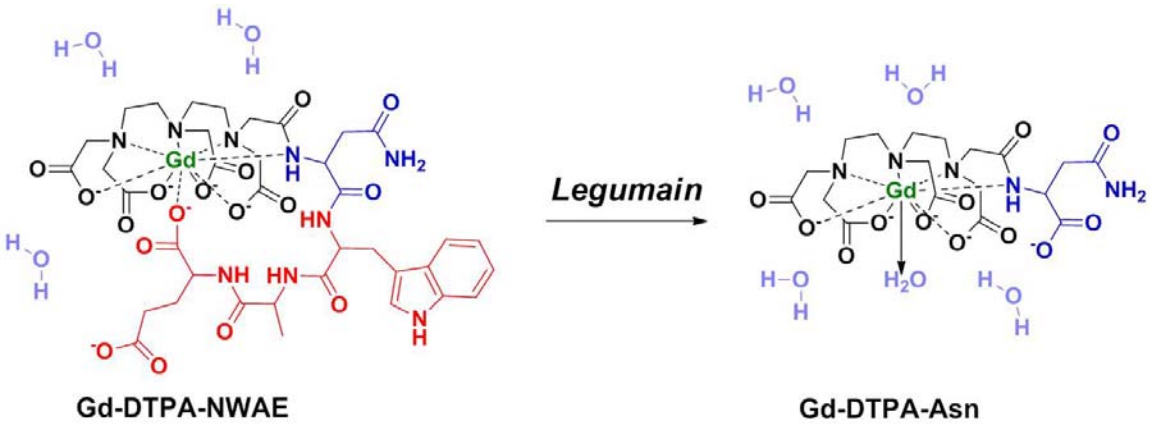

Figure 3.1 Proposed bioactivation of Gd-DTPA-NWAE

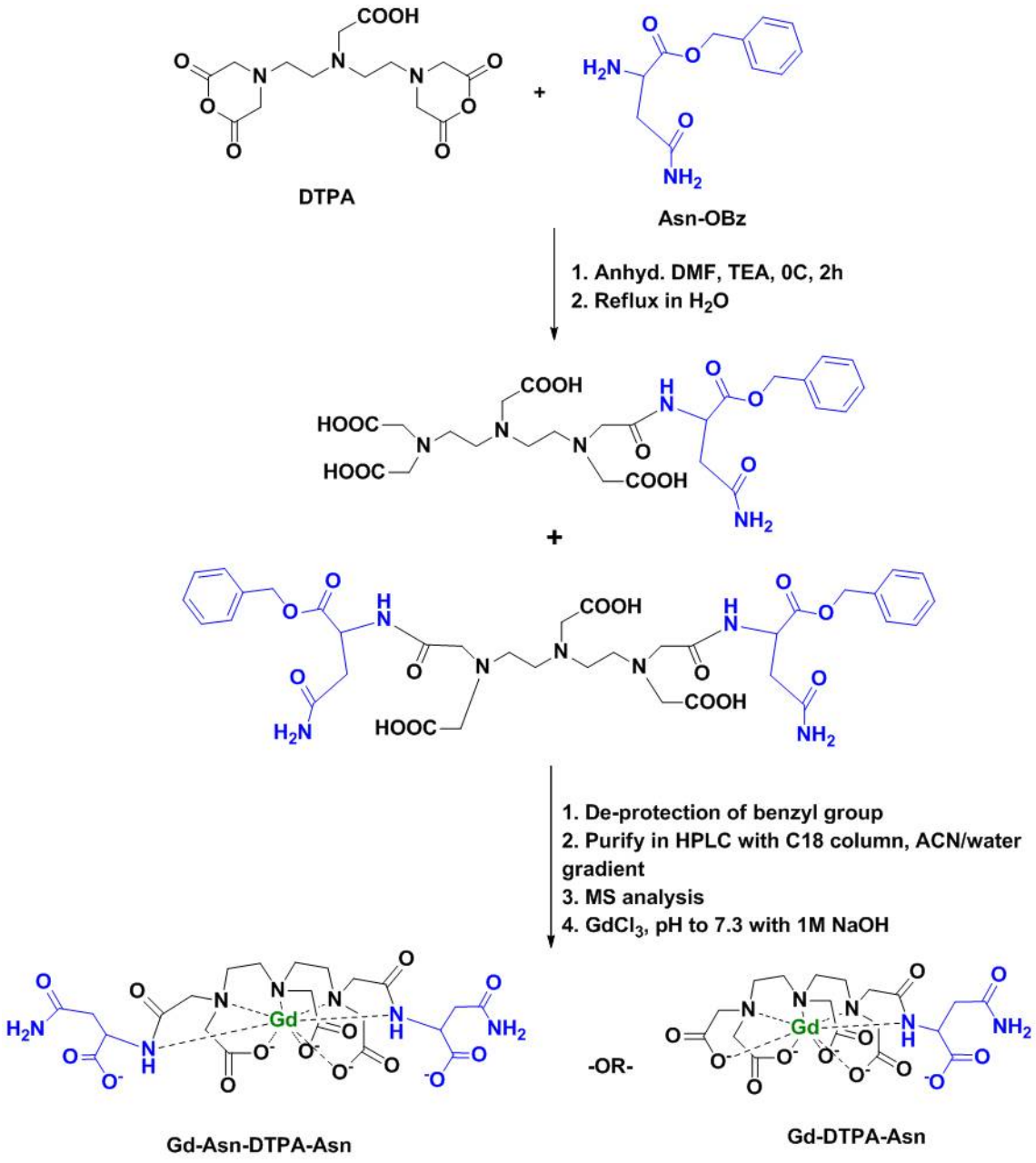

Figure 3.2 Synthesis Scheme for Gd-DTPA-Asn and Gd-Asn-DTPA-Asn

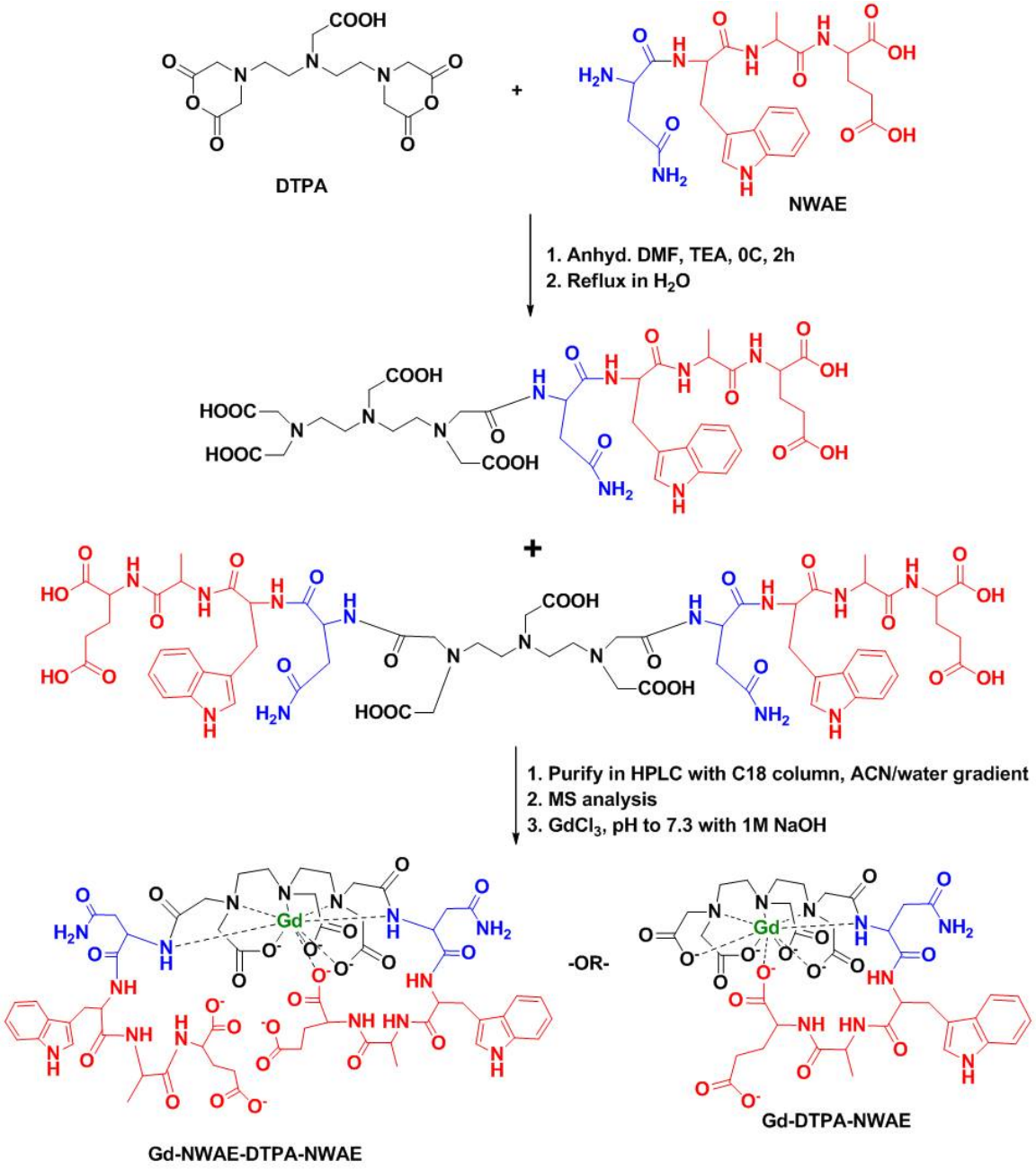

Figure 3.3 Synthesis scheme for Gd-DTPA-NWAE and Gd-NWAE-DTPA-NWAE

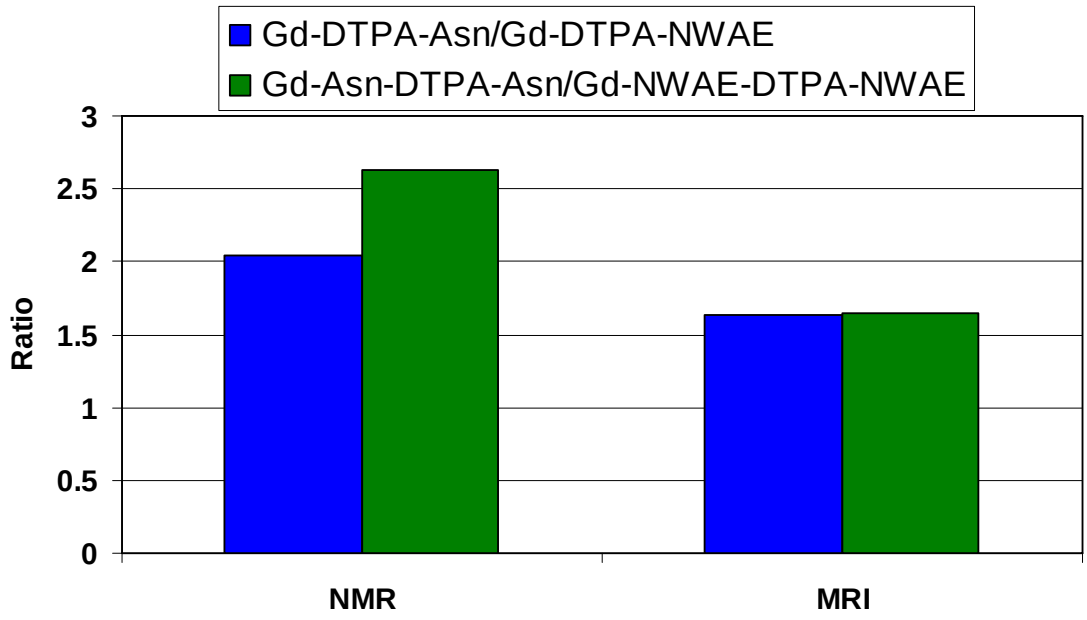

Figure 3.4 The relaxivity ratios for Gd-DTPA amino acid and tetrapeptide analogues.
The T1 times for Gd-DTPA-Asn, Gd-DTPA-NWAE, Gd-Asn-DTPA-Asn, and Gd-NWAE-DTPA-NWAE were measured by NMR (11.75T) and MRI (7T) at various concentrations. The inverse T1 times were first plotted against the concentrations to determine the relaxivity (R_1) for each compound. The relaxivities of the single amino acid metabolites were then divided by the relaxivities of the corresponding tetrapeptide contrast agents to obtain the relaxivity ratios shown here. The ratios suggest there would be observable signal enhancement upon activation *in vivo*.

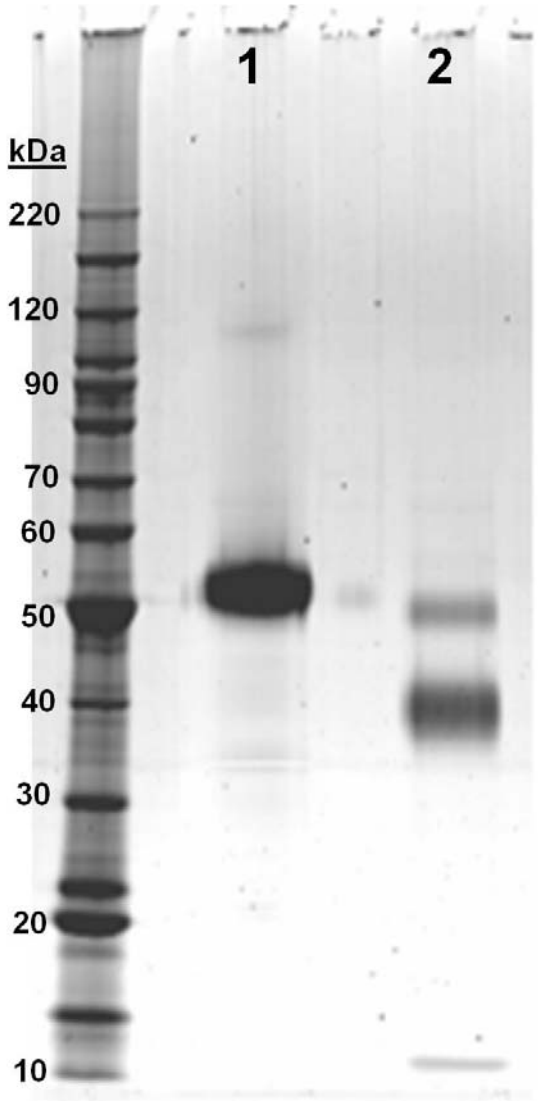

Figure 3.5 Purified recombinant mouse legumain is autocatalytically activated in acidic conditions.
Recombinant mouse legumain was expressed and purified from Sf9 insect cells. A portion of recombinant mouse legumain was incubated in acidic buffer for 4 hrs to allow for autocatalytic activation. His-legumain (lane 1) and activated legumain (lane 2) were run in a 4-12% Bis-Tris gel (Invitrogen) with BenchMark™ Protein Ladder (Invitrogen) to confirm approximate size and purity.

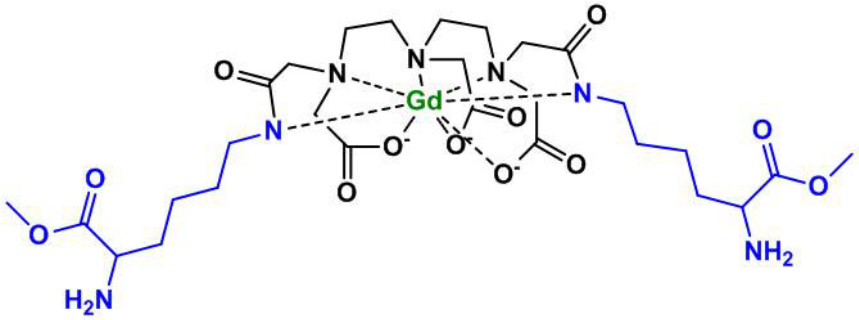

Figure 3.6 Structure of Gd-Lys-OMe-DTPA-Lys-OMe

Table 3.1 Relaxivities (R1) of Gd-DTPA analogues

The T1 times for Gd-DTPA-Asn, Gd-DTPA-NWAE, Gd-Asn-DTPA-Asn, and Gd-NWAE-DTPA-NWAE were measured in NMR (11.75T) and MRI (7T) at various concentrations. The inverse of the T1 times were plotted against the concentration of the compounds and the slope of the best fit line is equal to the relaxivity (R_1) of each compound.

Compounds	Relaxivity (R_1) (mM^{-1} s^{-1})	
	NMR	MRI
Gd-DTPA (synthesized)	4.59	6.971
Gd-Asn-DTPA-Asn	2.75	3.702
Gd-DTPA-Asn	1.73	2.602
Gd-NWAE-DTPA-NWAE	1.046	2.245
Gd-DTPA-NWAE	0.846	1.588

3.6 References

1. Adkison, A. M., Raptis, S. Z., Kelley, D. G., and Pham, C. T. (2002) Dipeptidyl peptidase I activates neutrophil-derived serine proteases and regulates the development of acute experimental arthritis, *J Clin.Invest 109*, 363-371.

2. Pagano, M. B., Bartoli, M. A., Ennis, T. L., Mao, D., Simmons, P. M., Thompson, R. W., and Pham, C. T. (2007) Critical role of dipeptidyl peptidase I in neutrophil recruitment during the development of experimental abdominal aortic aneurysms, *Proc.Natl.Acad.Sci.U.S.A 104*, 2855-2860.

3. Chen, J. M., Dando, P. M., Rawlings, N. D., Brown, M. A., Young, N. E., Stevens, R. A., Hewitt, E., Watts, C., and Barrett, A. J. (1997) Cloning, isolation, and characterization of mammalian legumain, an asparaginyl endopeptidase, *J Biol.Chem. 272*, 8090-8098.

4. Chen, J. M., Dando, P. M., Stevens, R. A., Fortunato, M., and Barrett, A. J. (1998) Cloning and expression of mouse legumain, a lysosomal endopeptidase, *Biochem.J 335 (Pt 1)*, 111-117.

5. Liu, C., Sun, C., Huang, H., Janda, K., and Edgington, T. (2003) Overexpression of legumain in tumors is significant for invasion/metastasis and a candidate enzymatic target for prodrug therapy, *Cancer Res. 63*, 2957-2964.

6. Engin, K., Leeper, D. B., Cater, J. R., Thistlethwaite, A. J., Tupchong, L., and McFarlane, J. D. (1995) Extracellular pH distribution in human tumours, *Int.J Hyperthermia 11*, 211-216.

7. Thistlethwaite, A. J., Leeper, D. B., Moylan, D. J., III, and Nerlinger, R. E. (1985) pH distribution in human tumors, *Int.J Radiat.Oncol.Biol.Phys. 11*, 1647-1652.

8. Vaupel, P., Kallinowski, F., and Okunieff, P. (1989) Blood flow, oxygen and nutrient supply, and metabolic microenvironment of human tumors: a review, *Cancer Res. 49*, 6449-6465.

9. Wu, W., Luo, Y., Sun, C., Liu, Y., Kuo, P., Varga, J., Xiang, R., Reisfeld, R., Janda, K. D., Edgington, T. S., and Liu, C. (2006) Targeting cell-impermeable prodrug activation to tumor microenvironment eradicates multiple drug-resistant neoplasms, *Cancer Res. 66*, 970-980.

10. Baruch, A., Jeffery, D. A., and Bogyo, M. (2004) Enzyme activity--it's all about image, *Trends Cell Biol. 14*, 29-35.

11. Buschmann, V., Weston, K. D., and Sauer, M. (2003) Spectroscopic study and evaluation of red-absorbing fluorescent dyes, *Bioconjug.Chem. 14*, 195-204.

12. Moats, R. A., Fraser, S. E., and Meade, T. J. (1997) A "Smart" Magnetic Resonance Imaging Agent That Reports on Specific Enzymatic Activity, *Angew.Chem.Int.Ed.Engl. 36*, 726-728.

13. Louie, A. Y., Huber, M. M., Ahrens, E. T., Rothbacher, U., Moats, R., Jacobs, R. E., Fraser, S. E., and Meade, T. J. (2000) In vivo visualization of gene expression using magnetic resonance imaging, *Nat.Biotechnol. 18*, 321-325.

14. Gries, H. (2002) Extracellular MRI Contrast Agents Based on Gadolinium, *Topics in Current Chemistry 221*, 2-24.

15. Barge, A., Cravotto, G., Gianolio, E., and Fedeli, F. (2006) How to determine free Gd and free ligand in solution of Gd chelates. A technical note, *Contrast Media Mol Imaging 1*, 184-188.

16. Dando, P. M., Fortunato, M., Smith, L., Knight, C. G., McKendrick, J. E., and Barrett, A. J. (1999) Pig kidney legumain: an asparaginyl endopeptidase with restricted specificity, *Biochem.J 339 (Pt 3)*, 743-749.

17. Halfon, S., Patel, S., Vega, F., Zurawski, S., and Zurawski, G. (1998) Autocatalytic activation of human legumain at aspartic acid residues, *FEBS Letters 438*, 114-118.

18. Li, D. N., Matthews, S. P., Antoniou, A. N., Mazzeo, D., and Watts, C. (2003) Multistep Autoactivation of Asparaginyl Endopeptidase in Vitro and in Vivo, *Journal of Biological Chemistry 278*, 38980-38990.

19. Kembhavi, A. A., Buttle, D. J., Knight, C. G., and Barrett, A. J. (1993) The Two Cysteine Endopeptidases of Legume Seeds: Purification and Characterization by Use of Specific Fluorometric Assays, *Archives of Biochemistry and Biophysics 303*, 208-213.

CHAPTER 4

Determination of differential peptide hydrolysis in whole cells using fluorescence

4.1 Summary

Identification of peptide promoities selectively cleaved in disease tissue such as cancer can be useful in designing target-activated prodrugs. Historically, sequences have been identified using purified proteases; however, there may be changes in protein abundance and/or activity in more complex systems, thus necessitating the development of a whole-cell screening system. The hydrolysis of amino acid sequences from the fluorescent compounds AMC (7-amino-4-methylcoumarin) and ACC (7-amino-4-carbamoylmethylcoumarin) can be monitored in real-time using a fluorescence plate reader without time-consuming sample preparation. In this chapter we demonstrate the ability of AMC conjugates to monitor proteolytic activity of proteases overexpressed in transfected whole cells with known substrates. We then apply this method to identifying peptide sequences differentially hydrolyzed by cancer cells with unknown protease abundances. The differential hydrolysis by peptide sequence was further confirmed with ACC conjugates.

4.2 Introduction

A major challenge in developing drugs is to reduce side effects caused by off-target activity. One approach to this challenge is to design prodrugs that are preferentially activated at the target site. As proteases make up approximately 2% of the mammalian

proteome, they represent a significant target for prodrug development (*1*).

One area in which this strategy has had moderate success is cancer chemotherapy. For example, peptides attached to anticancer compounds such as doxorubicin, 5-fluorodeoxyuridine, paclitaxel, thapsigargin, and vinblastine have been used to target proteases such as prostate-specific antigen, matrix metalloproteases 2 and 9, legumain, and cathepsin B (*2-15*). The development of these prodrugs has focused on identifying a single protease that is overexpressed in the tumor tissue and screening the purified protease for the most preferential peptide sequence, often several amino acids long. While this approach is reasonable, it inherently limits the number of potential peptide promoieties. Another drawback of this strategy is that it ignores the potential role of other proteases within the cell in prodrug activation. Furthermore, as seen in Chapter 3, there might be less activity in a whole-cell system as compared to screening with a purified protein. An improved strategy for prodrug design to overcome these drawbacks is to target not merely a single enzyme, but rather the proteolytic profile of the entire target cell. Cloutier et al. demonstrated the validity of this approach by using a phage display library to identify pentapeptides that were differentially cleaved by secreted proteases of three prostate cancer cell lines (*16*). However, their method was limited to identifying surface proteolytic activity, was labor intensive with multiple rounds of screening, and excluded aminopeptidase activity as the pentapeptide did not have an exposed N-terminus.

To overcome these limitations, we have developed a rapid, physiologically relevant screening system to determine whole-cell proteolytic activity using the fluorescent compound 7-amino-4-methylcoumarin (AMC). To further simplify prodrug

development, we selected AMC compounds with single amino acids, dipeptides or tripeptides conjugated, and screened for differential activation. While AMC compounds have been used extensively to determine purified protease activity, to our knowledge this is the first time they have been used in a whole-cell screening system. To verify the promoiety was responsible for differential hydrolysis, we also used ACC (7-amino-4-carbamoylmethylcoumarin) as a leaving group. ACC has a similar structure to AMC (Figure 4.1) and both compounds experience a shift in excitation/emission spectra when an amino acid or peptide is conjugated to the amine group.

To investigate the feasibility of this approach we monitored the hydrolysis of known substrates by proteases overexpressed in HEK-293 cells. We then wanted to see if there was differential hydrolysis of our existing repertoire of AMC compounds by two breast cancer cell lines (MCF7 and BT-549) and a non-cancerous fibroblast cell line (MRC-5) that expresses proteases involved in remodeling of the extracellular matrix. The rationale for this strategy was that if we could observe differential hydrolysis with a limited number of compounds in two similar cell lines, then this approach could likely be extended to include a more complete library of compounds with cells from different tissue sources.

4.3 Methods

4.3.1 Materials

AMC (7-amino-4-methylcoumarin) compounds were purchased from Bachem, except Met-AMC (Enzo Life Sciences) and Lys-Pro-AMC (MP Bio); unless otherwise noted, all amino acids are L-isomers. Cells were purchased from ATCC and cell culture media was purchased from GIBCO.

4.3.2 Synthesis of ACC compounds

ACC (7-amino-4-carbamoylmethylcoumarin) was synthesized and conjugated to Rink amide AM resin according to the method of Maly et al. (*17*). The single amino acid conjugates of valine and alanine were made as well as the dipeptide conjugate of lysine-alanine using the coupling conditions described previously (*17*). Compound identities and purity were confirmed by TOF mass spec (ES^+) and ^1H NMR.

4.3.3 Cell culture

All cells were maintained at 37°C in 90% humidity with 5% CO_2. HEK-293 and HepG2 cells were cultured in Dulbecco's Modified Eagle Medium (DMEM) containing 10% heat-inactivated fetal bovine serum (HI-FBS). MRC-5, MCF7, and BT-549 cells were maintained in RPMI-1640 medium supplemented with 10% HI-FBS. HepG2, MRC-5, MCF7, and BT-549 cells were plated in black wall, clear bottom, tissue culture treated 96-well plates at a density that resulted in 25000 cells/well at the time of assay. For assays with MRC-5, MCF7, and BT-549 cells, media was replaced with serum-free RPMI-1640 medium immediately prior to adding substrate.

4.3.4 Transfection of HEK-293 cells

The cDNA for hANPEP, hNPEPPS, hDPP4, hDPP7, and mDPP9 in the vector pCMV-SPORT6 were purchased from OpenBiosystems. Plasmids were prepared from 200 ml DH10B TonA cultures using a maxi-prep kit from QIAGEN. Plasmids were sequenced at the University of Michigan DNA Sequencing Core using the T7 and M13 reverse primers. For mock-transfections, the empty pcDNA3.1 vector (Invitrogen) was also purified using a maxi-prep kit. Approximately 20 min prior to plating cells, 0.32 µg DNA and 0.5 µL Lipofectamine 2000 in 50 µL OptiMEM were added to each well of a black wall with clear bottom 96-well plate with CellBIND® surface (Corning). HEK-293

cells were trypsinized, counted, and plated at a density of 120,000 cells/well in 100 µL DMEM containing 10% HI-FBS. Cells were incubated at 37°C in 5% CO_2 with 90% humidity for 48-72 hrs prior to assaying.

4.3.5 Whole cell hydrolysis of AMC and ACC conjugates

Val-AMC, Pro-AMC, Tyr-AMC, Met-AMC, Leu-AMC, Phe-AMC, Ala-AMC, Gly-Phe-AMC, Gly-Pro-AMC, Lys-Pro-AMC, Lys-Ala-AMC, Ala-Ala-Phe-AMC, AMC, Val-ACC, Ala-ACC, Lys-Ala-ACC, and ACC were dissolved in DMSO at a concentration of 10 mM to create stock solutions. For the competition assays, 10 mM Gly-Sar was added prior to adding AMC compounds. For permeabilized membrane studies, 0.2% Triton X-100 was added 15 min prior to assay. A final concentration of 100 µM AMC or ACC compounds (1% DMSO) was added to the media and plates were incubated 2 hrs at 37°C. AMC fluorescence was measured every 2 min at $400_{ex}/508_{em}$ nm in a BioTek Synergy HT plate reader. The fluorescence reading for the DMSO negative control was subtracted. The amount of compound hydrolyzed to AMC or ACC was calculated from the fluorescence values and plotted against time to obtain the initial velocities (V_0, nmol/min) of hydrolysis.

4.3.6 Hydrolysis of AMC conjugates in mouse serum

Mouse serum was obtained from Invitrogen and diluted to 50% (v/v) in phosphate buffered saline, pH 7.4 (PBS). The diluted serum as well as PBS were aliquoted in opaque 96-well plates. AMC conjugates were added at a final concentration of 100 µM. AMC fluorescence was measured every 5 min at $400_{ex}/508_{em}$ nm in a BioTek Synergy HT plate reader heated to 37°C. The amount of compound hydrolyzed to AMC was calculated from the fluorescence values and plotted against time to obtain the initial velocities (V_0, nmol/min) of hydrolysis.

4.3.7 mRNA expression data

The mRNA expression data were obtained from the National Cancer Institute database, which is normalized using GC-content-based Robust Multiarray Averaging (GCRMA). The MEROPS peptidase database (http://merops.sanger.ac.uk/) (*18*) was used to identify potential peptidases involved in AMC substrate hydrolysis. TreeView software (EisenSoftware, Stanford University) was used to create a heat map of the mRNA expression data of the relevant proteases.

4.3.8 Statistical analysis

Data were analyzed by two-way ANOVA with a Bonferroni posttest using GraphPad Prism 4 (GraphPad Software, Inc). A P-value of < 0.05 was considered statistically significant.

4.4 Results

4.4.1 Single amino acid conjugates of AMC in transfected cells

To examine the feasibility of studying proteolytic activity in a whole-cell system, we transiently transfected HEK-293 cells with ANPEP and NPEPPS cDNA and screened several single amino acid conjugates of AMC known to be substrates of the aminopeptidases. The selected amino acids included valine, proline, tyrosine, methionine, phenylalanine, alanine, and leucine. While the transfected cells appeared to have slightly increased hydrolytic activity against several of the compounds, only Leu-AMC was hydrolyzed significantly faster by ANPEP-transfected cells compared to mock-transfected control cells (Figure 4.2).

4.4.2 Hydrolysis of peptide-AMC conjugates in transfected cells

The rapid hydrolysis of single amino acid substrates in mock-transfected cells make them less than ideal candidates for targeted prodrug promoieties. To examine the

potential for dipeptide promoieties, we transiently transfected HEK-293 cells with DPP4, DPP7, and DPP9 and screened with the known substrates of these dipeptidases: Gly-Pro-AMC, Lys-Pro-AMC, and Lys-Ala-AMC, with Gly-Phe-AMC as a control substrate. The initial velocities, V_0 (nmol/min), of hydrolysis are shown in Figure 4.3. Gly-Pro-AMC and Lys-Pro-AMC were good substrates for DPP4, DPP7, and DPP9 (>5-fold faster V_0 compared to mock-transfected cells). Interestingly, only cells expressing DPP7 and not DPP4 or DPP9 showed significantly faster hydrolysis of Lys-Ala-AMC compared to mock-transfected cells (1.16 ± 0.238 nmol/min compared to 0.02 ± 0.003 nmol/min, respectively). The hydrolysis assays were repeated in the presence of 10 mM Gly-Sar, a competitive inhibitor of PEPT1. This did not result in any significant changes in hydrolysis rates (data not shown). This was repeated in detergent-permeabilized cells, which resulted in faster rates of hydrolysis in DPP4-, DPP7-, and DPP9-transfected cells, while the trends remained the same (Figure 4.4). The hydrolysis of dipeptide substrates were also measured in ANPEP- and NPEPPS-transfected cells (Figure 4.3). The most noteworthy finding was the significant hydrolysis of Gly-Phe-AMC and Lys-Ala-AMC in HEK-293 cells overexpressing ANPEP.

4.4.3 Hydrolysis of single amino acid conjugates by three cell lines

We determined that we could measure differential hydrolysis in cells artificially overexpressing select proteases. To determine whether endogenous protease levels were sufficiently different to observe differential hydrolysis of AMC compounds, we selected the breast cancer cell lines MCF7 and BT-549 as well as the fibroblast cell line MRC-5. Again we started the screening with single amino acid substrates including D-Ala-, Val-, Pro-, Tyr-, Phe-, Leu-, Met-, and L-Ala-AMC and determined the initial velocities of hydrolysis. Unlike the transfected HEK-293 cells, there were significant differences in

hydrolysis rates among the three cell lines (Figure 4.5). The two breast cancer cell lines, MCF7 and BT-549, had similar hydrolysis rates for most compounds with the exception of Met- and Ala-AMC. Also, the preferential hydrolysis seemed to be stereo-specific, as BT-549 cells hydrolyzed L-Ala-AMC significantly faster than the other two cell lines, but there was virtually no hydrolysis of D-Ala-AMC in any cell line.

4.4.4 Differential hydrolysis of peptide-AMC conjugates by BT-549 cells

While there was significantly faster hydrolysis of select single amino acid substrates by the two breast cancer cells, there was still hydrolysis of these compounds by MRC-5 fibroblast cells. In an effort to achieve greater specificity, we tested the hydrolysis of several di- and tripeptide AMC conjugates by the three cell lines. The promoieties Lys-Ala, Gly-Phe, and Ala-Ala-Phe were hydrolyzed significantly faster by BT-549 cells compared to MCF7 or MRC-5 cells (Figure 4.6). Moreover, there was minimal hydrolysis of Lys-Ala-AMC in MRC-5 or MCF7 cells resulting in 10-fold and 100-fold differences in initial velocities, respectively, compared to BT-549 cells.

4.4.5 Hydrolysis of ACC conjugates

To verify whether this promoiety specificity can be conferred to other leaving groups, we synthesized ACC and conjugated valine, alanine, and lysine-alanine to ACC and compared the hydrolysis of these compounds by MRC-5, MCF7, and BT-549 cells to their respective AMC counterparts. Regardless of whether the leaving group was AMC or ACC, alanine and lysine-alanine substrates were hydrolyzed significantly faster by BT-549 cells as compared to MRC-5 and MCF7 cells (Figure 4.7). The hydrolysis of the ACC conjugates was significantly faster than the hydrolysis of the AMC conjugates by BT-549 cells.

4.4.6 Serum and liver stability of AMC conjugates

Ideally, there should be minimal hydrolysis of enzyme-activated prodrugs prior to reaching their target site. The blood stream and liver represent two potential sites of off-target activation. To begin to estimate the off-target activation that may occur, we measured the hydrolysis of our AMC compounds in 50% mouse serum and HepG2 liver cells. The hydrolysis rates were quite similar between serum and liver cells, with only Gly-Pro-AMC and Lys-Pro-AMC being hydrolyzed significantly faster in serum as compared to HepG2 cells (Figure 4.8). The three lead compounds from the breast cancer cell screen, Lys-Ala-, Gly-Phe-, and Ala-Ala-Phe-AMC, tended to be hydrolyzed more slowly than the majority of the compounds tested in both serum and HepG2 cells.

4.4.7 Protease expression levels in breast cancer cells

Using the MEROPS database (*18*), proteases that could potentially cleave single amino acids, dipeptides or tripeptides from AMC were selected. Figure 4.9 is a heat map of the mRNA expression levels of these proteases in MCF7 and BT-549 cells. The expression levels of many of these proteases are very similar between the two cell lines. The most notable differences in expression are the cathepsins (B, C, and D), tripeptidyl peptidases 1 and 2, and alanyl aminopeptidase.

4.5 Discussion

According to studies done with purified proteases, Ala, Met, and Leu are good substrates of alanyl aminopeptidase and puromycin-sensitive aminopeptidase while Pro and Val are poor substrates (*19-21*). However, as seen in Chapter 3 with legumain, there can be significant differences in hydrolytic activity between a purified protease and an overexpressed protease in a whole-cell system. Thus, screening prodrug substrates against purified proteases may not be the best predictor of their activation *in vivo*, as

subcellular localization and environment may affect the hydrolytic activity of an enzyme. To test this hypothesis, we transfected HEK-293 cells with the membrane-bound alanyl aminopeptidase (ANPEP, aminopeptidase N, APN, CD13) which has been previously characterized in its purified form due to its purported role in tumor progression (*19, 20, 22-26*). The cytosolic puromycin-senstive aminopeptidase (NPEPPS, APP-S) was also selected for transfection because it prefers substrates similar to those of APN, and because the purified protease has previously been characterized in our laboratory (*27*) and by others (*21, 28-31*). When APN and APP-S were overexpressed in HEK-293 cells, there was only slightly increased hydrolysis of single amino acid substrates compared to mock-transfected cells, and only Leu-AMC was hydrolyzed significantly faster by ANPEP-transfected cells. This lack of differential hydrolysis makes single amino acid promoieties less than ideal for a targeted prodrug approach, but makes them good candidates for to ensure rapid activation upon absorption of orally administered prodrugs.

The lack of significantly increased hydrolysis may be due to the already rapid hydrolysis of single amino acid substrates in mock-transfected cells. With this in mind, we selected several dipeptide substrates including Gly-Pro-, Lys-Pro-, and Lys-Ala-AMC which are known substrates of dipeptidyl peptidase IV (DPP4) (*32*), dipeptidyl peptidase VII (DPP7) (*33*), and dipeptidyl peptidase IX (DPP9) (*34*). We also tested the hydrolysis of Gly-Phe-AMC, which is not a known substrate of the previously listed dipeptidases and has been reported to be a substrate of cathepsin C and possibly APP-S (*35, 36*). In agreement with previous literature, Gly-Pro-AMC and Lys-Pro-AMC were good substrates for DPP4, DPP7, and DPP9. The k_{cat} values reported in the literature (*33*) indicate Lys-Ala-AMC should be hydrolyzed faster than Gly-Pro- or Lys-Pro-AMC by

DPP7. Our data are in partial agreement with this, as the V_0 for Lys-Ala-AMC was significantly faster than the V_0 for Gly-Pro-AMC ($P < 0.05$). Interestingly, the initial velocities of hydrolysis for Gly-Pro and Lys-Pro substrates by DPP9-transfected cells were similar in our system, whereas k_{cat} values reported in literature for Gly-Pro substrates are 2- to 4-fold greater than the k_{cat} values for Lys-Pro substrates (*34, 37*). Finally, Lys-Ala-AMC is reported to be a DPP4 substrate in literature (*32*), but the hydrolysis of Lys-Ala-AMC in DPP4-transfected cells was not significantly faster than mock-transfected cells. These results further emphasize the potential differences in enzymatic activity between purified proteases and proteases in live cells.

The hydrolysis of the dipeptide substrates were also tested in the ANPEP- and NPEPPS-transfected HEK-293 cells. The work of Ishii et al. (*20*) showed that Gly-Pro- and Lys-Ala-AMC were poor substrates for alanyl aminopeptidase, with Lys-Ala-AMC being the worse of the two. However, in HEK-293 cells transfected with ANPEP, we saw that Lys-Ala-AMC was hydrolyzed almost as fast as Ala-AMC, while there was no detectable increase in Lys-Pro-AMC hydrolysis. Alternatively, Huang et al. found Lys-Ala-AMC was almost as good a substrate for alanyl aminopeptidase as Ala-AMC (*19*). Similarly, Feracci et al. (*22*) found the peptide Lys-Ala-Ala was a better substrate for APN than Ala-*p*-nitroanilide. Huang et al. (*19*) proposed that alanyl aminopeptidase hydrolyzes Lys-Ala-AMC in a two-step reaction based on the concave curve of activity plotted against time. Therefore, it is possible Ishii et al. (*20*) only measured the slow step of the two-step reaction. Furthermore, based on the reported enzymatic activity of alanyl aminopeptidase against Gly- and Phe-AMC (*19, 20, 22*), the rapid hydrolysis of Gly-Phe-AMC by ANPEP-transfected cells was unexpected, which further highlights the need for

screening whole-cell proteolytic activity. However, it was previously suggested that APP-S may be involved in Gly-Phe-AFC hydrolysis based on inhibitor profile characteristics (*36*).

There was a possibility that the differences in substrate hydrolysis could be due to accessibility of the substrate to the enzyme, as DPP IV is a membrane protease (*38*), while DPP VII is lysosomal (*33, 39*), and DPP IX is localized to the cytosol (*34*). To rule out this possibility, cell membranes were permeabilized with Triton X-100. The differential pattern of hydrolysis remained in detergent-permeabilized cells suggesting the pattern was not due to substrate accessibility.

Using the MEROPS database, we identified 31 proteases potentially involved in the hydrolysis of our AMC compounds and compared the mRNA expression levels of these proteases in the two breast cancer cell lines. Based on our hydrolysis results we were not surprised to find increased expression levels of alanyl aminopeptidase, cathepsin C, and tripeptidyl peptidases 1 and 2 in BT-549 cells, which are known activators of Ala-AMC, Gly-Phe-AMC, and Ala-Ala-Phe-AMC, respectively (*19, 20, 40-44*). Similarly, the lack of differences in mRNA expression levels of dipeptidyl peptidasesIV, VII, and IX fit with the lack of differential hydrolysis of their known substrates, Gly-Pro-AMC and Lys-Pro-AMC (*32-34*). As was shown in DPP7-transfected cells, Lys-Ala-AMC is a DPP VII substrate and there was faster hydrolysis of Lys-Ala-AMC in BT-549 cells compared to MCF7 cells, yet there was no difference in DPP7 mRNA expression levels between the two breast cancer cell lines. The increased V_0 of Lys-Ala-AMC hydrolysis in BT-549 cells could be explained by the increased expression of alanyl aminopeptidase (ANPEP) in BT-549 cells rather than DPP7. This further highlights the ability to target more than

one protease with a single substrate and the need to know the entire proteolytic profile of a target cell.

To successfully design target activated prodrugs using single amino acid or peptide promoieties, it is first necessary to identify promoieties that will be differentially hydrolyzed. As the results of this chapter have shown, relying on the *in vivo* mRNA transcript level and *in vitro* substrate specificity of a single protease is not sufficient to predict the hydrolysis pattern of even a select number of promoieties. By screening a whole-cell system we can achieve differential activation through the combined activity of multiple proteases. These promoieties can be used to not only design prodrugs to treat a disease such as cancer, but can also be attached to imaging agents for diagnostic purposes.

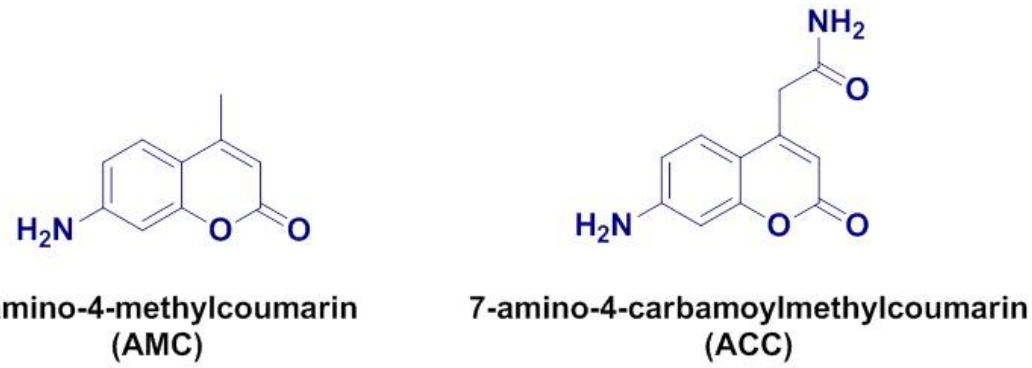

Figure 4.1 Chemical structures of AMC and ACC.

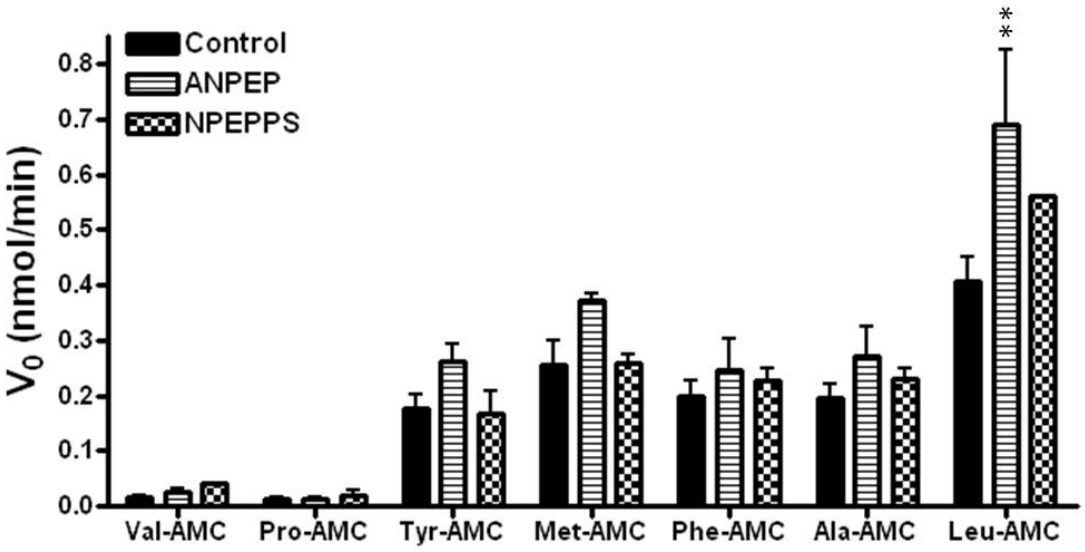

Figure 4.2 Single amino acids are not ideal candidates for targetd prodrug promoieties.
HEK-293 cells were transiently transfected with ANPEP or NPEPPS cDNA or mock-transfected with pcDNA3.1 (empty vector). Fluorescence values were converted to amount of AMC and plotted against time to determine the initial velocity (V_o, nmol/min). Data were analyzed by two-way ANOVA with a Bonferroni posttest. Asterisks indicate that the value is significantly different from mock-transfected cells (**P<0.01).

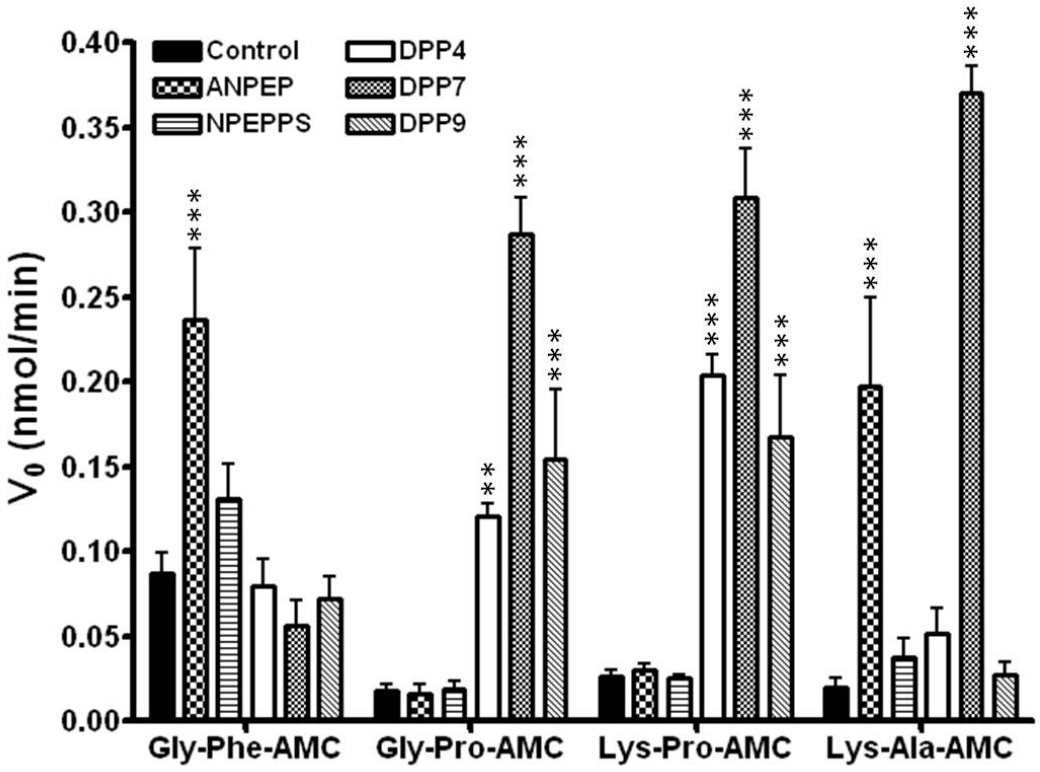

Figure 4.3 Dipeptide promoieties are sufficient for differential hydrolysis in transfected HEK-293 cells.

HEK-293 cells were transiently-transfected with ANPEP, NPEPPS, DPP4, DPP7 or DPP9 cDNA or mock-transfected (control). Compounds were added at a final concentration of 100 uM and fluorescence was measured. Fluorescence values were converted to amount of AMC and plotted against time to determine the initial velocity (V_o, nmol/min). Data were analyzed by two-way ANOVA with a Bonferroni post-test using GraphPad Prism 4.0. Bars with asterisks are significantly different from mock-transfected control cells (**P < 0.01, ***P < 0.001).

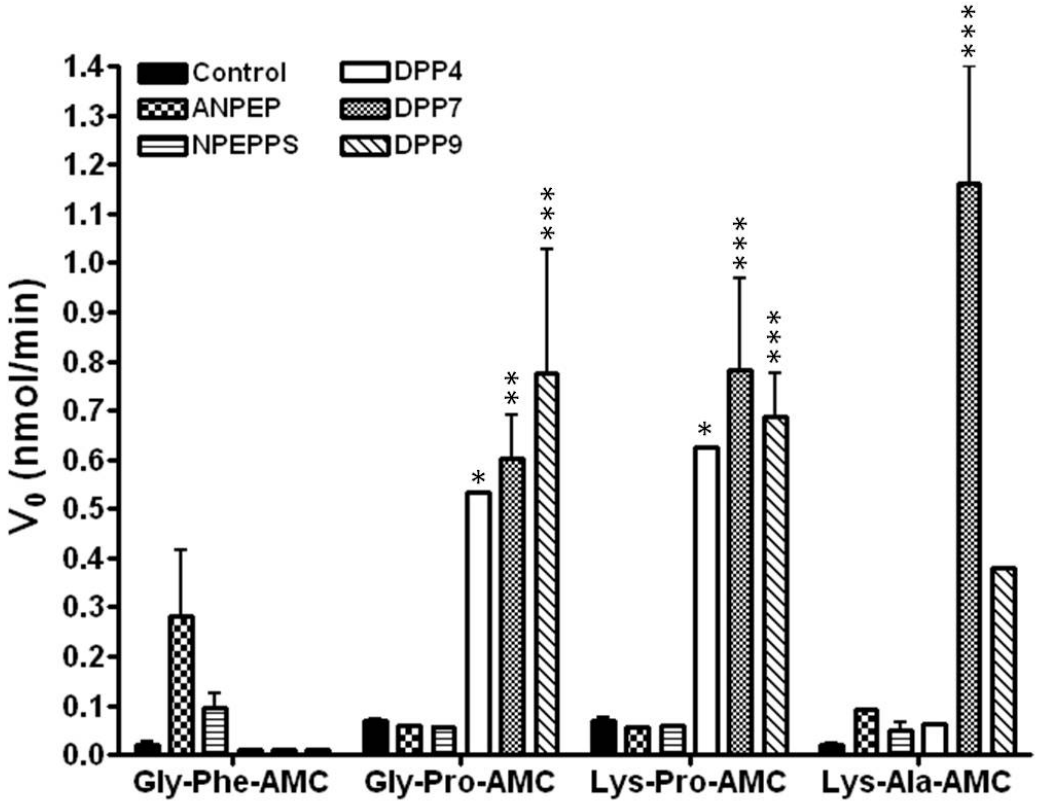

Figure 4.4 Membrane permeabilization by Triton X-100 changes the rate of hydrolysis by transfected HEK-293 cells

HEK-293 cells were transfected with ANPEP, NPEPPS, DPP4, DPP7 or DPP9 cDNA or empty vector (control). Cell membranes were permeabilized with detergent prior to performing assay. The hydrolysis of the compounds to AMC was measured by the change in fluorescence over time. The initial velocity of hydrolysis (V_0, nmol/min) was determined by the slope of the linear portion of the hydrolysis curve. Bars with asterisks are significantly different from the mock-transfected (control) cells (*P < 0.05, **P < 0.01, ***P < 0.001).

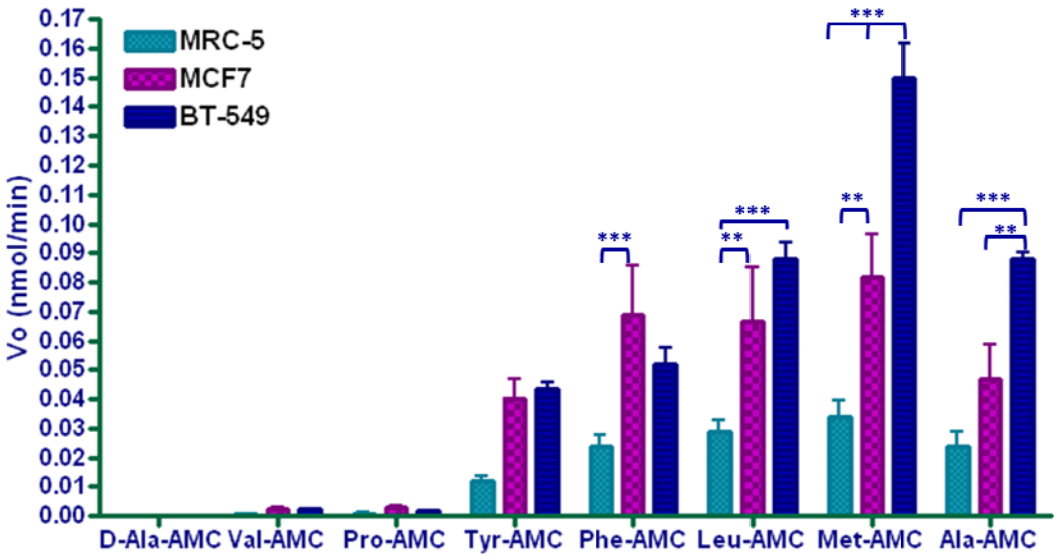

Figure 4.5 Differential hydrolysis can be achieved with single amino acid substrates. AMC conjugates were added to MRC-5, MCF7, and BT-549 cells and the change in fluorescence was measured over time. Fluorescence values were converted to amount of AMC and plotted against time to determine the initial velocity (V_o, nmol/min). Data were analyzed by two-way ANOVA with a Bonferroni post-test using GraphPad Prism 4.0. Bars with asterisks are significantly different (**P < 0.01, ***P < 0.001).

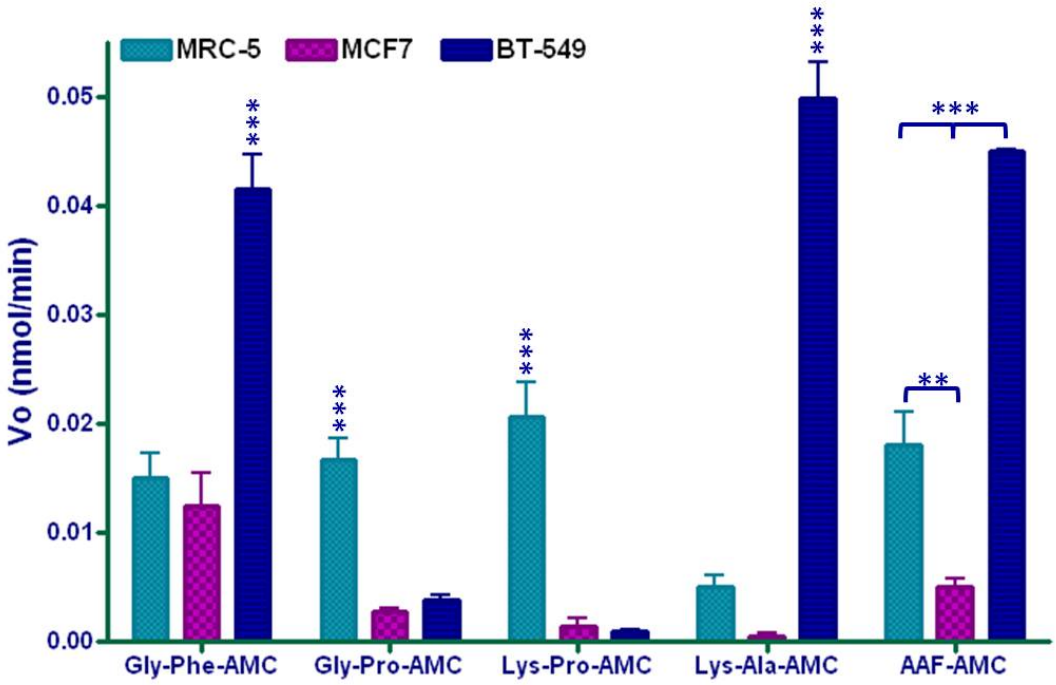

Figure 4.6 Di- and tripeptide promoieties resulted in greater differential hydrolysis. AMC conjugates were added to MRC-5, MCF7, and BT-549 cells and change in fluorescence was measured over time. Fluorescence values were converted to amount of AMC and plotted against time to determine the initial velocity (V_o, nmol/min). Data were analyzed by two-way ANOVA with a Bonferroni post-test using GraphPad Prism 4.0. Bars with asterisks are significantly different (**P < 0.01, ***P < 0.001).

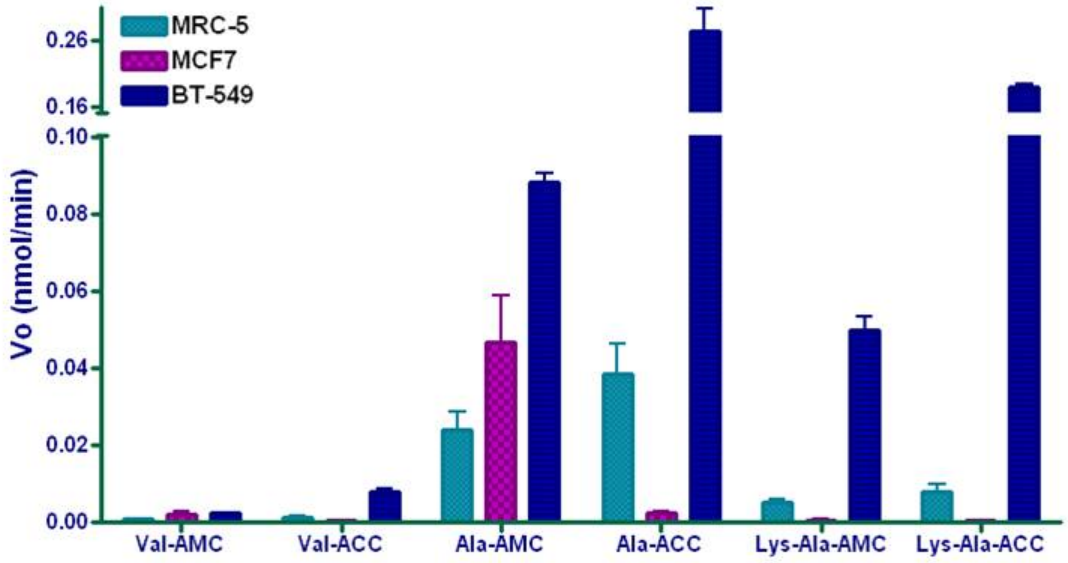

Figure 4.7 The promoiety confers differential hydrolysis despite changing the leaving group.

AMC and ACC conjugates were added to MRC-5, MCF7, and BT-549 cells and change in fluorescence was measured over time. Fluorescence values were converted to amount of AMC or ACC and plotted against time to determine the initial velocity (V_o, nmol/min). Data were analyzed by two-way ANOVA with a Bonferroni post-test using GraphPad Prism 4.0. Bars with asterisks are significantly different from other cell lines with the same compound (**P < 0.01, ***P < 0.001).

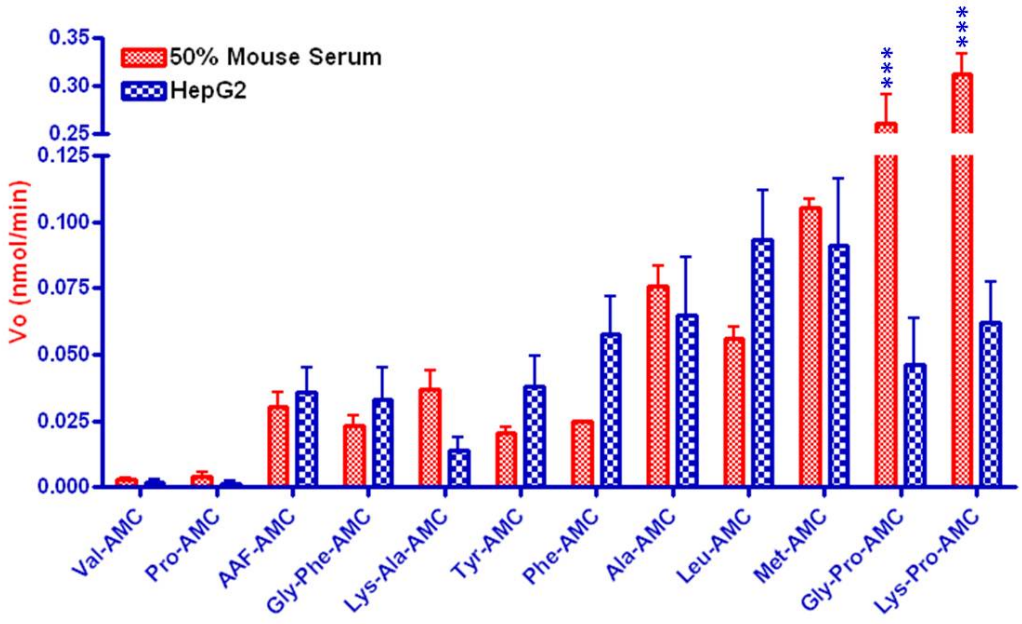

Figure 4.8 There is significant X-prolyl peptidase activity in mouse serum. AMC conjugates were added to wells containing 50% mouse serum or HepG2 cells. Fluorescence values were converted to amount of AMC and plotted against time to determine the initial velocity (V_0, nmol/min). Data were analyzed by two-way ANOVA with a Bonferroni post-test using GraphPad Prism 4.0. Bars with asterisks are significantly different between the serum and HepG2 groups (***$P < 0.001$).

Figure 4.9 mRNA expression levels of select proteases in MCF7 and BT-549 cells. Proteases were selected using the MEROPS database and expression levels (GCRMA normalized) were obtained from the National Cancer Institute. The heat map was created using TreeView software (EisenSoftware) with high expression in red and low expression in black.

4.6 References

1. Lim, M. D., and Craik, C. S. (2009) Using specificity to strategically target proteases, *Bioorganic & Medicinal Chemistry 17*, 1094-1100.

2. Mhaka, A., Denmeade, S. R., Yao, W., Isaacs, J. T., and Khan, S. R. (2002) A 5-fluorodeoxyuridine prodrug as targeted therapy for prostate cancer, *Bioorganic & Medicinal Chemistry Letters 12*, 2459-2461.

3. Dubowchik, G. M., Mosure, K., Knipe, J. O., and Firestone, R. A. (1998) Cathepsin B-sensitive dipeptide prodrugs. 2. Models of anticancer drugs paclitaxel (Taxol), mitomycin C and doxorubicin, *Bioorg Med Chem Lett 8*, 3347-3352.

4. DiPaola, R. S., Rinehart, J., Nemunaitis, J., Ebbinghaus, S., Rubin, E., Capanna, T., Ciardella, M., Doyle-Lindrud, S., Goodwin, S., Fontaine, M., Adams, N., Williams, A., Schwartz, M., Winchell, G., Wickersham, K., Deutsch, P., and Yao, S. L. (2002) Characterization of a novel prostate-specific antigen-activated peptide-doxorubicin conjugate in patients with prostate cancer, *J Clin Oncol 20*, 1874-1879.

5. Young, L., Di Salvo, A., Turnbull, A., Lyle, J., Bibby, M. C., Double, J. A., Kay, G., Loadman, P. M., and Mincher, D. (2003) Design of Tumour-Activated Prodrugs that Harness the 'Dark Side' of MMP-9, *Br J Cancer 88*, S27.

6. Kratz, F., Drevs, J., Bing, G., Stockmar, C., Scheuermann, K., Lazar, P., and Unger, C. (2001) Development and in vitro efficacy of novel MMP2 and MMP9 specific doxorubicin albumin conjugates, *Bioorganic & Medicinal Chemistry Letters 11*, 2001-2006.

7. Hu, Z., Jiang, X., Albright, C. F., Graciani, N., Yue, E., Zhang, M., Zhang, S. Y., Bruckner, R., Diamond, M., Dowling, R., Rafalski, M., Yeleswaram, S., Trainor, G. L., Seitz, S. P., and Han, W. (2010) Discovery of matrix metalloproteases selective and activated peptide-doxorubicin prodrugs as anti-tumor agents, *Bioorg Med Chem Lett 20*, 853-856.

8. Denmeade, S. R., Nagy, A., Gao, J., Lilja, H., Schally, A. V., and Isaacs, J. T. (1998) Enzymatic activation of a doxorubicin-peptide prodrug by prostate-specific antigen, *Cancer Res 58*, 2537-2540.

9. Khan, S. R., and Denmeade, S. R. (2000) In vivo activity of a PSA-activated

doxorubicin prodrug against PSA-producing human prostate cancer xenografts, *Prostate 45*, 80-83.

10. Liu, C., Sun, C., Huang, H., Janda, K., and Edgington, T. (2003) Overexpression of legumain in tumors is significant for invasion/metastasis and a candidate enzymatic target for prodrug therapy, *Cancer Res. 63*, 2957-2964.

11. Lee, G. Y., Song, J. h., Kim, S. Y., Park, K., and Byun, Y. (2006) Peptide-doxorubicin conjugates specifically degraded by matrix metalloproteinases expressed from tumor, *Drug Development Research 67*, 438-447.

12. DeFeo-Jones, D., Garsky, V. M., Wong, B. K., Feng, D. M., Bolyar, T., Haskell, K., Kiefer, D. M., Leander, K., McAvoy, E., Lumma, P., Wai, J., Senderak, E. T., Motzel, S. L., Keenan, K., Van Zwieten, M., Lin, J. H., Freidinger, R., Huff, J., Oliff, A., and Jones, R. E. (2000) A peptide-doxorubicin 'prodrug' activated by prostate-specific antigen selectively kills prostate tumor cells positive for prostate-specific antigen in vivo, *Nat Med 6*, 1248-1252.

13. DeFeo-Jones, D., Brady, S. F., Feng, D.-M., Wong, B. K., Bolyar, T., Haskell, K., Kiefer, D. M., Leander, K., McAvoy, E., Lumma, P., Pawluczyk, J. M., Wai, J., Motzel, S. L., Keenan, K., Van Zwieten, M., Lin, J. H., Garsky, V. M., Freidinger, R., Oliff, A., and Jones, R. E. (2002) A Prostate-specific Antigen (PSA)-activated Vinblastine Prodrug Selectively Kills PSA-secreting Cells in Vivo, *Molecular Cancer Therapeutics 1*, 451-459.

14. Denmeade, S. R., Jakobsen, C. M., Janssen, S., Khan, S. R., Garrett, E. S., Lilja, H., Christensen, S. B., and Isaacs, J. T. (2003) Prostate-Specific Antigen-Activated Thapsigargin Prodrug as Targeted Therapy for Prostate Cancer, *Journal of the National Cancer Institute 95*, 990-1000.

15. Kumar, S. K., Williams, S. A., Isaacs, J. T., Denmeade, S. R., and Khan, S. R. (2007) Modulating paclitaxel bioavailability for targeting prostate cancer, *Bioorganic & Medicinal Chemistry 15*, 4973-4984.

16. Cloutier, S. M., Kundig, C., Gygi, C. M., Jichlinski, P., Leisinger, H. J., and Deperthes, D. (2004) Profiling of proteolytic activities secreted by cancer cells using phage display substrate technology, *Tumour Biol 25*, 24-30.

17. Maly, D. J., Leonetti, F., Backes, B. J., Dauber, D. S., Harris, J. L., Craik, C. S., and Ellman, J. A. (2002) Expedient solid-phase synthesis of fluorogenic protease substrates using the 7-amino-4-carbamoylmethylcoumarin (ACC) fluorophore, *J*

Org Chem 67, 910-915.

18. Rawlings, N. D., Morton, F. R., and Barrett, A. J. (2006) MEROPS: the peptidase database, *Nucleic Acids Res 34*, D270-272.

19. Huang, K., Takahara, S., Kinouchi, T., Takeyama, M., Ishida, T., Ueyama, H., Nishi, K., and Ohkubo, I. (1997) Alanyl aminopeptidase from human seminal plasma: purification, characterization, and immunohistochemical localization in the male genital tract, *J Biochem 122*, 779-787.

20. Ishii, K., Usui, S., Sugimura, Y., Yoshida, S., Hioki, T., Tatematsu, M., Yamamoto, H., and Hirano, K. (2001) Aminopeptidase N regulated by zinc in human prostate participates in tumor cell invasion, *International Journal of Cancer 92*, 49-54.

21. Sengupta, S., Horowitz, P. M., Karsten, S. L., Jackson, G. R., Geschwind, D. H., Fu, Y., Berry, R. W., and Binder, L. I. (2006) Degradation of tau protein by puromycin-sensitive aminopeptidase in vitro, *Biochemistry 45*, 15111-15119.

22. Feracci, H., Benajiba, A., Gorvel, J. P., Doumeng, C., and Maroux, S. (1981) Enzymatic and immunological properties of the protease form of aminopeptidases N and A from pig and rabbit intestinal brush border, *Biochimica et Biophysica Acta (BBA) - Enzymology 658*, 148-157.

23. Piedfer, M., Dauzonne, D., Tang, R., N'Guyen, J., Billard, C., and Bauvois, B. (2011) Aminopeptidase-N/CD13 is a potential proapoptotic target in human myeloid tumor cells, *The FASEB Journal*.

24. Terauchi, M., Kajiyama, H., Shibata, K., Ino, K., Nawa, A., Mizutani, S., and Kikkawa, F. (2007) Inhibition of APN/CD13 leads to suppressed progressive potential in ovarian carcinoma cells, *BMC Cancer 7*, 140.

25. Wickström, M., Larsson, R., Nygren, P., and Gullbo, J. (2011) Aminopeptidase N (CD13) as a target for cancer chemotherapy, *Cancer Science 102*, 501-508.

26. Drag, M., Bogyo, M., Ellman, J. A., and Salvesen, G. S. (2010) Aminopeptidase Fingerprints, an Integrated Approach for Identification of Good Substrates and Optimal Inhibitors, *Journal of Biological Chemistry 285*, 3310-3318.

27. Tehler, U., Nelson, C. H., Peterson, L. W., Provoda, C. J., Hilfinger, J. M., Lee, K.-D., McKenna, C. E., and Amidon, G. L. (2010) Puromycin-sensitive aminopeptidase: An antiviral prodrug activating enzyme, *Antiviral Research 85*, 482-489.

28. Constam, D. B., Tobler, A. R., Rensing-Ehl, A., Kemler, I., Hersh, L. B., and Fontana, A. (1995) Puromycin-sensitive aminopeptidase. Sequence analysis, expression, and functional characterization, *J Biol.Chem. 270*, 26931-26939.

29. Thompson, M. W., Govindaswami, M., and Hersh, L. B. (2003) Mutation of active site residues of the puromycin-sensitive aminopeptidase: conversion of the enzyme into a catalytically inactive binding protein, *Arch.Biochem.Biophys. 413*, 236-242.

30. Mantle, D., Hardy, M. F., Lauffart, B., McDermott, J. R., Smith, A. I., and Pennington, R. J. (1983) Purification and characterization of the major aminopeptidase from human skeletal muscle, *Biochem J 211*, 567-573.

31. Sharma, K. K., and Ortwerth, B. J. (1986) Isolation and characterization of a new aminopeptidase from bovine lens, *J Biol Chem 261*, 4295-4301.

32. Bar, J., Weber, A., Hoffmann, T., Stork, J., Wermann, M., Wagner, L., Aust, S., Gerhartz, B., and Demuth, H. U. (2003) Characterisation of human dipeptidyl peptidase IV expressed in Pichia pastoris. A structural and mechanistic comparison between the recombinant human and the purified porcine enzyme, *Biol Chem 384*, 1553-1563.

33. Maes, M. B., Lambeir, A. M., Gilany, K., Senten, K., Van der Veken, P., Leiting, B., Augustyns, K., Scharpe, S., and De Meester, I. (2005) Kinetic investigation of human dipeptidyl peptidase II (DPPII)-mediated hydrolysis of dipeptide derivatives and its identification as quiescent cell proline dipeptidase (QPP)/dipeptidyl peptidase 7 (DPP7), *Biochem J 386*, 315-324.

34. Geiss-Friedlander, R., Parmentier, N., Moller, U., Urlaub, H., Van den Eynde, B. J., and Melchior, F. (2009) The Cytoplasmic Peptidase DPP9 Is Rate-limiting for Degradation of Proline-containing Peptides, *Journal of Biological Chemistry 284:*, 27211-27219.

35. Doughty, M. J., and Gruenstein, E. I. (1986) Chloride-insensitive, glycine-phenylalanine-naphthylamide hydrolysis at neutral pH in human skin fibroblasts, *Biochem Cell Biol 64*, 772-781.

36. Niles, A. L., Moravec, R. A., Eric Hesselberth, P., Scurria, M. A., Daily, W. J., and Riss, T. L. (2007) A homogeneous assay to measure live and dead cells in the same sample by detecting different protease markers, *Analytical Biochemistry 366*, 197-206.

37. Tang, H. K., Tang, H. Y., Hsu, S. C., Chu, Y. R., Chien, C. H., Shu, C. H., and Chen, X. (2009) Biochemical properties and expression profile of human prolyl dipeptidase DPP9, *Arch Biochem Biophys 485*, 120-127.

38. Kotackova, L., Balaziova, E., and Sedo, A. (2009) Expression pattern of dipeptidyl peptidase IV activity and/or structure homologues in cancer, *Folia Biol (Praha) 55*, 77-84.

39. Maes, M.-B., Scharpé, S., and De Meester, I. (2007) Dipeptidyl peptidase II (DPPII), a review, *Clinica Chimica Acta 380*, 31-49.

40. Ezaki, J., Takeda-Ezaki, M., Oda, K., and Kominami, E. (2000) Characterization of endopeptidase activity of tripeptidyl peptidase-I/CLN2 protein which is deficient in classical late infantile neuronal ceroid lipofuscinosis, *Biochem Biophys Res Commun 268*, 904-908.

41. Kuribayashi, M., Yamada, H., Ohmori, T., Yanai, M., and Imoto, T. (1993) Endopeptidase Activity of Cathepsin C, Dipeptidyl Aminopeptidase I, from Bovine Spleen, *Journal of Biochemistry 113*, 441-449.

42. McGuire, M. J., Lipsky, P. E., and Thiele, D. L. (1992) Purification and characterization of dipeptidyl peptidase I from human spleen, *Archives of Biochemistry and Biophysics 295*, 280-288.

43. Tian, Y., Sohar, I., Taylor, J. W., and Lobel, P. (2006) Determination of the substrate specificity of tripeptidyl-peptidase I using combinatorial peptide libraries and development of improved fluorogenic substrates, *J Biol Chem 281*, 6559-6572.

44. Tomkinson, B. (2000) Association and dissociation of the tripeptidyl-peptidase II complex as a way of regulating the enzyme activity, *Arch Biochem Biophys 376*, 275-280.

CHAPTER 5

Selective Hydrolysis of Doxorubicin Prodrugs

5.1 Summary

To more selectively target chemotherapeutics, it is useful to identify peptide sequences that are preferentially hydrolyzed by cancer cells. The proteolytic profiles of cells can be determined by a variety of methods. In the previous chapter, AMC and ACC conjugates were used to screen whole cells to identify peptide sequences differentially hydrolyzed by cancer cells. In this chapter, the results from the AMC screen are applied to the rational design of a peptide prodrug. The lead sequence from the AMC screen, lysyl-alanine is conjugated to doxorubicin (Dox), as well as control amino acid and dipeptide sequences. The prodrugs are characterized by measuring the rate of hydrolysis in lysed and whole cells and the cytotoxicity is compared to that of free Dox using IC_{50} values. Finally, microscopy is used to explore distribution of free Dox and Dox prodrugs within the cells.

5.2 Introduction

The lack of tumor selectivity continues to limit the dosage of many anti-cancer compounds on the market. It has become increasingly common to use a prodrug approach to target existing drugs in order to improve selectivity (*1-4*). One such prodrug approach involves conjugating a peptide to a drug that is hydrolyzed by a protease overexpressed in the tumor tissue. Proteases are required for degradation of the

extracellular matrix, which is essential for tumor metastasis (*4*). In addition, proteases make up almost 2% of mammalian genes (*5*), making them an attractive target for prodrug activation. Chemotherapeutic prodrugs have been targeted to a variety of cysteine, serine, and metalloproteases including cathepsins (*6-8*), prostate-specific antigen (*9-18*), matrix metalloproteinases (*19-24*), legumain (*25-27*), and urokinase plasminogen activator (*28*). However, there can be variability in expression and activity of a single protease, making this approach less reliable. Furthermore, these targets tend to be extracellular, thus ignoring the ~50% of proteases that are intracellular (*5*).

Protease-activated prodrugs have been developed to improve the selectivity of 5-fluorodeoxyuridine (*17, 29*), camptothecin (*30*), vinblastine (*9*), paclitaxel (*15*), thapsigargin (*12*), and, most extensively, doxorubicin (*8, 10, 13, 14, 20, 22, 23, 25, 31, 32*). The anthracyline doxorubicin (Dox) is one the most commonly used chemotherapeutics and has a broad spectrum of activity (*33*). Breast cancer is the most commonly diagnosed cancer among women and the median 5-year survival rate for metastatic breast cancer (MBC) is less than 25% (*34*). In a population-based study in British Columbia, ~35% of women with MBC were treated with an anthracycline (*35*). Despite its widespread use, cytotoxic side effects continue to plague the use of Dox, with cardiotoxicity being one of the most significant problems leading to dose limitations (*33*). The need for improved selectivity combined with the presence of a primary amine group on Dox make it a good candidate for a peptide-prodrug approach.

In the previous chapter, we established a method to screen peptide promoities to aid in the design of target-activated prodrugs. In this chapter, we conjugated the lead promoiety from that screen, L-Lys-L-Ala, to doxorubicin and measured the hydrolysis and

cytotoxicity in MRC-5, MCF7, and BT-549 cells. We also attempted to identify some of the proteases involved in hydrolysis using inhibitors and transfected cells.

5.3 Methods

5.3.1 Materials

Doxorubicin hydrochloride was obtained from Pharmacia & Upjohn. Fmoc-L-lysine(Fmoc)-L-alanine and Fmoc-L-lysine(Fmoc)-D-alanine dipeptides were synthesized by Genscript (≥98% purity). Fmoc- L-alanine-OH and Fmoc- D-alanine-OH were purchased from NovaBiochem. MRC-5, MCF7, and BT-549 cells were purchased from American Type Culture Collection (ATCC) and cell culture media was purchased from Gibco/Invitrogen. All other chemicals used were purchased from Thermo Fischer Scientific.

5.3.2 Synthesis of doxorubicin prodrugs

Peptide prodrugs of doxorubicin were synthesized using the methods of Chung and Kratz (*28*) and Schmid et al. (*8*) with modifications. Yields shown are for L-Lys-D-Ala-Dox. Briefly, doxorubicin hydrochloride (17.18 mg, 0.0296 mmol) and Fmoc-L-lysine(Fmoc)-L-alanine-OH, Fmoc-L-lysine(Fmoc)-D-alanine-OH, Fmoc-L-alanine-OH or Fmoc-D-alanine-OH (0.0296 mmol) were mixed in 4 mL of dimethylformamide (DMF), and then treated with *N*,*N*-diisopropylethylamine (DIPEA) for 10 min. HATU (2-(7-Aza-1H-benzotriazole-1-yl)-1,1,3,3-tetramethyluronium hexafluorophosphate) (12.38 mg, 0.03256 mmol) was added and the reaction mixture was stirred at room temperature for 2 h. The product was precipitated in ethyl ether and washed three times. The filtrate was collected and purified through chromatography on silica gel using chloroform/methanol 93:7, affording 21.7 mg (62%) of red powder as pure product.

The Fmoc protecting group was removed by dissolving Fmoc-L-Lys(Fmoc)-L-Ala-Dox, Fmoc-L-Lys(Fmoc)-D-Ala-Dox, Fmoc- L-Ala-Dox, and Fmoc-D-Ala-Dox in 1.25 mL of DMF with 20% piperadine. The blue mixture was stirred at room temperature for 5 min followed by precipitation of the product in 15 mL of diethyl ether. The pure product was filtered and vacuumed overnight to give 10.5 mg (78%) dark red powder. Compound identity was confirmed by mass spec (ESI-MS: m/z 743.3 $[M+H]^+$ for dipeptide prodrugs and m/z 637.1 $[M+Na]^+$ for single amino acid prodrugs) and purity was determined by HPLC (>90%).

5.3.3 HPLC analysis

Samples were analyzed using an HPLC system (Agilent) consisting of a reverse-phase column (Agilent Zorbax Eclipse XDB-C18, 3.5 µm, 4.6 × 150 mm), an 1100 series pump (Hewlett Packard), an 1100 series fluorescence detector (Agilent), and a 1200 series autosampler (Agilent). The mobile phase consisted of 8 mM triethylamine in 28 mM sodium phosphate, pH 3.7 with 22-35% acetonitrile gradient with a flow rate of 1 ml/min with fluorescence detection at $480_{ex}/560_{em}$ nm. The amount of prodrug and doxorubicin present were calculated from standard curves based on peak areas.

5.3.4 pH stability of prodrugs

Prodrugs were incubated in 0.2 M sodium citrate/citric acid buffer (pH 4.0), 10 mM Hepes, 100 mM NaCl (pH 7.4) or 0.1 M sodium borate buffer (pH 9.8) at room temperature for 24 hrs. Samples were analyzed by HPLC as described above at 0 and 24 hrs.

5.3.5 Cell culture

All Cells were maintained at 37°C in 90% humidity with 5% CO_2. HEK-293

were cultured in Dulbecco's Modified Eagle Medium (DMEM) containing 10% heat-inactivated fetal bovine serum (HI-FBS). MRC-5, MCF7, and BT-549 cells were maintained in RPMI-1640 medium supplemented with 10% HI-FBS. MRC-5, MCF7, and BT-549 cells were plated in black wall, clear bottom, tissue culture treated 96-well plates at a density that resulted in 5000 cells/well at the time of assay.

5.3.6 Transfection of HEK-293 cells

The human cDNAs for alanyl aminopeptidase (ANPEP), puromycin-sensitive aminopeptidase (NPEPPS), and dipeptidyl peptidase VII (DPP7) in the vector pCMV-SPORT6 were purchased from OpenBiosystems. Plasmids were prepared from 200 ml DH10B TonA cultures using a maxi-prep kit from Qiagen. Plasmids were sequenced at the University of Michigan DNA Sequencing Core using the T7 and M13 reverse primers. For mock-transfections, the empty pcDNA3.1 vector (Invitrogen) was also purified using a maxi-prep kit. Approximately 20 min prior to plating cells, 0.32 μg DNA and 0.5 μL Lipofectamine 2000 (Invitrogen) in 50 μL OptiMEM were added to each well of a black wall with clear bottom 96-well plate with CellBIND® surface (Corning). HEK-293 cells were trypsinized, counted, and plated at a density of 120,000 cells/well in 100 μL DMEM containing 10% HI-FBS. Cells were incubated at 37°C in 5% CO_2 with 90% humidity for 48-72 hrs prior to assaying.

5.3.7 Hydrolysis of prodrugs

L-Lys-L-Ala-Dox, L-Lys-D-Ala-Dox, L-Ala-Dox, and D-Ala-Dox were dissolved in methanol to obtain a stock concentration of 1 mM. Cells were plated in black wall, clear bottom, tissue culture treated 96-well plates at a density that resulted in 5000 cells/well at the time of assay. For the assay with lysed cells, 0.2% Triton X-100 was

added 15 min prior to adding prodrug. The prodrugs were added to wells containing cells at a final concentration of 1-20 μM. At predetermined time points (0-24 hrs), 100 μL media or buffer was removed and quenched in 400 μL methanol. Samples were placed on a vortex at 4°C for ≥30 min followed by centrifugation at 12000 × g for 8 min at 4°C. The supernatant was then analyzed by HPLC. Data were fitted to one-phase exponential association curves in GraphPad Prism 4.0.

5.3.8 Whole-cell hydrolysis of L-Lys-L-Ala-AMC

L-Lys-L-Ala-AMC and AMC were dissolved in DMSO at a concentration of 10 mM to create stock solutions. A final concentration of 100 μM AMC compounds (1% DMSO) was added to the media and plates were incubated 30 min at 37°C with or without 100 μM bestatin. AMC fluorescence was measured every 2 min at $400_{ex}/508_{em}$ nm in a BioTek Synergy HT plate reader. The fluorescence reading for the DMSO negative control was subtracted. The amount of compound hydrolyzed to AMC was calculated from the fluorescence values and plotted against time. The data were fitted to one-phase exponential association curves by GraphPad Prism 4.0.

5.3.9 Cell viability

Doxorubicin was added to the media at a final concentration of 0.01 - 100 μM and dox prodrugs were added to the media at a final concentration of 1 - 500 μM. After 12 hrs of incubation at 37°C, drug-containing media was replaced with fresh media and cells were incubated an additional 48 hrs. Doxorubicin, prodrugs or solvent were added to the media at a final concentration of 10 μM and incubated with cells with or without 100 μM bestatin for 12 hours. Cell viability was determined by adding 20 μL of CellTiter-Blue® (Promega) to each well and incubating at 37°C for 1 hr. Fluorescence was measured at

$530_{ex}/590_{em}$ nm on a BioTek Synergy HT plate reader and cell viability was expressed as percent of solvent-treated control. Data were fitted to sigmoidal dose-response curves in GraphPad Prism 4.0 to determine IC_{50} values.

5.3.10 Microscopy

Glass cover slips were treated with poly-L-lysine for 1 hr at room temperature and then washed with PBS. Cells were seeded at a density of ~13000 cells/cm^2 approximately 36 hrs prior to drug treatment. Cells were treated with 15 μM prodrug or doxorubicin and incubated at 37°C for 6 hrs or 24 hrs. Cover slips were washed in serum-free, phenol-free RPMI-1640 media and mounted on glass slides. Cells were imaged with a Zeiss Axiovert 135 TV microscope (Carl Zeiss MicroImaging, LLC, Thornwood, NY) using a 63× oil immersion objective lens. A xenon lamp with 490 nm excitation filter and an 83101m emission filter (Chroma Technology Corp, Bellows Fall, VT) was used to acquire images of doxorubicin and doxorubicin prodrugs. Phase contrast and fluorescence images captured by a cooled CCD camera were overlayed using MetaMorph software.

5.3.11 Statistical analysis

Data were analyzed using GraphPad Prism 4 (GraphPad Software, Inc). A P-value of < 0.05 was considered statistically significant.

5.4 Results

5.4.1 Synthesis and pH stability

L-Lys-L-Ala-Dox, L-Lys-D-Ala-Dox, L-Ala-Dox, and D-Ala-Dox were synthesized according to the scheme shown in Figure 5.1 and purified to >90% purity. All prodrugs were stable in acidic (pH 4.0) and physiologic (pH 7.4) buffers, but not in a

basic (pH 9.8) buffer. When analyzed by HPLC, there was loss of total fluorescenceat pH 9.8, suggesting that doxorubicin itself is not stable in basic pH.

5.4.2 Hydrolysis of L-Lys-L-Ala-Doxorubicin by lysed cells

To verify that our screening system can be useful for rational prodrug design, we selected the promoiety lysine-alanine to make a doxorubicin prodrug. Because we did not know the subcellular localization of the protease responsible for hydrolyzing the lysine-alanine promoiety or the permeability of the doxorubicin prodrug, we began with lysed cells. MRC-5, MCF7, and BT-549 cells were lysed by incubating with 0.2% Triton X-100. The metabolite L-Ala-Dox was detectable in the BT-549 samples starting at the 10 min time point, while it was not detectable in the MRC-5 or MCF7 samples until the 30 min time point (Figure 5.2). This resulted in significantly higher amounts of L-Ala-Dox in the BT-549 cell lysates as compared to MRC-5 or MCF7 cell lysates at 60 min.

5.4.3 Hydrolysis of Dox prodrugs by whole cells

L-Lys-L-Ala-Dox (10 μM) was added to the media of whole cells in 96-well plates and incubated 0 to 24 hrs. The amount of prodrug and metabolites in the media was determined at several time points. The amount of L-Lys-L-Ala-Dox in the media decreased over time, with a corresponding increase in L-Ala-Dox (Figure 5.3). The rate at which this hydrolysis occurred was faster in the media of BT-549 cells compared to that in media of MRC-5 or MCF7 cells or media alone. The hydrolysis of L-Lys-L-Ala-Dox was significantly inhibited in all three cell lines by 100 μM bestatin (Figure 5.4); bestatin had no effect on the 48 hr cell viability (data not shown). There was no detectable hydrolysis of the other prodrugs, L-Lys-D-Ala-Dox, L-Ala-Dox or D-Ala-Dox, after 12 hrs.

5.4.4 Hydrolysis of L-Lys-L-Ala-Dox by transfected cells

HEK-293 cells were transfected with ANPEP, NPEPPS or DPP7 cDNA or mock-transfected (control). L-Lys-L-Ala-Dox (10 μM) was added to the media of the transfected cells and incubated 0 to 6 hrs. As seen in Figure 5.5, cells transfected with ANPEP or NPEPPS were able to hydrolyze L-Lys-L-Ala-Dox significantly faster than mock-transfected cells. This resulted in significantly shorter half-life values for L-Lys-L-Ala-Dox in ANPEP- and NPEPPS-transfected cells compared to mock-transfected cells (1.9 ± 0.3 hrs and 7.4 ± 0.7 hrs vs. 14.4 ± 1.1 hrs, respectively). There was no difference in hydrolysis rates of L-Lys-L-Ala-Dox in DPP7-transfected cells compared with mock-transfected (pcDNA3.1) cells.

5.4.5 Hydrolysis of L-Lys-L-Ala-AMC by transfected cells

HEK-293 cells were transfected with ANPEP or DPP7 cDNA or mock-transfected with empty pcDNA3.1 vector. L-Lys-L-Ala-AMC (100 μM) was added cells and incubated 30 min. As seen in Figure 5.5, cells transfected with ANPEP or DPP7 were able to hydrolyze L-Lys-L-Ala-AMC significantly faster than mock-transfected cells. When co-incubated with the inhibitor bestatin, hydrolysis of L-Lys-L-Ala-AMC was significantly inhibited in ANPEP-transfected cells, while bestatin had very little effect on L-Lys-L-Ala-AMC in DPP7-transfected cells.

5.4.6 Cytotoxicity of prodrugs

The IC_{50} of doxorubicin was similar for all three cell lines following a 12 hr incubation period (Figure 5.6). L-Lys-L-Ala-Dox, L-Lys-D-Ala-Dox, L-Ala-Dox, and D-Ala-Dox were incubated with cells for 12 hrs followed by a 48 hr incubation. As shown in Figure 5.6, all of the prodrugs significantly decreased cell viability compared to the

vehicle-treated control cells; however, they were not as toxic as the parent compound doxorubicin. The calculated IC_{50} values of the compounds are shown in Table 5.1. The MCF7 cells tended to be more resistant to the prodrugs than the other two cell lines. Despite the more extensive hydrolysis of L-Lys-L-Ala-Dox to L-Ala-Dox by BT-549 cells compared to MRC-5 cells, the IC_{50} values for L-Lys-L-Ala-Dox in the two cells were not significantly different. Furthermore, L-Ala-Dox had a lower IC_{50} value than L-Lys-L-Ala-Dox and L-Lys-D-Ala-Dox in all cell lines. The unhydrolyzed dipeptide prodrugs had higher IC_{50} values than their corresponding single amino acid prodrugs.

5.4.7 Microscopy

Fluorescence microscopy was used to image cells treated with dox and dox prodrugs. Despite the lack of hydrolysis to the parent compound doxorubicin, the prodrugs were able to accumulate in cells. All four prodrugs exhibited similar patterns of accumulation, with no differences between 6 hr and 24 hr incubation (24 hr data not shown). There was very little accumulation of the prodrugs in the nuclei of the cells, whereas the parent compound, doxorubicin, accumulated almost exclusively in the nuclei, as seen in the images in Figure 5.7. These differences in accumulation patterns may partially explain the differences in cytotoxicity between the prodrugs and doxorubicin.

5.5 Discussion

The dipeptide promoiety L-Lys-L-Ala was selected as the most promising promoiety from the screen with AMC and ACC compounds in Chapter 4. This promoiety was conjugated to doxorubicin to create the prodrug L-Lys-L-Ala-Dox. The prodrug L-Lys-D-Ala-Dox was synthesized and used as a negative control, as mixed D/L

dipeptides have been shown to be more resistant to hydrolysis (*36*); furthermore, we saw no hydrolysis of D-Ala-AMC in our screening system (Chapter 4). In addition, the potential intermediate metabolites L-Ala-Dox and D-Ala-Dox were synthesized. An HPLC method was established to separate the dipeptide prodrugs from the single amino acid intermediates and the parent compound, doxorubicin. All of the prodrugs were stable in acidic (pH 4.0) and physiologic (pH 7.4) buffers, so we would not expect to see any significant non-specific chemical hydrolysis *in vivo*.

The L-Lys-L-Ala promoiety, when conjugated to AMC or ACC, was previously shown to be hydrolyzed faster by BT-549 cells compared to MRC-5 or MCF7 cells (Chapter 4). We tested the hydrolysis of L-Lys-L-Ala-Dox in detergent-permeabilized MRC-5, MCF7, and BT-549 cells to ensure that hydrolysis was not limited by membrane permeability. As seen with the AMC and ACC compounds, L-Lys-L-Ala-Dox was hydrolyzed faster by BT-549 cells compared to MRC-5 or MCF7 cells. However, in the case of AMC or ACC conjugates, the entire peptide promoiety was removed from the parent compound. In the case of L-Lys-L-Ala-Dox, the lysine amino acid was cleaved from the prodrug to leave the intermediate metabolite L-Ala-Dox. Unfortunately, the cells appeared to be unable to remove the alanine amino acid from doxorubicin to generate the parent compound.

We then tested the hydrolysis of all four prodrugs in whole cells. Again, L-Lys-L-Ala-Dox was the only prodrug hydrolyzed, but was only hydrolyzed to L-Ala-Dox and not the parent compound, doxorubicin. The hydrolysis occurred significantly faster and to a greater extent in BT-549 cells compared to the other two cell lines or serum-containing media. As was shown in Chapter 4, alanyl aminopeptidase (APN, gene ID

ANPEP) is able to hydrolyze L-Lys-L-Ala-AMC and has greater mRNA expression in BT-549 cells. This, combined with the fact that only the lysine amino acid is cleaved from L-Lys-L-Ala-Dox suggests that an aminopeptidase, possibly APN, is involved in the faster hydrolysis of the prodrug in BT-549 cells. This conclusion is also supported by the observation that hydrolysis of L-Lys-L-Ala-Dox was significantly inhibited in cells that were preincubated with the aminopeptidase inhibitor bestatin. The lack of hydrolysis of L-Ala-Dox is potentially due to steric hindrance and could possibly be overcome through the use of a linker, which would be hydrolyzed following cleavage of L-Lys-L-Ala. One potential linker is the amino acid leucine. The prodrug N-L-leucyl-doxorubicin (Leu-Dox) has previously been synthesized and characterized and shown to be rapidly hydrolyzed in plasma following intravenous administration in humans (*37-41*). In the case of the hypothetical prodrug L-Lys-L-Ala-L-Leu-Dox, the Lys-Ala promoiety would be preferentially cleaved by BT-549 cells followed by cleavage of Leu, most likely by a different protease.

To further investigate which proteases might be involved in the prodrug hydrolysis, L-Lys-L-Ala-Dox was incubated with HEK-293 cells transfected with ANPEP, APP-S or DPP7 cDNA and the hydrolysis rates and half-lives were compared to the values from mock-transfected cells. While the promoiety L-Lys-L-Ala is a known substrate of DPP VII (*42*), there was no difference in the hydrolysis of L-Lys-L-Ala-Dox between DPP7- and mock-transfected cells. Alternatively, cells overexpressing the two aminopeptidases, APN and APP-S, were able to hydrolyze L-Lys-L-Ala-Dox to L-Ala-Dox significantly faster than mock-transfected cells. Once again, the cells were not able to cleave L-Ala from doxorubicin to generate the parent compound. Bestatin was able to inhibit

hydrolysis of L-Lys-L-Ala-AMC in ANPEP-transfected cells, but not in DPP7-transfected cells. Taken together with the ability of bestatin to inhibit hydrolysis in BT-549 cells, an aminopeptidase is the most likely responsible for the hydrolysis of L-Lys-L-Ala-Dox in whole cells.

Hydrolysis is only one factor in the design of a target-activated prodrug. It is also important that the prodrug have little to no cytotoxicity until activated. The IC_{50} values for all four prodrugs were significantly higher than the IC_{50} values for doxorubicin in MRC-5, MCF7, and BT-549 cells. While the differences were not as dramatic, the IC_{50} values for the single amino acid metabolites were significantly lower than the IC_{50} values for their corresponding dipeptide prodrugs, i.e. L-Ala-Dox compared to L-Lys-L-Ala-Dox and D-Ala-Dox compared to L-Lys-D-Ala-Dox. This suggests that lengthening the peptide promoiety could further decrease the cytotoxicity of the prodrug.

It was interesting that, despite the lack of hydrolysis, even L-Lys-D-Ala-Dox was able to affect the cell viability of all three cell lines. While doxorubicin has many proposed mechanisms of action (*33*), they all involve intracellular targets. Therefore, we hypothesized that the unhydrolyzed prodrugs were still able to permeate the cell membrane. This was tested by incubating the cells with each prodrug and using the fluorescent properties of doxorubicin to image the cellular accumulation and distribution in live cells. It appeared that all of the prodrugs and doxorubicin could permeate the cell membrane and accumulate inside the cells. However, the prodrugs appeared to accumulate outside the nucleus of the cell while doxorubicin mostly accumulated in the nucleus. The major mechanisms of doxorubicin action appear to be intercalation into the DNA helix and covalent binding to proteins involved in the replication and transcription

of DNA (*33*). Doxorubicin enters the cell by simple diffusion, but is believed to bind to the 20S proteasome to translocate into the nucleus through nuclear pores (*33*). The conjugation of amino acids or dipeptides to doxorubicin most likely prevents the binding of doxorubicin to the proteasome. Hence, the lack of hydrolysis of the prodrugs is most likely preventing it from being transported to the nucleus, thus mitigating its ability to affect cell viability.

While we were not able to achieve complete hydrolysis of the prodrugs to the parent compound, we did see differential hydrolysis of the lysyl group from L-Lys-L-Ala-Dox. It was encouraging to find that the screening with AMC/ACC compounds was partially able to predict differential hydrolysis. The partial hydrolysis might be able to be overcome through the use of a linking group. The prodrugs themselves retained some cytotoxicity, but were significantly less toxic than the parent compound doxorubicin. Also, the single amino acid prodrugs were more cytotoxic than their corresponding dipeptide prodrugs. Therefore, we may be able to render doxorubicin inactive by attaching longer peptide sequences. If that were the case, the single amino acid prodrug could then be the active metabolite at the target site. The inability of DPP7-transfected cells to activate the prodrug L-Lys-L-Ala-Dox emphasizes the need for future screening systems to contain several parent compounds with different physical characteristics including molecular weight and charge.

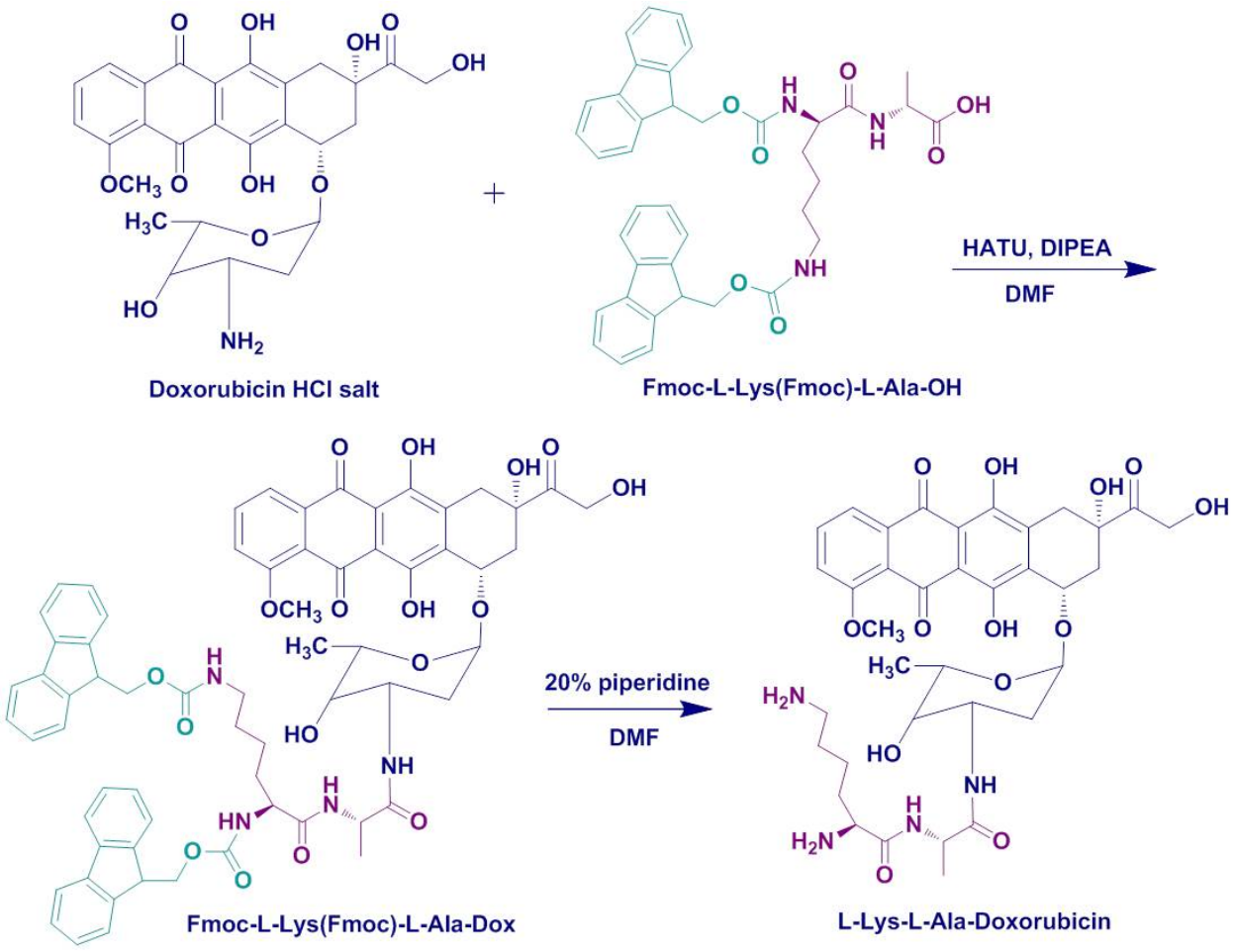

Figure 5.1 Synthesis scheme for L-Lys-L-Ala-Doxorubicin

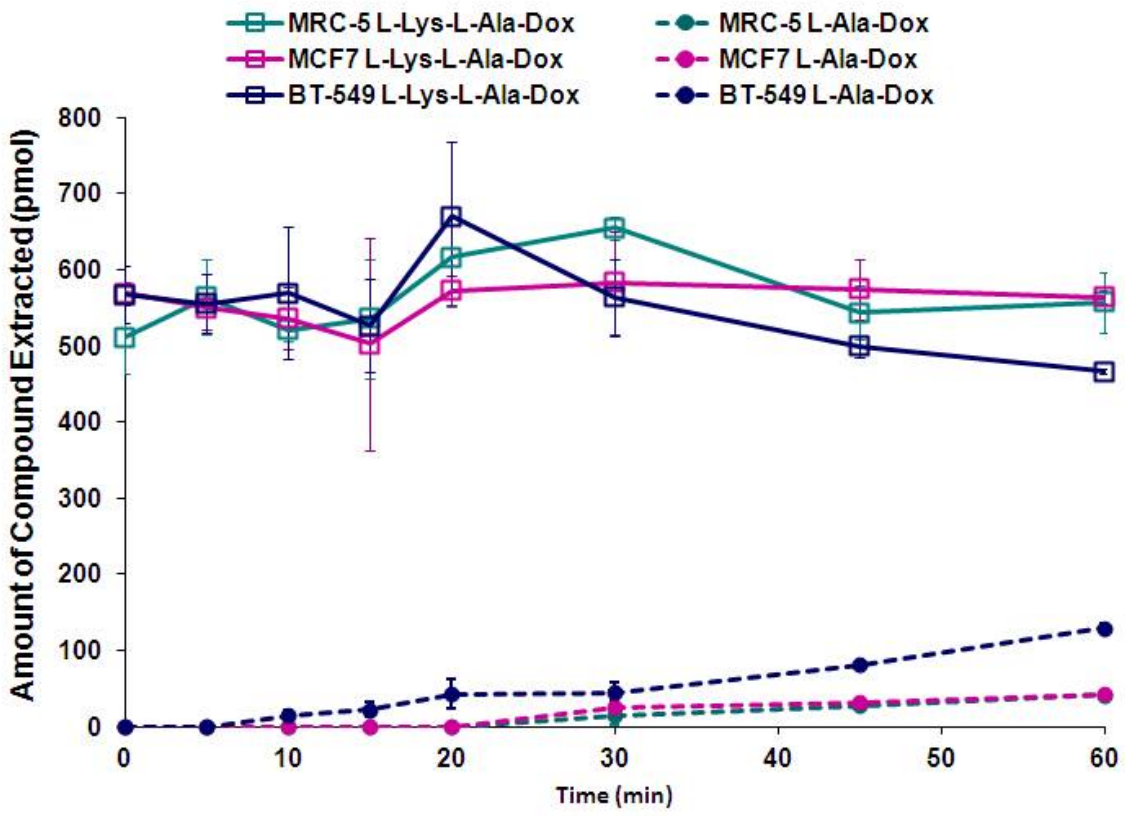

Figure 5.2 L-Lys-L-Ala-Dox is hydrolyzed significantly faster by detergent-permeabilized BT-549 cells.
L-Lys-L-Ala-Dox was incubated with MRC-5, MCF7, and BT-549 cells with detergent-permeabilized membranes. Samples (n = 3) were collected at 0, 5, 10, 15, 20, 30, 45, and 60 min and analyzed by HPLC with fluorescence detection. The amount of L-Lys-L-Ala-Dox and the metabolite L-Ala-Dox were plotted against time and analyzed by non-linear regression.

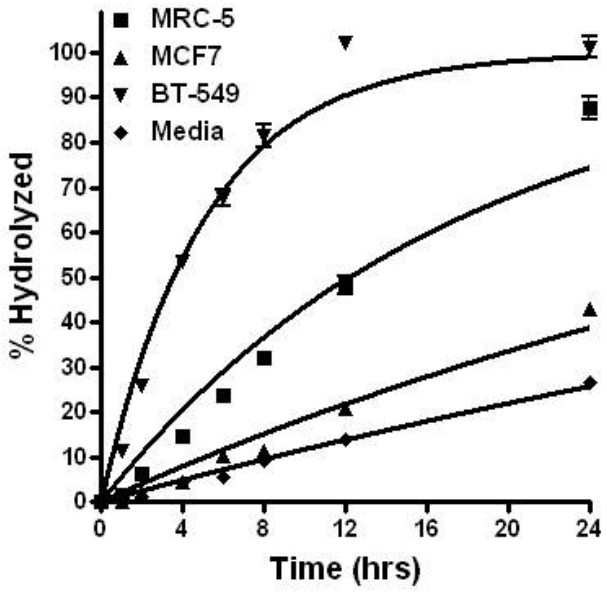

Figure 5.3 BT-549 cells hydrolyze L-Lys-L-Ala-Dox to L-Ala-Dox significantly faster than MRC-5 or MCF7 cells.
L-Lys-L-Ala-Dox was added to MRC-5, MCF7 or BT-549 cells or serum containing media. At 0, 1, 2, 3, 6, 12, and 24 hrs, media were collected and analyzed by HPLC. The amount of prodrug hydrolyzed to L-Ala-Dox was converted to the percent of total prodrug added at time 0 and plotted against time. GraphPad Prism was used to fit curves to the data using one phase exponential association.

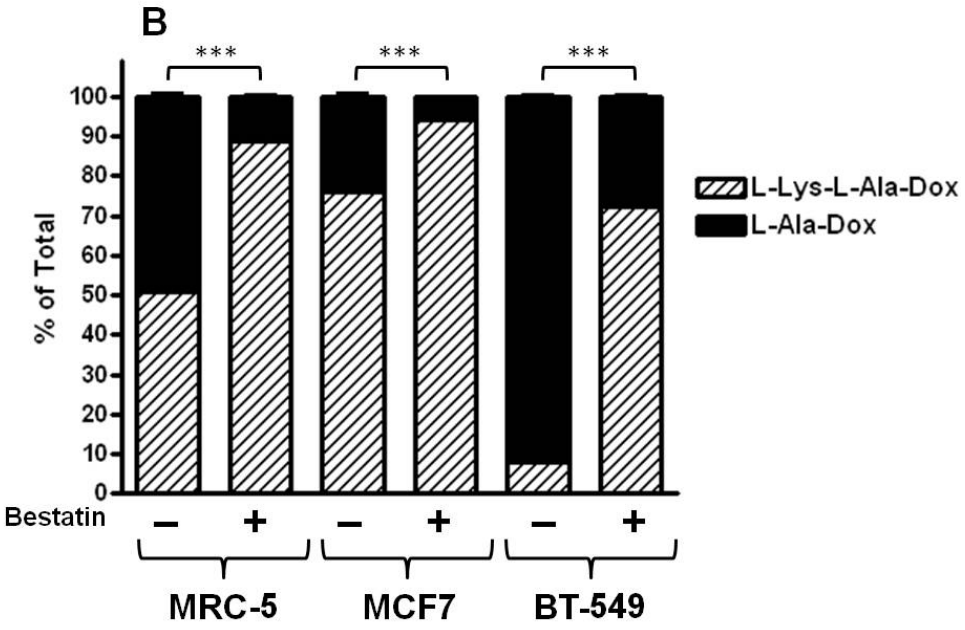

Figure 5.4 Bestatin inhibits whole-cell hydrolysis of L-Lys-L-Ala-Dox.
L-Lys-L-Ala-Dox was added to wells containing MRC-5, MCF7 or BT-549 cells pre-incubated with or without 100 μM bestatin, an aminopeptidase inhibitor. After a 12 hr incubation at 37°C, media were collected and analyzed by HPLC. The amount of prodrug (hashed bars) and the metabolite L-Ala-Dox (black bars) were calculated using a standard curve and converted to the percent of total compound recovered. Asterisks represent significant differences between cells with and without bestatin (***$P < 0.001$).

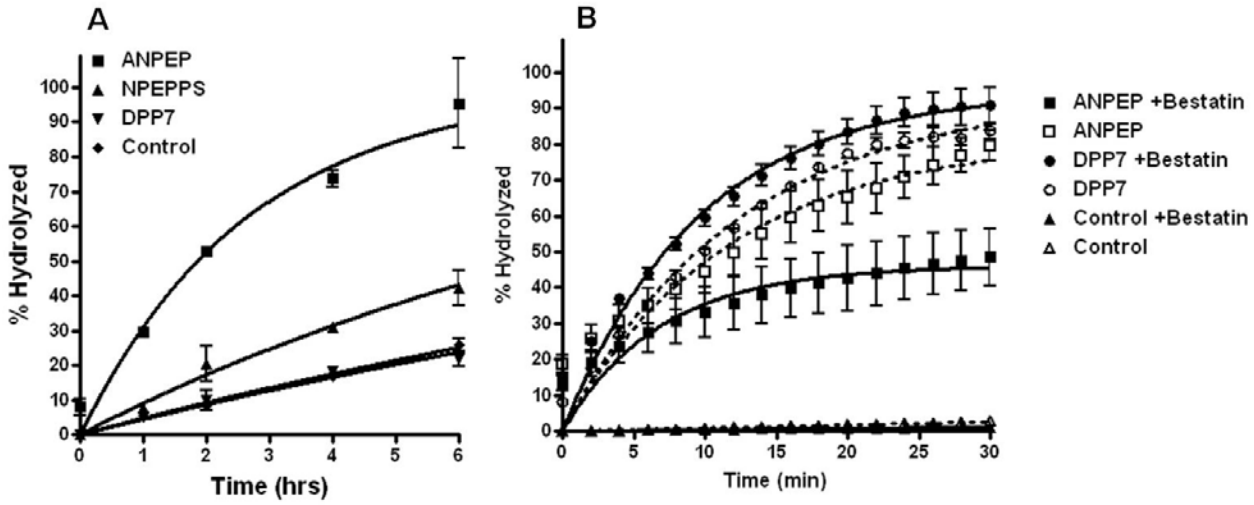

Figure 5.5 L-Lys-L-Ala-Dox and L-Lys-L-Ala-AMC are hydrolyzed faster by ANPEP-transfected HEK-293 cells.

HEK-293 cells were transiently transfected with ANPEP, NPEPPS or DPP7 cDNA or empty plasmid-transfected (control), 48-72 hrs prior to assays. (A) Following the addition of L-Lys-L-Ala-Dox, media were collected at 0, 1, 2, 4, and 6 hrs and analyzed by HPLC. Data are expressed as the percent of prodrug hydrolyzed over time. (B) L-Lys-L-Ala-AMC was incubated with transfected cells in the presence or absence of the inhibitor bestatin. Data are expressed as the percent of L-Lys-L-Ala-AMC hydrolyzed to AMC over time. GraphPad Prism was used to fit curves to the data using one phase exponential association.

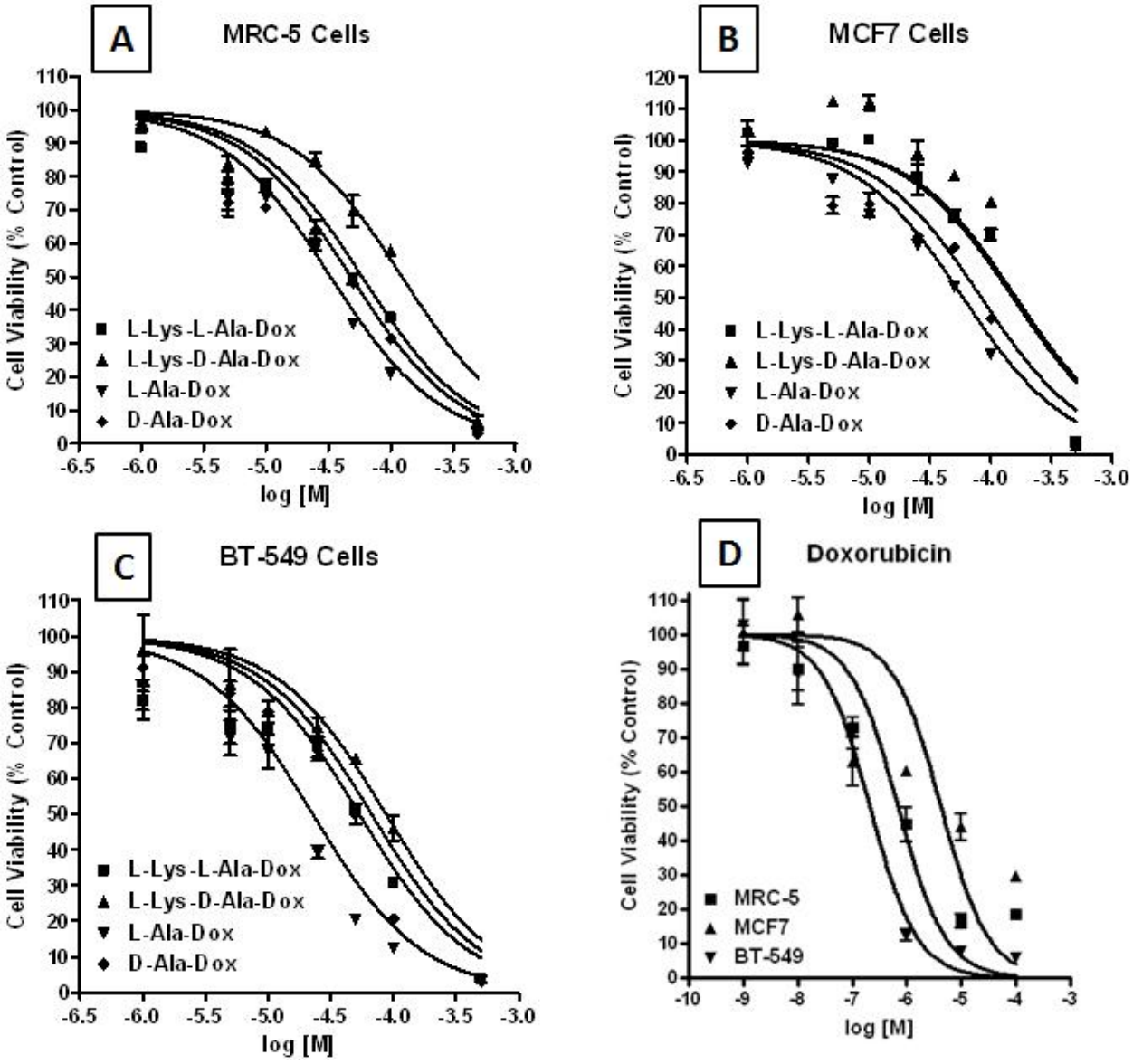

Figure 5.6 Prodrugs of doxorubicin retain some cytotoxicity.
L-Lys-L-Ala-Dox, L-Lys-D-Ala-Dox, L-Ala-Dox, and D-Ala-Dox were incubated at a final concentration of 1 to 500 μM to MRC-5, MCF7 or BT-549 cells for 12 hrs. Similarly, doxorubicin was incubated at a final concentration of 1 to 100 μM. Cell viability was determined by CellTiter Blue assay 48 hrs later. The percent cell viability was plotted against the log transformed concentration of prodrug to determine IC_{50} values for each compound using GraphPad Prism 4.0.

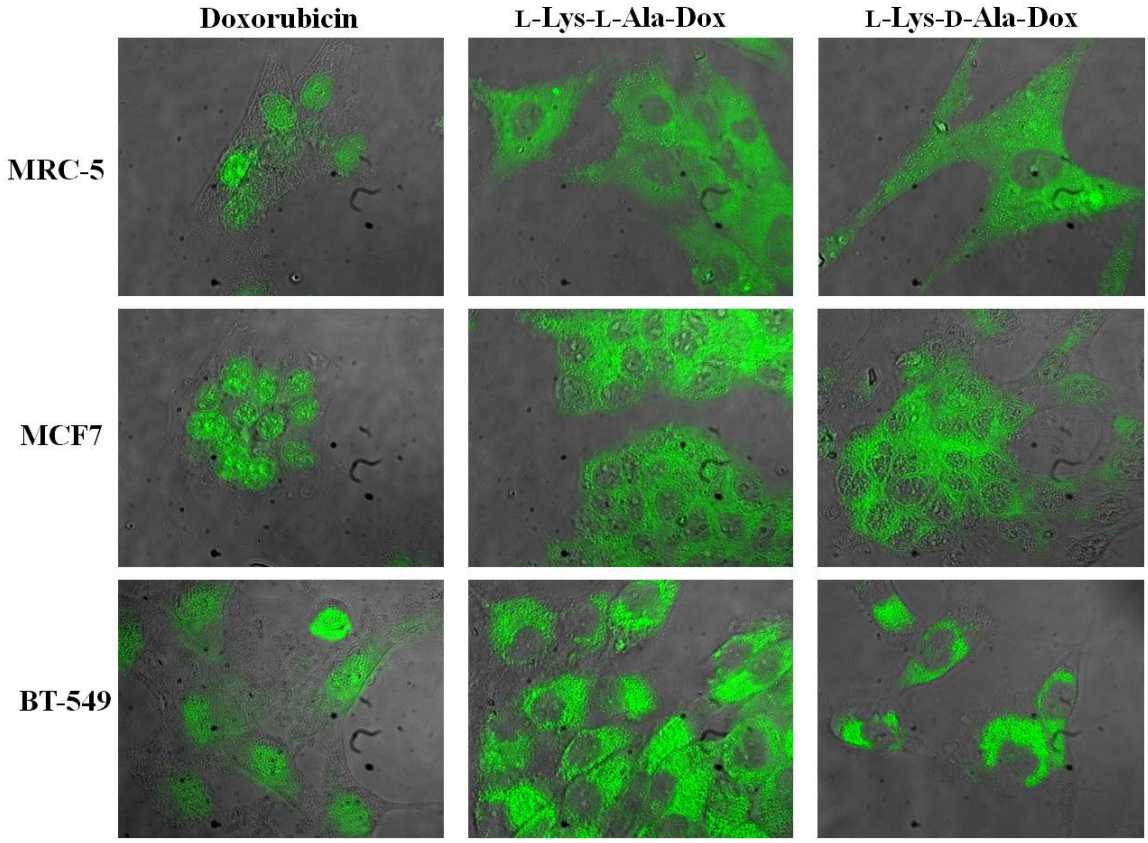

Figure 5.7 Doxorubicin prodrugs accumulate outside the nucleus.
Doxorubicin or L-Lys-L-Ala-Dox added at a final concentration of 15 μM MRC-5, MCF7 or BT-549 cells and incubated at 37°C for 6 hrs. Doxorubicin and doxorubicin prodrugs in live cells were imaged with a Zeiss Axiovert 135 TV microscope using a 63× oil immersion objective lens and a xenon lamp with a 490 nm excitation filter. Phase contrast and fluorescence images were overlayed using MetaMorph software.

Table 5.1 IC_{50} values of doxorubicin and dox prodrugs in MRC-5, MCF7, and BT-549 cells

L-Lys-L-Ala-Dox, L-Lys-D-Ala-Dox, L-Ala-Dox, and D-Ala-Dox were added at a final concentration of 1 to 500 μM to 96-well plates containing 5,000 MRC-5, MCF7 or BT-549 cells per well and incubated at 37°C. Similarly, doxorubicin was incubated at a final concentration of 1 to 100 μM. After 12 hrs, drug-containing media were replaced with fresh media and cells were incubated an additional 48 hrs. Cell viability was determined by CellTiter Blue assay. The IC_{50} values for each compound were compared by Two-way ANOVA using GraphPad Prism 4.0.

	MRC-5			MCF7			BT-549		
Compound	**Mean IC_{50} (M)**	**SD**	**Diff.**	**Mean IC_{50} (M)**	**SD**	**Diff.**	**Mean IC_{50} (M)**	**SD**	**Diff.**
L-Lys-L-Ala-Dox	5.83E-05	5.78E-06	a,d,†	1.48E-04	1.40E-05	a,‡	6.70E-05	3.97E-06	a,†
L-Lys-D-Ala-Dox	1.21E-04	4.76E-06	b,†	1.59E-04	7.12E-06	a,‡	9.00E-05	3.57E-05	b,§
L-Ala-Dox	3.31E-05	4.07E-06	c,†,‡	5.88E-05	2.12E-06	b,†	2.34E-05	4.79E-06	c,‡
D-Ala-Dox	4.76E-05	3.84E-06	c,d,†	8.31E-05	2.38E-06	c,‡	5.28E-05	4.48E-06	a,†
Dox	4.48E-07	2.92E-07	e,†	3.30E-07	5.55E-08	d,†	1.33E-07	7.76E-08	d,†

*Values with different letters within a column are significantly different from each other ($P < 0.05$) and values with different symbols within a row are significantly different from each other ($P < 0.05$).

5.6 References

1. Atkinson, J. M., Siller, C. S., and Gill, J. H. (2008) Tumour endoproteases: the cutting edge of cancer drug delivery?, *Br J Pharmacol 153*, 1344-1352.

2. Denny, W. A. (2001) Prodrug strategies in cancer therapy, *Eur J Med Chem 36*, 577-595.

3. Huang, P. S., and Oliff, A. (2001) Drug-targeting strategies in cancer therapy, *Curr Opin Genet Dev 11*, 104-110.

4. Lee, M., Fridman, R., and Mobashery, S. (2004) Extracellular proteases as targets for treatment of cancer metastases, *Chemical Society Reviews 33*, 401-409.

5. Overall, C. M., and Blobel, C. P. (2007) In search of partners: linking extracellular proteases to substrates, *Nat Rev Mol Cell Biol 8*, 245-257.

6. Dubowchik, G. M., and Firestone, R. A. (1998) Cathepsin B-sensitive dipeptide prodrugs. 1. A model study of structural requirements for efficient release of doxorubicin, *Bioorg Med Chem Lett 8*, 3341-3346.

7. Dubowchik, G. M., Mosure, K., Knipe, J. O., and Firestone, R. A. (1998) Cathepsin B-sensitive dipeptide prodrugs. 2. Models of anticancer drugs paclitaxel (Taxol), mitomycin C and doxorubicin, *Bioorg Med Chem Lett 8*, 3347-3352.

8. Schmid, B., Chung, D. E., Warnecke, A., Fichtner, I., and Kratz, F. (2007) Albumin-binding prodrugs of camptothecin and doxorubicin with an Ala-Leu-Ala-Leu-linker that are cleaved by cathepsin B: synthesis and antitumor efficacy, *Bioconjug Chem 18*, 702-716.

9. DeFeo-Jones, D., Brady, S. F., Feng, D.-M., Wong, B. K., Bolyar, T., Haskell, K., Kiefer, D. M., Leander, K., McAvoy, E., Lumma, P., Pawluczyk, J. M., Wai, J., Motzel, S. L., Keenan, K., Van Zwieten, M., Lin, J. H., Garsky, V. M., Freidinger, R., Oliff, A., and Jones, R. E. (2002) A Prostate-specific Antigen (PSA)-activated Vinblastine Prodrug Selectively Kills PSA-secreting Cells in Vivo, *Molecular Cancer Therapeutics 1*, 451-459.

10. DeFeo-Jones, D., Garsky, V. M., Wong, B. K., Feng, D. M., Bolyar, T., Haskell, K., Kiefer, D. M., Leander, K., McAvoy, E., Lumma, P., Wai, J., Senderak, E. T.,

Motzel, S. L., Keenan, K., Van Zwieten, M., Lin, J. H., Freidinger, R., Huff, J., Oliff, A., and Jones, R. E. (2000) A peptide-doxorubicin 'prodrug' activated by prostate-specific antigen selectively kills prostate tumor cells positive for prostate-specific antigen in vivo, *Nat Med 6*, 1248-1252.

11. Denmeade, S. R., and Isaacs, J. T. (1998) Enzymatic activation of prodrugs by prostate-specific antigen: targeted therapy for metastatic prostate cancer, *Cancer J Sci Am 4 Suppl 1*, S15-21.

12. Denmeade, S. R., Jakobsen, C. M., Janssen, S., Khan, S. R., Garrett, E. S., Lilja, H., Christensen, S. B., and Isaacs, J. T. (2003) Prostate-Specific Antigen-Activated Thapsigargin Prodrug as Targeted Therapy for Prostate Cancer, *Journal of the National Cancer Institute 95*, 990-1000.

13. Denmeade, S. R., Nagy, A., Gao, J., Lilja, H., Schally, A. V., and Isaacs, J. T. (1998) Enzymatic activation of a doxorubicin-peptide prodrug by prostate-specific antigen, *Cancer Res 58*, 2537-2540.

14. DiPaola, R. S., Rinehart, J., Nemunaitis, J., Ebbinghaus, S., Rubin, E., Capanna, T., Ciardella, M., Doyle-Lindrud, S., Goodwin, S., Fontaine, M., Adams, N., Williams, A., Schwartz, M., Winchell, G., Wickersham, K., Deutsch, P., and Yao, S. L. (2002) Characterization of a novel prostate-specific antigen-activated peptide-doxorubicin conjugate in patients with prostate cancer, *J Clin Oncol 20*, 1874-1879.

15. Elsadek, B., Graeser, R., Esser, N., Schäfer-Obodozie, C., Ajaj, K. A., Unger, C., Warnecke, A., Saleem, T., El-Melegy, N., Madkor, H., and Kratz, F. (2010) Development of a novel prodrug of paclitaxel that is cleaved by prostate-specific antigen: An in vitro and in vivo evaluation study, *European Journal of Cancer 46*, 3434-3444.

16. Khan, S. R., and Denmeade, S. R. (2000) In vivo activity of a PSA-activated doxorubicin prodrug against PSA-producing human prostate cancer xenografts, *Prostate 45*, 80-83.

17. Mhaka, A., Denmeade, S. R., Yao, W., Isaacs, J. T., and Khan, S. R. (2002) A 5-fluorodeoxyuridine prodrug as targeted therapy for prostate cancer, *Bioorganic & Medicinal Chemistry Letters 12*, 2459-2461.

18. Wong, B. K., DeFeo-Jones, D., Jones, R. E., Garsky, V. M., Feng, D. M., Oliff, A., Chiba, M., Ellis, J. D., and Lin, J. H. (2001) PSA-specific and non-PSA-

specific conversion of a PSA-targeted peptide conjugate of doxorubicin to its active metabolites, *Drug Metab Dispos 29*, 313-318.

19. Albright, C. F., Graciani, N., Han, W., Yue, E., Stein, R., Lai, Z., Diamond, M., Dowling, R., Grimminger, L., Zhang, S. Y., Behrens, D., Musselman, A., Bruckner, R., Zhang, M., Jiang, X., Hu, D., Higley, A., Dimeo, S., Rafalski, M., Mandlekar, S., Car, B., Yeleswaram, S., Stern, A., Copeland, R. A., Combs, A., Seitz, S. P., Trainor, G. L., Taub, R., Huang, P., and Oliff, A. (2005) Matrix metalloproteinase-activated doxorubicin prodrugs inhibit HT1080 xenograft growth better than doxorubicin with less toxicity, *Mol Cancer Ther 4*, 751-760.

20. Hu, Z., Jiang, X., Albright, C. F., Graciani, N., Yue, E., Zhang, M., Zhang, S. Y., Bruckner, R., Diamond, M., Dowling, R., Rafalski, M., Yeleswaram, S., Trainor, G. L., Seitz, S. P., and Han, W. (2010) Discovery of matrix metalloproteases selective and activated peptide-doxorubicin prodrugs as anti-tumor agents, *Bioorg Med Chem Lett 20*, 853-856.

21. Kline, T., Torgov, M. Y., Mendelsohn, B. A., Cerveny, C. G., and Senter, P. D. (2004) Novel antitumor prodrugs designed for activation by matrix metalloproteinases-2 and -9, *Mol Pharm 1*, 9-22.

22. Kratz, F., Drevs, J., Bing, G., Stockmar, C., Scheuermann, K., Lazar, P., and Unger, C. (2001) Development and in vitro efficacy of novel MMP2 and MMP9 specific doxorubicin albumin conjugates, *Bioorganic & Medicinal Chemistry Letters 11*, 2001-2006.

23. Lee, G. Y., Song, J. h., Kim, S. Y., Park, K., and Byun, Y. (2006) Peptide-doxorubicin conjugates specifically degraded by matrix metalloproteinases expressed from tumor, *Drug Development Research 67*, 438-447.

24. Van Valckenborgh, E., Mincher, D., Di Salvo, A., Van Riet, I., Young, L., Van Camp, B., and Vanderkerken, K. (2005) Targeting an MMP-9-activated prodrug to multiple myeloma-diseased bone marrow: a proof of principle in the 5T33MM mouse model, *Leukemia 19*, 1628-1633.

25. Liu, C., Sun, C., Huang, H., Janda, K., and Edgington, T. (2003) Overexpression of legumain in tumors is significant for invasion/metastasis and a candidate enzymatic target for prodrug therapy, *Cancer Res. 63*, 2957-2964.

26. Stern, L., Perry, R., Ofek, P., Many, A., Shabat, D., and Satchi-Fainaro, R. (2009) A Novel Antitumor Prodrug Platform Designed to Be Cleaved by the

Endoprotease Legumain, *Bioconjugate Chemistry 20*, 500-510.

27. Wu, W., Luo, Y., Sun, C., Liu, Y., Kuo, P., Varga, J., Xiang, R., Reisfeld, R., Janda, K. D., Edgington, T. S., and Liu, C. (2006) Targeting cell-impermeable prodrug activation to tumor microenvironment eradicates multiple drug-resistant neoplasms, *Cancer Res. 66*, 970-980.

28. Chung, D.-E., and Kratz, F. (2006) Development of a novel albumin-binding prodrug that is cleaved by urokinase-type-plasminogen activator (uPA), *Bioorganic & Medicinal Chemistry Letters 16*, 5157-5163.

29. Tsume, Y., Hilfinger, J. M., and Amidon, G. L. (2008) Enhanced Cancer Cell Growth Inhibition by Dipeptide Prodrugs of Floxuridine: Increased Transporter Affinity and Metabolic Stability, *Molecular Pharmaceutics 5*, 717-727.

30. Schmid, B. r., Warnecke, A., Fichtner, I., Jung, M., and Kratz, F. (2007) Development of Albumin-Binding Camptothecin Prodrugs Using a Peptide Positional Scanning Library, *Bioconjugate Chemistry 18*, 1786-1799.

31. Garsky, V. M., Lumma, P. K., Feng, D. M., Wai, J., Ramjit, H. G., Sardana, M. K., Oliff, A., Jones, R. E., DeFeo-Jones, D., and Freidinger, R. M. (2001) The synthesis of a prodrug of doxorubicin designed to provide reduced systemic toxicity and greater target efficacy, *J Med Chem 44*, 4216-4224.

32. Fernandez, A. M., Van Derpoorten, K., Dasnois, L., Lebtahi, K., Dubois, V., Lobl, T. J., Gangwar, S., Oliyai, C., Lewis, E. R., Shochat, D., and Trouet, A. (2001) N-Succinyl-(beta-alanyl-L-leucyl-L-alanyl-L-leucyl)doxorubicin: an extracellularly tumor-activated prodrug devoid of intravenous acute toxicity, *J Med Chem 44*, 3750-3753.

33. Carvalho, C., Santos, R. X., Cardoso, S., Correia, S., Oliveira, P. J., Santos, M. S., and Moreira, P. I. (2009) Doxorubicin: the good, the bad and the ugly effect, *Curr Med Chem 16*, 3267-3285.

34. Luu, T., Chung, C., and Somlo, G. Combining Emerging Agents in Advanced Breast Cancer, *Oncologist*.

35. Chia, S. K., Speers, C. H., D'Yachkova, Y., Kang, A., Malfair-Taylor, S., Barnett, J., Coldman, A., Gelmon, K. A., O'Reilly, S. E., and Olivotto, I. A. (2007) The impact of new chemotherapeutic and hormone agents on survival in a population-

based cohort of women with metastatic breast cancer, *Cancer 110*, 973-979.

36. Sykes, A. P., Lister, N., Bailey, P. D., Boyd, C. A. R., and Bronk, J. R. (1995) Dipeptide transport and hydrolysis in rat small intestine, in vitro, *Biochimica et Biophysica Acta (BBA) - Biomembranes 1237*, 70-76.

37. Bennis, S., Garcia, C., and Robert, J. (1993) Aspects of the cellular pharmacology of N-l-leucyldoxorubicin in human tumor cell lines, *Biochem Pharmacol 45*, 1929-1931.

38. Breistol, K., Hendriks, H. R., Berger, D. P., Langdon, S. P., Fiebig, H. H., and Fodstad, O. (1998) The antitumour activity of the prodrug N-L-leucyl-doxorubicin and its parent compound doxorubicin in human tumour xenografts, *Eur J Cancer 34*, 1602-1606.

39. Breistol, K., Hendriks, H. R., and Fodstad, O. (1999) Superior therapeutic efficacy of N-L-leucyl-doxorubicin versus doxorubicin in human melanoma xenografts correlates with higher tumour concentrations of free drug, *Eur J Cancer 35*, 1143-1149.

40. de Jong, J., Geijssen, G. J., Munniksma, C. N., Vermorken, J. B., and van der Vijgh, W. J. (1992) Plasma pharmacokinetics and pharmacodynamics of a new prodrug N-l-leucyldoxorubicin and its metabolites in a phase I clinical trial, *J Clin Oncol 10*, 1897-1906.

41. de Jong, J., Klein, I., Bast, A., and van der Vijgh, W. J. F. (1992) Analysis and pharmacokinetics of N-l-leucyldoxorubicin and metabolites in tissues of tumor-bearing BALB/c mice, *Cancer Chemotherapy and Pharmacology 31*, 156-160.

42. Maes, M. B., Lambeir, A. M., Gilany, K., Senten, K., Van der Veken, P., Leiting, B., Augustyns, K., Scharpe, S., and De Meester, I. (2005) Kinetic investigation of human dipeptidyl peptidase II (DPPII)-mediated hydrolysis of dipeptide derivatives and its identification as quiescent cell proline dipeptidase (QPP)/dipeptidyl peptidase 7 (DPP7), *Biochem J 386*, 315-324.

CHAPTER 6

Conclusions

6.1 Significance

We identified puromycin-sensitive aminopeptidase (APP-S) as one of the major proteases involved in the activation of the prodrug Val-Ser-cHPMPC. To our knowledge, we are the first to identify APP-S as an antiviral prodrug-activating enzyme. The broad tissue distribution of APP-S and other neutral aminopeptidases, as well as their homology and expression in a variety of species (*1-4*) can be advantageous for ensuring complete and rapid prodrug activation upon absorption, as was previously noted for Val-Ser-cHPMPC *in situ* (*5*). Additionally, APP-S has been shown to have a broad substrate specificity, with preference for hydrophobic and basic amino acids, (*6-10*). Thus, the amino acid/peptide promoiety of a prodrug could be modified to a variety of sequences to achieve desired chemical stability and/or solubility and still be a substrate of APP-S. The wide-range of substrates of APP-S make it an attractive target for future design of orally absorbed prodrugs. As evidenced by several leaving groups, APP-S appears to prefer the Ala residue over Val. This suggests the rate of prodrug activation *in vivo* could be controlled by modifying the amino acid promoiety.

APP-S has the potential to activate orally absorbed peptide prodrugs with a variety of sequences. Another application of peptide prodrugs is to target a specific protease in a target tissue as a way to improve site-specific delivery. We selected the cysteine endoprotease legumain, as it has been previously shown to be overexpressed in tumors

and effective in prodrug activation in cell culture and *in vivo* (*11-13*). However, some of the experiments showed that prodrugs were more effectively cleaved by the purified protease than by cells overexpressing legumain (*12*). To design a prodrug that is effectively cleaved at the target site, it would be useful to have a minimally invasive imaging agent to monitor cleavage of the promoiety *in vivo*. We synthesized a peptide-Gd-DTPA conjugate that, theoretically, should have been activated by legumain. We found we could detect 1.5-2.5-fold differences in relaxivities between the procontrast agents and their theoretical metabolites. Louie et al. (*14*) observed a 3-fold difference in relaxivity corresponded to a 57% enhancement in signal intensity *in vivo* when the procontrast agent EgadMe was activated by β-galactosidase. This suggests the 1.5-2.5-fold differences in the measured relaxivities for our peptide-Gd-DTPA procontrast agents should be sufficient to observe differences in signal enhancement upon activation *in vivo*. However, recombinant mouse legumain was unable to cleave the procontrast agent to a detectable amount. The protein structure of legumain has not been solved, but it is possible steric hindrance prevented legumain from activating the procontrast agents. The amino acid in the P1' position seems to have very little effect on substrate hydrolysis (*15*), however, legumain does require Asn in the P1 position and at least two amino acids N-terminal to the Asn residue in order to hydrolyze the substrate (*16*). In the case of Gd-DTPA-NWAE, if Asn is the P1 amino acid, this positions Gd-DTPA is the P2 amino acid. Gd-DTPA may be too dissimilar from a naturally occurring amino acid for legumain to recognize it as a substrate or the lack of an amino acid in the P3 position are also potential reasons for the lack of Gd-DTPA-NWAE activation by legumain. These issues could possibly be overcome by altering the structure of the procontrast agent such

that Gd-DTPA is in the P1' or P2' position through the use of a linker such as propanediamine. Additionally, we found that while purified recombinant legumain was able to efficiently hydrolyze the model substrate Z-AAN-AMC, there was minimal hydrolysis (<12% over 2 hrs) of the compound when incubated with legumain-expressing HEK-293 (HEK-LEG) cells. While our procontrast agent may be an effective way to monitor protease activity *in vivo*, legumain may not be the best target for a prodrug approach. Furthermore, screening the activity of a purified protease may not be the most effective strategy for rational prodrug design.

As an alternative to producing and purifying recombinant proteases, we a more accurate approach would be to screen promoieties in a whole-cell system to account for the activity of other proteases as well as changes in protease activity in live cells compared to a purified recombinant protease. The MRI procontrast agent has the potential to be used for in *vivo* monitoring of enzymatic activity, but a less labor intensive approach for was desired for promoiety screening purposes. Therefore, we selected the fluorescent compound 7-amino-4-methylcoumarin (AMC), which allowed us to monitor hydrolysis in real-time in a 96-well format. After verifying we could monitor the activity of artificially overexpressed proteases in live cells using known substrates, we began screening endogenously expressed proteases in cultured cells. We selected MCF7 cells, a relatively noninvasive breast cancer cell line (*17*), BT-549 cells, a highly invasive breast cancer cell line (*17*), and MRC-5 cells, an immortalized fibroblast cell line. A fibroblast cell line was chosen as our control cells because fibroblasts are known to express proteases involved in extracellular matrix (ECM) remodeling (*18, 19*), while highly invasive cancer cells have been shown to overexpress proteases needed for ECM

degradation (*20-22*). Without knowing the exact expression levels of proteases, we were able to identify several substrates that were preferentially hydrolyzed by BT-549 cells compared to MCF7 and MRC-5 cells. These substrate preferences held true even when the AMC leaving group was replaced with ACC (7-amino-4-carbamoylmethylcoumarin). There have been other attempts to determine whole cell proteolytic activity (*23*, *24*) and coumarin-based compounds have been used to screen selectivity of purified proteases (*25-27*). However, to our knowledge, this is the first time these fluorescent compounds have been used to determine proteolytic profiles of live whole cells.

The screening with AMC and ACC conjugates showed select peptides such as Lys-Ala were preferentially cleaved by the highly invasive BT-549 breast cancer cells, however, for this system to be useful in prodrug design, the screening results should be applicable to a pharmacologically active drug. To test this, we synthesized L-Lys-L-Ala-doxorubicin as well as the negative control L-Lys-D-Ala-doxorubicin and the theoretical metabolites L-Ala-doxorubicin and D-Ala-doxorubicin . We found that the prodrug L-Lys-L-Ala-doxorubicin was preferentially, but incompletely, hydrolyzed by BT-549 cells, while there was no hydrolysis of the other doxorubicin prodrugs. Also, L-Lys-L-Ala-doxorubicin did not appear to be hydrolyzed by dipeptidyl peptidase VII (DPP7), the expected protease, but was hydrolyzed by the aminopeptidases alanyl aminopeptidase (APN) and puromycin-sensitive aminopeptidase (APP-S). The L-Lys-L-Ala promoiety was preferentially and completely cleaved by DPP7, APN, and BT-549 cells when conjugated to AMC, but hydrolysis was incomplete when conjugated to Dox. The inability to hydrolyze L-Ala-Dox to Dox may be due to steric hindrance, thus, a linker between L-Lys-L-Ala and Dox may result in more complete hydrolysis. The prodrug

leucine-doxorubicin (Leu-Dox) has previously been synthesized and characterized *in vitro* and *in vivo* (*28-32*). Leu-Dox was shown to be rapidly converted to Dox as determined by plasma concentrations following intravenous administration in human subjects (*31*). Based on the rapid hydrolysis of Leu-Dox, the use of leucine as a linker to form the prodrug L-Lys-L-Ala-L-Leu-Dox could result in more complete hydrolysis of the prodrug to the more active parent compound, Dox, while maintaining selective activation by BT-549 cells due to the L-Lys-L-Ala promoiety.

The IC_{50} values for all four doxorubicin prodrugs were significantly higher than those of doxorubicin itself in each of the tested cell lines, but the unhydrolyzed prodrugs were still able to affect cell viability. When drug distribution was visualized by microscopy, it was seen that the parent compound doxorubicin appeared to accumulate in the nuclei of cells while the prodrugs primarily accumulated in the cytosol of cells. Interestingly, even L-Lys-D-Ala-doxorubicin was able to accumulate in the cells. As L-Lys-D-Ala-doxorubicin was not hydrolyzed and L-D-dipeptides are poor substrates for transporters like PEPT1 (*33, 34*), it is most likely the prodrugs, like doxorubicin itself, enter the cell through passive diffusion. It has been proposed that doxorubicin binds the 20S proteasomal subunit for translocation into the nucleus, where is dissociates from the proteasome and binds DNA due to its higher affinity for DNA (*35*). Conjugation of an amino acid or peptide to doxorubicin may affect its ability to bind to the proteasome, resulting in reduced accumulation in the nuclei of cells. Furthermore, it has been shown that amino acid and dipeptide derivatives of daunorubicin, an anthracycline with a similar structure to doxorubicin as shown in Figure 6.1, have significantly reduced DNA binding affinities (*36*). The reduced affinity for DNA may also play a role in the reduced

accumulation of doxorubicin prodrugs in cell nuclei. The intracellular accumulation, reduced cytotoxicity, and limited hydrolysis to the parent compound seen with the doxorubicin prodrugs were similar to the results reported by Baurain et al. for amino acid and dipeptide prodrugs of daunorubicin (*37*). When given intravenously, the daunorubicin prodrugs delayed tumor development significantly better than daunorubicin with reduced acute toxicity as determined by weight loss and mouse survival (*37*). The results from Baurain et al. (*37*) suggest that L-Lys-L-Ala-doxorubicin has the potential to limit BT-549 tumor cell progression with reduced overall toxicity as compared to doxorubicin *in vivo*.

6.2 Future Directions

Rational prodrug design could be significantly improved with a better understanding of how proteases work together to activate a peptide prodrug. As previously mentioned, the screening system should be composed of a variety of imaging agents with different physicochemical properties. As previously noted by Harris et al. (*26*), the ability of ACC to be attached to Rink amide resin allows for the efficient solid-phase synthesis of a library of amino acid and peptide conjugates of ACC. Thus, synthesis of a more complete library for screening would be highly beneficial. We were able to identify amino acid and dipeptide promoieties that were preferentially hydrolyzed by BT-549 breast cancer cells compared to the control cells, MRC-5 fibroblasts, from a very small subset of compounds. Based on this, we would expect to find additional promoieties that are differentially activated in a more complete library of dipeptides.

Any future screening should include screening proteolytic activity of serum and metabolic tissues such as liver cells. As was seen in Chapter 4, there can be significant

hydrolysis of peptide prodrugs in serum and liver cells, two potential sites of metabolism *in vivo*, and a targeted prodrug should have minimal hydrolysis prior to reaching the target tissue. It would also be useful to explore the use of N-terminal protecting groups such as Boc (*tert*-Butyl carbamate) or Ac (acetyl) to improve the enzymatic stability of the prodrugs in plasma to limit the activation of the prodrug prior to reaching the target site.

ACC and many ACC conjugates are readily able to permeate cell membranes and are useful in determining the proteolytic profile of the entire cell, including intracellular proteases. However, not all prodrugs are cell-permeant. To distinguish between intracellular and extracellular proteolytic activity, it would be useful to have an imaging agent that does not permeate the cell membrane. The contrast agent Gd-DTPA is non-cell permeant, and we were able to distinguish between peptide conjugates of Gd-DTPA and the parent compound by changes in NMR signal enhancement. A procontrast agent would also be useful in determining enzymatic activity *in vivo* in a minimally invasive manner. However, it is not very practical to synthesize and analyze a complete library of contrast agents; therefore, a procontrast agent approach might be more suitable for confirming activation of lead promoieties. A compound that might better suit our screening needs is aminoluciferin. Luciferin and aminoluciferin are substrates for firefly luciferase and emit light when oxidized by luciferase (*38*). However, when an amino acid or peptide is conjugated to aminoluciferin, it is no longer a substrate for luciferase (*38, 39*). Cleavage of the peptide bond can therefore be monitored by the subsequent oxidation of aminoluciferin by luciferase and emission of bioluminescence, as illustrated in Figure 6.2. Similarly to AMC and ACC, this bioluminescence can be assayed in a 96-

well format and protease activity measured in real-time. Unlike AMC and ACC, however, aminoluciferin does not require excitation by an external light source; thus it has a lower background signal and is more suitable for *in vivo* imaging in luciferase-transgenic small animals (*40-42*). Aminoluciferin has different physicochemical properties from AMC and ACC and does not permeate the cell membrane as easily (*42*). This was evidenced when Gly-Pro-aminoluciferin was incubated with HEK-293 cells expressing the cytosolic dipeptidase DPP9. Gly-Pro-aminoluciferin hydrolysis was similar in mock-transfected and DPP9-transfected cells, but significantly enhanced in DPP9-transfected cells that were co-transfected with the peptide transporter PepT1 (Z. Walls and K-D Lee, *unpublished data*).

In conclusion, we believe this screening system can be applied to select promoieties for the design of target-activated prodrugs with a wide range of chemical structures. While doxorubicin contains a primary amine group for direct conjugation of peptides, this strategy does not exclude drugs without a primary amine group. The lack of a primary amine group could be overcome through the use of a linker, which may also be useful in overcoming steric hindrance. Finally, a similar screening strategy could be applied to ester peptide prodrugs with variations of the screening compounds previously mentioned. For example, a valylester conjugate of D-luciferin has been shown to be preferentially hydrolyzed by *E. coli* expressing valacyclovirase (Z. Walls, J. Sun, and K-D Lee, *unpublished data*). Once the proteolytic profiles of all cells are more clearly understood, the *in vivo* activation of targeted peptide prodrugs can be more accurately predicted.

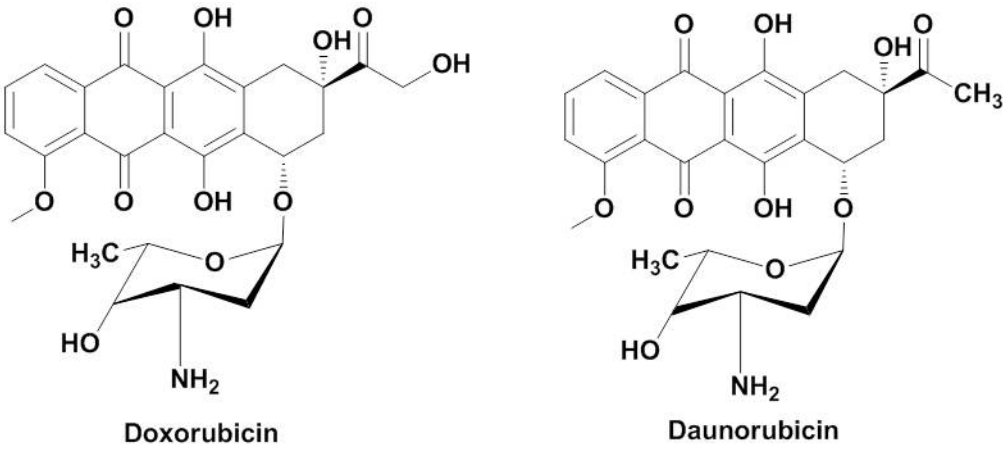

Figure 6.1 Structures of doxorubicin (Dox) and Daunorubicin (DNR)

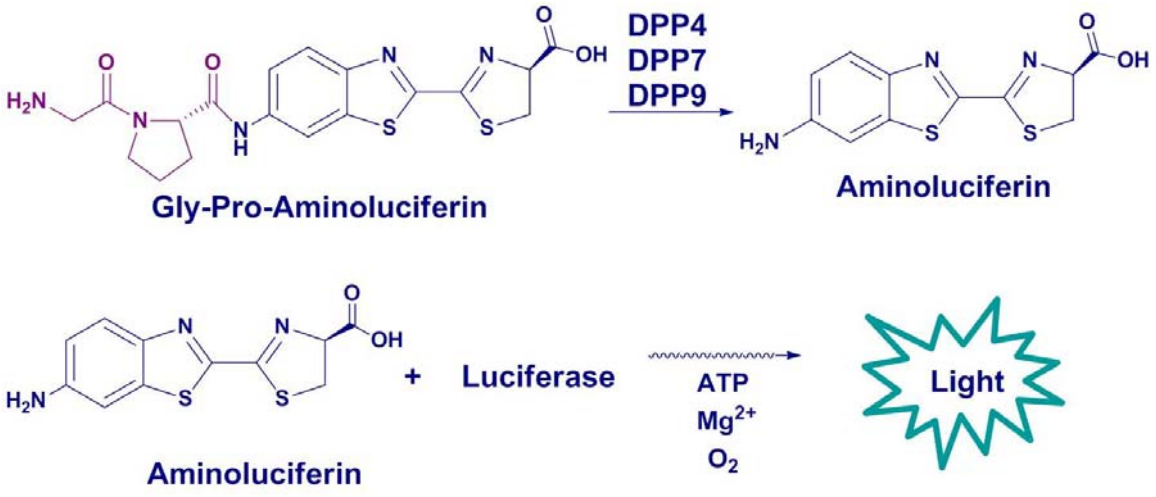

Figure 6.2 Activation of Gly-Pro-Aminoluciferin

6.3 References

1. Constam, D. B., Tobler, A. R., Rensing-Ehl, A., Kemler, I., Hersh, L. B., and Fontana, A. (1995) Puromycin-sensitive aminopeptidase. Sequence analysis, expression, and functional characterization, *J Biol.Chem. 270*, 26931-26939.

2. McLellan, S., Dyer, S. H., Rodriguez, G., and Hersh, L. B. (1988) Studies on the tissue distribution of the puromycin-sensitive enkephalin-degrading aminopeptidases, *J Neurochem 51*, 1552-1559.

3. Schulz, C., Perezgasga, L., and Fuller, M. T. (2001) Genetic analysis of dPsa, the Drosophila orthologue of puromycin-sensitive aminopeptidase, suggests redundancy of aminopeptidases, *Dev Genes Evol 211*, 581-588.

4. Tobler, A. R., Constam, D. B., Schmitt-Graff, A., Malipiero, U., Schlapbach, R., and Fontana, A. (1997) Cloning of the human puromycin-sensitive aminopeptidase and evidence for expression in neurons, *J Neurochem. 68*, 889-897.

5. Eriksson, U., Peterson, L. W., Kashemirov, B. A., Hilfinger, J. M., Drach, J. C., Borysko, K. Z., Breitenbach, J. M., Kim, J. S., Mitchell, S., Kijek, P., and McKenna, C. E. (2008) Serine Peptide Phosphoester Prodrugs of Cyclic Cidofovir: Synthesis, Transport, and Antiviral Activity, *Molecular Pharmaceutics 5*, 598-609.

6. Hui, K. S., Wang, Y. J., and Lajtha, A. (1983) Purification and characterization of an enkephalin aminopeptidase from rat brain membranes, *Biochemistry (Mosc). 22*, 1062-1067.

7. Johnson, G. D., and Hersh, L. B. (1990) Studies on the subsite specificity of the rat brain puromycin-sensitive aminopeptidase, *Arch. Biochem. Biophys. 276*, 305-309.

8. Schnebli, H. P., Phillipps, M. A., and Barclay, R. K. (1979) Isolation and characterization of an enkephalin-degrading aminopeptidase from rat brain, *Biochim. Biophys. Acta 569*, 89-98.

9. Sengupta, S., Horowitz, P. M., Karsten, S. L., Jackson, G. R., Geschwind, D. H., Fu, Y., Berry, R. W., and Binder, L. I. (2006) Degradation of Tau Protein by Puromycin-Sensitive Aminopeptidase in Vitro, *Biochemistry (Mosc). 45*, 15111-15119.

10. Wagner, G. W., Tavianini, M. A., Herrmann, K. M., and Dixon, J. E. (1981) Purification and characterization of an enkephalin aminopeptidase from rat brain, *Biochemistry (Mosc). 20*, 3884-3890.

11. Liu, C., Sun, C., Huang, H., Janda, K., and Edgington, T. (2003) Overexpression of legumain in tumors is significant for invasion/metastasis and a candidate enzymatic target for prodrug therapy, *Cancer Res. 63*, 2957-2964.

12. Stern, L., Perry, R., Ofek, P., Many, A., Shabat, D., and Satchi-Fainaro, R. (2009) A Novel Antitumor Prodrug Platform Designed to Be Cleaved by the Endoprotease Legumain, *Bioconjugate Chemistry 20*, 500-510.

13. Wu, W., Luo, Y., Sun, C., Liu, Y., Kuo, P., Varga, J., Xiang, R., Reisfeld, R., Janda, K. D., Edgington, T. S., and Liu, C. (2006) Targeting cell-impermeable prodrug activation to tumor microenvironment eradicates multiple drug-resistant neoplasms, *Cancer Res. 66*, 970-980.

14. Louie, A. Y., Huber, M. M., Ahrens, E. T., Rothbacher, U., Moats, R., Jacobs, R. E., Fraser, S. E., and Meade, T. J. (2000) In vivo visualization of gene expression using magnetic resonance imaging, *Nat.Biotechnol. 18*, 321-325.

15. Schwarz, G., Brandenburg, J., Reich, M., Burster, T., Driessen, C., and Kalbacher, H. (2002) Characterization of legumain, *Biol Chem 383*, 1813-1816.

16. Dando, P. M., Fortunato, M., Smith, L., Knight, C. G., McKendrick, J. E., and Barrett, A. J. (1999) Pig kidney legumain: an asparaginyl endopeptidase with restricted specificity, *Biochem.J 339 (Pt 3)*, 743-749.

17. Nagaraja, G. M., Othman, M., Fox, B. P., Alsaber, R., Pellegrino, C. M., Zeng, Y., Khanna, R., Tamburini, P., Swaroop, A., and Kandpal, R. P. (2006) Gene expression signatures and biomarkers of noninvasive and invasive breast cancer cells: comprehensive profiles by representational difference analysis, microarrays and proteomics, *Oncogene 25*, 2328-2338.

18. Kurihara, Y., Hatori, M., Ando, Y., Ito, D., Toyoshima, T., Tanaka, M., and Shintani, S. (2009) Inhibition of cyclooxygenase-2 suppresses the invasiveness of oral squamous cell carcinoma cell lines via down-regulation of matrix metalloproteinase-2 production and activation, *Clin Exp Metastasis 26*, 425-432.

19. Amenta, J. S., Sargus, M. J., and Baccino, F. M. (1978) Inhibition of basal protein

degradation in rat embryo fibroblasts by cycloheximide: Correlation with activities of lysosomal proteases, *Journal of Cellular Physiology 97*, 267-283.

20. Fingleton, B. (2006) Matrix metalloproteinases: roles in cancer and metastasis, *Front Biosci 11*, 479-491.

21. Terauchi, M., Kajiyama, H., Shibata, K., Ino, K., Nawa, A., Mizutani, S., and Kikkawa, F. (2007) Inhibition of APN/CD13 leads to suppressed progressive potential in ovarian carcinoma cells, *BMC Cancer 7*, 140.

22. Decock, J., Paridaens, R., and Cufer, T. (2005) Proteases and metastasis: clinical relevance nowadays?, *Curr Opin Oncol 17*, 545-550.

23. Cloutier, S. M., Kundig, C., Gygi, C. M., Jichlinski, P., Leisinger, H. J., and Deperthes, D. (2004) Profiling of proteolytic activities secreted by cancer cells using phage display substrate technology, *Tumour Biol 25*, 24-30.

24. Trouet, A., Passioukov, A., Van derpoorten, K., Fernandez, A. M., Abarca-Quinones, J., Baurain, R., Lobl, T. J., Oliyai, C., Shochat, D., and Dubois, V. (2001) Extracellularly tumor-activated prodrugs for the selective chemotherapy of cancer: application to doxorubicin and preliminary in vitro and in vivo studies, *Cancer Res 61*, 2843-2846.

25. Gosalia, D. N., Salisbury, C. M., Maly, D. J., Ellman, J. A., and Diamond, S. L. (2005) Profiling serine protease substrate specificity with solution phase fluorogenic peptide microarrays, *PROTEOMICS 5*, 1292-1298.

26. Harris, J. L., Backes, B. J., Leonetti, F., Mahrus, S., Ellman, J. A., and Craik, C. S. (2000) Rapid and general profiling of protease specificity by using combinatorial fluorogenic substrate libraries, *Proc Natl Acad Sci U S A 97*, 7754-7759.

27. Maly, D. J., Huang, L., and Ellman, J. A. (2002) Combinatorial strategies for targeting protein families: application to the proteases, *Chembiochem 3*, 16-37.

28. Bennis, S., Garcia, C., and Robert, J. (1993) Aspects of the cellular pharmacology of N-l-leucyldoxorubicin in human tumor cell lines, *Biochem Pharmacol 45*, 1929-1931.

29. Breistol, K., Hendriks, H. R., Berger, D. P., Langdon, S. P., Fiebig, H. H., and Fodstad, O. (1998) The antitumour activity of the prodrug N-L-leucyl-doxorubicin and its parent compound doxorubicin in human tumour xenografts, *Eur J Cancer 34*, 1602-1606.

30. Breistol, K., Hendriks, H. R., and Fodstad, O. (1999) Superior therapeutic efficacy of N-L-leucyl-doxorubicin versus doxorubicin in human melanoma xenografts correlates with higher tumour concentrations of free drug, *Eur J Cancer 35*, 1143-1149.

31. de Jong, J., Geijssen, G. J., Munniksma, C. N., Vermorken, J. B., and van der Vijgh, W. J. (1992) Plasma pharmacokinetics and pharmacodynamics of a new prodrug N-l-leucyldoxorubicin and its metabolites in a phase I clinical trial, *J Clin Oncol 10*, 1897-1906.

32. de Jong, J., Klein, I., Bast, A., and van der Vijgh, W. J. F. (1992) Analysis and pharmacokinetics of N-l-leucyldoxorubicin and metabolites in tissues of tumor-bearing BALB/c mice, *Cancer Chemotherapy and Pharmacology 31*, 156-160.

33. Brandsch, M., Knütter, I., and Leibach, F. H. (2004) The intestinal H+/peptide symporter PEPT1: structure-affinity relationships, *European Journal of Pharmaceutical Sciences 21*, 53-60.

34. Lister, N., Sykes, A. P., Bailey, P. D., Boyd, C. A., and Bronk, J. R. (1995) Dipeptide transport and hydrolysis in isolated loops of rat small intestine: effects of stereospecificity, *J Physiol 484 (Pt 1)*, 173-182.

35. Carvalho, C., Santos, R. X., Cardoso, S., Correia, S., Oliveira, P. J., Santos, M. S., and Moreira, P. I. (2009) Doxorubicin: the good, the bad and the ugly effect, *Curr Med Chem 16*, 3267-3285.

36. Masquelier, M., Baurain, R., and Trouet, A. (1980) Amino acid and dipeptide derivatives of daunorubicin. 1. Synthesis, physicochemical properties, and lysosomal digestion, *Journal of Medicinal Chemistry 23*, 1166-1170.

37. Baurain, R., Masquelier, M., Deprez-De Campeneere, D., and Trouet, A. (1980) Amino acid and dipeptide derivatives of daunorubicin. 2. Cellular pharmacology and antitumor activity of L1210 leukemic cells in vitro and in vivo, *Journal of Medicinal Chemistry 23*, 1171-1174.

38. Takakura, H., Kojima, R., Urano, Y., Terai, T., Hanaoka, K., and Nagano, T. (2011) Aminoluciferins as Functional Bioluminogenic Substrates of Firefly Luciferase, *Chemistry – An Asian Journal 6*, 1800-1810.

39. Moravec, R. A., O'Brien, M. A., Daily, W. J., Scurria, M. A., Bernad, L., and Riss, T. L. (2009) Cell-based bioluminescent assays for all three proteasome activities in a homogeneous format, *Analytical Biochemistry 387*, 294-302.

40. Dragulescu-Andrasi, A., Liang, G., and Rao, J. (2009) In Vivo Bioluminescence Imaging of Furin Activity in Breast Cancer Cells Using Bioluminogenic Substrates, *Bioconjugate Chemistry 20*, 1660-1666.

41. Hickson, J., Ackler, S., Klaubert, D., Bouska, J., Ellis, P., Foster, K., Oleksijew, A., Rodriguez, L., Schlessinger, S., Wang, B., and Frost, D. (2010) Noninvasive molecular imaging of apoptosis in vivo using a modified firefly luciferase substrate, Z-DEVD-aminoluciferin, *Cell Death Differ 17*, 1003-1010.

42. Shinde, R., Perkins, J., and Contag, C. H. (2006) Luciferin Derivatives for Enhanced in Vitro and in Vivo Bioluminescence Assays *Biochemistry 45*, 11103-11112.

APPENDIX A

Effect of pH and serum starvation on proteolytic profiles of cells

A.1 Summary

In addition to being targets for anticancer compounds, proteases have been used for prognostic purposes. While many proteases have already been identified, there are probably many more yet to be identified. We used cell lysates to determine whether pH had an effect on the hydrolysis of a simple compound such as AMC (7-amino-4-methylcoumarin) conjugated to a single amino acid. To better mimic the conditions of a solid tumor, we then measured the hydrolysis of Ala-AMC in whole cells under serum-starvation conditions at two different pHs. Finally, we chose cell lines from three different tissue sources known to play a role in metabolism and examined their proteolytic profiles. Based on whole-cell data, we found that a simple compound such as X-AMC (where X equals an amino acid) can be used to differentiate the extent of substrate hydrolysis between cell lines. Furthermore, we found that differences in the initial velocities of hydrolysis do not always correlate with differences in extent of hydrolysis. There were less significant differences in the initial velocities of hydrolysis among culture conditions and cells lines, making it the more conservative parameter for determination of differences in protease activity.

A.2 Introduction

It has been established there is a need to better understand the proteolytic profiles

of cells, especially in the diseased state (*1*). However, in diseased tissue such as tumors, the microenvironment is often very different from that of normal tissue. The extracellular matrix of tumors, for example, tends to be more acidic, and there is poor diffusion of nutrients between the circulatory system and the interior of the tumor (*2*). Researchers have recognized the importance of proteases in cancer progression and have begun identifying proteases associated with cancer progression for diagnostic and therapeutic purposes (*3*). These proteases are often identified by mRNA or immunohistochemistry of tumor cells, but protease activity might be more useful for the development of therapeutics. For a more high-throughput analysis of proteolytic profiles, it would be useful to use cell cultures rather than tumor tissue. Unfortunately, the proteases of interest may not be differentially expressed under normal cell culture conditions, as was the case with legumain (*4*). We have attempted to mimic some of these physiological changes in cell culture by manipulating pH and nutrient availability in cell culture to see what effect, if any, they have on protease activity against select substrates. We used cell lines from different tissue sources to determine if these cells react differently to changes in environment.

A.3 Methods

A.3.1 Materials

NIH-3T3, MCF7, HepG2, and Caco-2 cells were purchased from ATCC. HEK-LEG cells were generously provided by Dr. G. David Roodman (University of Pittsburgh). Cell culture reagents were purchased from Gibco/Invitrogen. Amino acid conjugates of 7-amino-4-methylcoumarin (AMC) were purchased from Bachem.

A.3.2 Cell Culture

HEK-293 cells stably overexpressing legumain (HEK-LEG), NIH-3T3, MCF7, HepG2, and Caco-2 cells were cultured in Dulbecco's Modified Eagle Medium (DMEM) containing 10% heat-inactivated fetal bovine serum (HI-FBS). Cells were maintained at 37°C in 90% humidity with 5% CO_2. Cells were plated in black wall, clear bottom, tissue culture treated 96-well plates at a density of 50,000 HEK-LEG cells/well and 100,000 MCF7 cells/well for serum-starvation and pH experiments. For assays with HEK-LEG, HepG2 and Caco-2 cells, RPMI-1640 medium with 10% HI-FBS was used to plate the cells at a density of 10,000 cells/well.

A.3.3 AMC Hydrolysis in cell lysates

NIH-3T3, MCF7, and NIH-3T3 cells were washed and pelleted in PBS and stored at -20°C until time of assay. Cell pellets were thawed, resuspended, and sonicated on ice for 3× 5 sec. Protein concentration was determined using the Pierce BCA assay (Thermo Fisher Scientific) after adding 2% SDS to prevent lipid interference with assay. For the hydrolysis assay, cell lysates were diluted to 65 µg/ml in 10 mM Hepes, 100 mM NaCl (pH 7.4) or 50 mM MES, 0.25 M NaCl (pH 5.5) in black 96-well plates. AMC compounds were added at a final concentration of 100 µM. Rate of hydrolysis was measured by fluorescence detection of AMC at $480_{ex}/560_{em}$ nm in a BioTek Synergy Plate Reader maintained at 37°C. Fluorescence values were converted to concentration using AMC standards and plotted against time to obtain the initial velocity of hydrolysis (V_0, nmol/min•mg protein).

A.3.4 AMC Hydrolysis in whole cells

HEK-LEG and MCF7 cells were plated in serum-containing media in black wall

clear bottom 96-well plates (Costar) ~24 hrs prior to assay. For serum-starved cells, the media werereplaced with serum-free media approximately 4 hrs prior to beginning the assay. Immediately prior to adding AMC compounds the media were replaced with 10 mM Hepes, 100 mM NaCl (pH 7.4) or 50 mM MES, 0.25 M NaCl (pH 5.5). AMC compounds were added at a final concentration of 100 μM. HEK-LEG, MCF7, HepG2, and Caco-2 cells were plated in black wall, clear bottom 96-well plates in serum-containing RPMI-1640 media approximately 2.5 hrs prior to beginning the assay. AMC compounds were added to the media at a final concentration of 100 μM. Rate of hydrolysis was measured by fluorescence detection of AMC at $480_{ex}/560_{em}$ nm in a BioTek Synergy Plate Reader maintained at 37°C. Fluorescence values were converted to concentration using AMC standards and plotted against time to obtain the initial velocity of hydrolysis (V_0, nmol/min).

A.4 Results

A.4.1 Effect of pH on hydrolysis in cell lysates

Cells were collected and lysed by sonication. The hydrolysis rate of three AMC conjugates were measured in two different buffers at pH 7.4 and pH 5.5. There were no significant differences in the initial velocity of hydrolysis (V_0) between the lysates of HEK-293 cells and the lysates of HEK-293 cells overexpressing legumain (HEK-LEG) as shown in Figure A.1. However, there was a slightly faster rate of hydrolysis of Z-AAN-AMC by HEK-LEG cell lysates at pH 5.5. In the pH 7.4 buffer, Leu-AMC was hydrolyzed significantly faster by MCF7 cell lysates than by NIH-3T3 cell lysates, with a similar trend at pH 5.5.

A.4.2 Effect of serum-starvation on hydrolysis by whole cells

Serum-starved HEK-LEG and MCF7 cells were incubated with several AMC conjugates in buffers of pH 7.4 and pH 5.5. The extent and rate of hydrolysis were compared to those of non-serum-starved cells (Figure A.2). Interestingly, the extent of hydrolysis of Ala-AMC was decreased in serum-starved MCF7 cells at pH 7.4 and pH 5.5, whereas it was increased in serum-starved HEK-LEG cells at pH 5.5. Conversely, the initial velocity of hydrolysis of Ala-AMC was not significantly different in MCF7 cells, although there was a slightly increased rate in serum-starved cells at pH 5.5. There was a significantly increased rate of hydrolysis of Ala-AMC in serum-starved cells at pH 5.5.

A.4.3 Proteolytic profiles of cells from different tissue sources

The extent and rates of hydrolysis of several AMC conjugates were compared in three different cell lines: HEK-LEG, Caco-2, and HepG2 (Figure A.3). Once again the rates of hydrolysis did not coincide with the extent of hydrolysis. The extents of hydrolysis of Leu-, Phe-, and Ala-AMC were significantly different between all three cell lines, with the lowest hydrolysis extent of all three compounds in MCF7 cells. There were no significant differences in the initial velocity of hydrolysis among the cell lines for any of the compounds. However, there was a trend toward faster V_0's for Leu-, Phe-, and Ala-AMC by MCF7 cells.

A.5 Conclusions

We have shown that pH does not have a profound effect on the rates of hydrolysis of three AMC substrates in the cell lysates of three different cell lines. While the hydrolysis of Z-AAN-AMC was not significantly faster in HEK-LEG cells at pH 5.5,

there did appear to be a trend toward increased initial velocity. This was expected as legumain, which hydrolyzes Z-ANN-AMC, is more active at acidic pH (*5-7*). While we only used three substrates, there were significant differences in the hydrolysis rate of Leu-AMC by MCF7 and NIH-3T3 cell lysates at pH 7.4. This led us to believe that we might be able to detect differences in proteolytic profiles of whole cells.

As mentioned previously, the microenvironment of solid tumors is often deprived of nutrients. This microenvironment can cause stress-induced changes in protein expression and localization. For example, while legumain is not usually detectable in cells under normal culture conditions, its expression appears to be upregulated during serum-starvation or when cells are implanted *in vivo (4)*. We hypothesized that the expression and activity of other proteases might also be affected by conditions such as pH and serum-starvation. The extent of, as well as the initial velocity of, Ala-AMC hydrolysis were determined in two cell lines with and without serum at physiologic and acidic pH. When comparing the extents of hydrolysis, the MCF7 breast cancer cell lines appeared to have the opposite reaction to serum-starvation compared to the HEK-LEG cells. However, when comparing the initial velocities of hydrolysis, the two cell lines appeared to behave more similarly. In order to avoid overestimating differences in protease activity between cells, it may therefore be best to compare the initial velocities of hydrolysis rather than extents of hydrolysis.

When the extent and rates of hydrolysis of Val-, Z-AAN-, Leu-, Phe-, and Ala-AMC were compared among three cell lines, there were significant differences in the extents of hydrolysis. However, when the initial velocities of hydrolysis were compared there were no significant differences. This further suggests the initial velocity of

hydrolysis might be the more conservative estimate of differences in protease activity. Based on these data, we monitored rates of hydrolysis in all future studies.

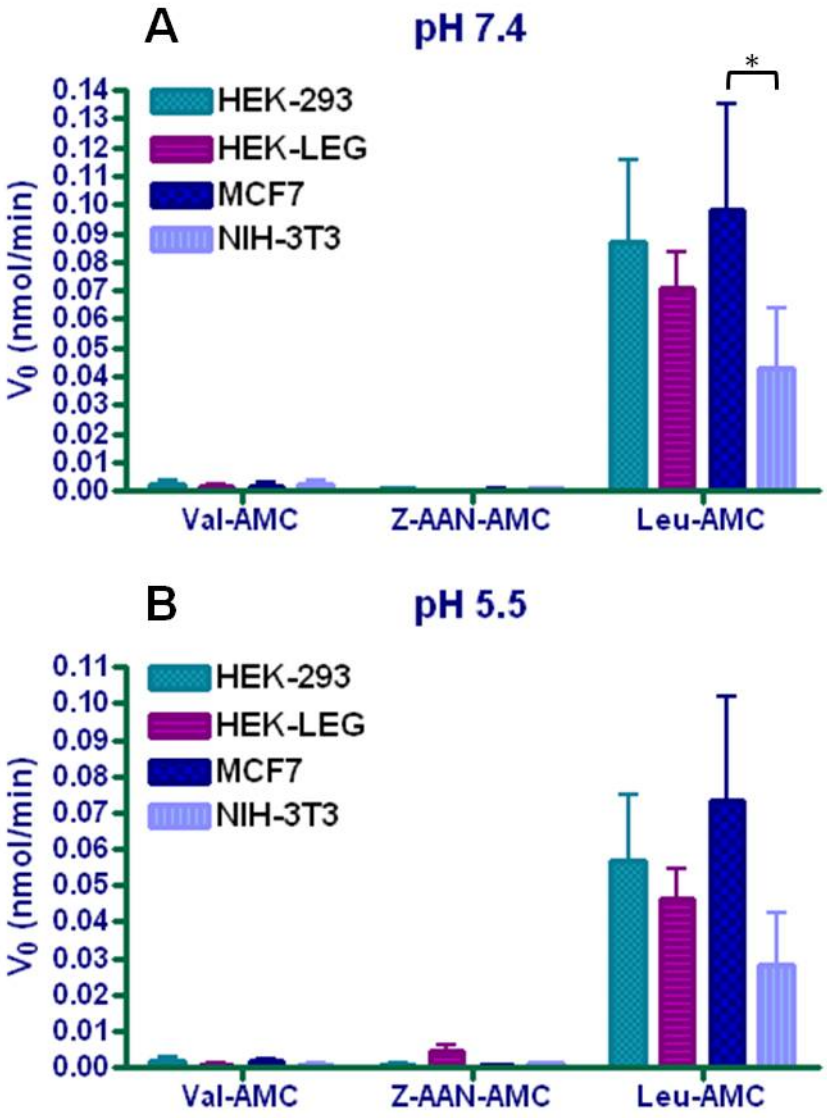

Figure A.1 pH has minimal effect on proteolytic profiles of cell lysates.
HEK-293, legumain-expressing HEK-293 (HEK-LEG), MCF7, and NIH-3T3 cell pellets were lysed and diluted to the same protein concentration in buffers at pH 7.4 (A) and pH 5.5 (B). Val-AMC, Z-AAN-AMC, and Leu-AMC were incubated with cell lysates and fluorescence was measured over time. Fluorescence values were converted to amount of AMC and plotted against time to determine the initial velocity of hydrolysis (V_0, nmol/min). Data were analyzed by two-way ANOVA and asterisks indicate significant differences (*$P < 0.05$).

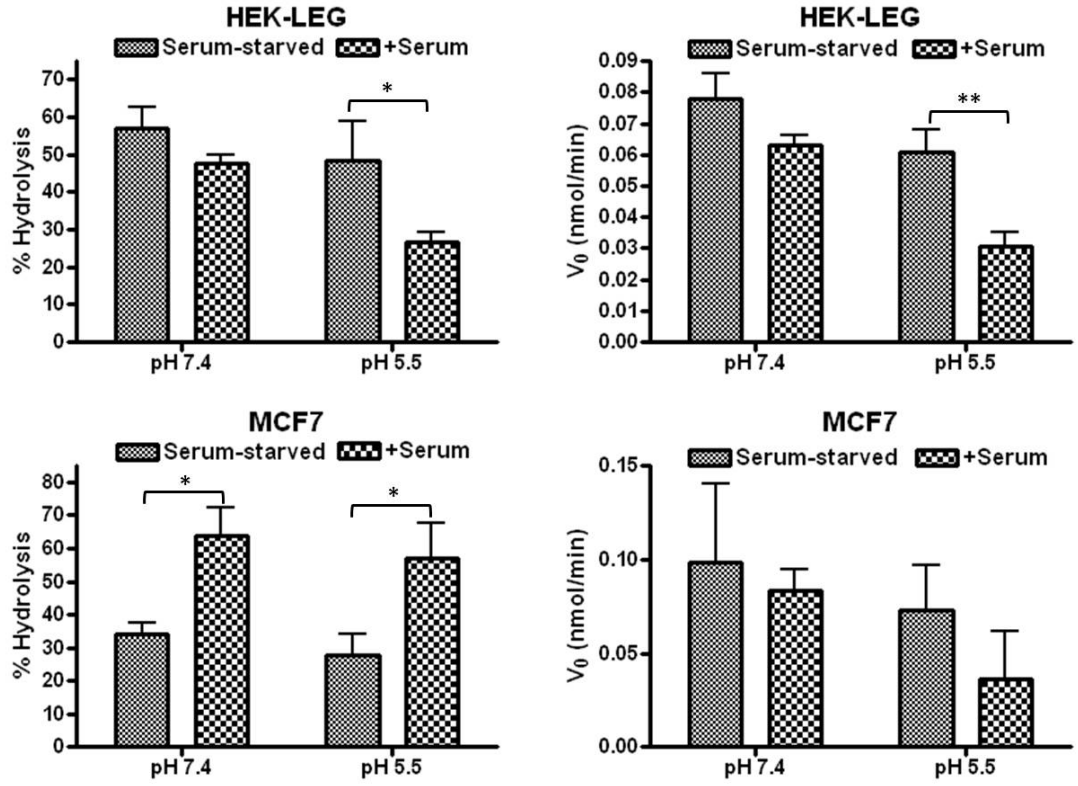

Figure A.2 Serum starvation has the opposite effect on extent of Ala-AMC hydrolysis in MCF7 and HEK-LEG cells.
HEK-LEG and MCF7 cells were serum-starved and media were replaced with buffer (pH 7.4 or 5.5) just prior to adding AMC conjugates. Fluorescence was measured over 2 hrs and values were converted to amount of AMC. The percent of Ala-AMC hydrolyzed to AMC at 2 hrs is plotted in the graphs on the left and the initial velocity of hydrolysis (V_0, nmol/min) is plotted in the graphs on the right. Data were analyzed by two-way ANOVA and asterisks indicate statistically significant differences (*$P < 0.05$, **$P < 0.01$).

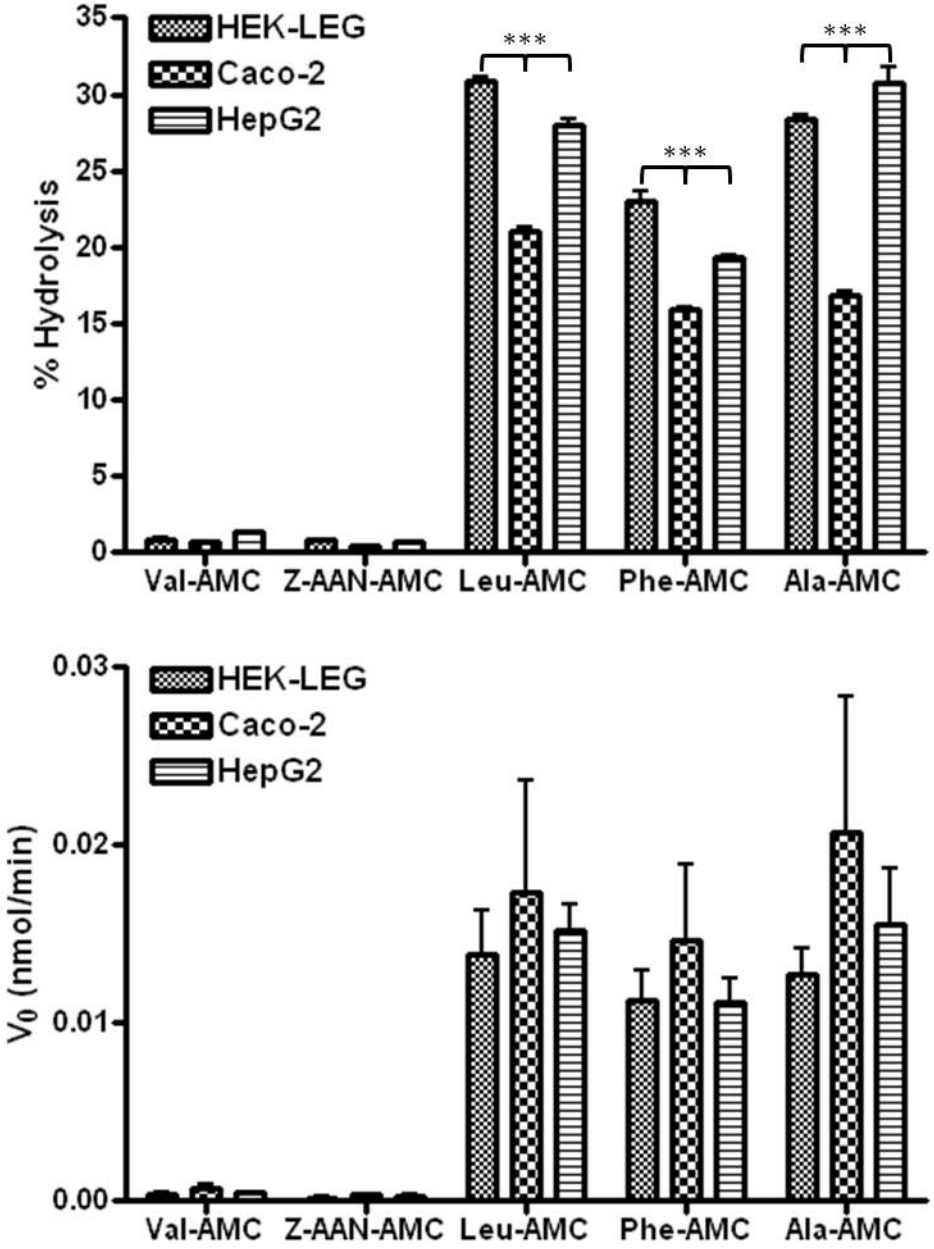

Figure A.3 Cells from different tissue sources have different proteolytic profiles at physiologic pH.

AMC compounds were added to wells containing the same number of HEK-LEG, Caco-2, and HepG2 cells in pH 7.4 or 5.5 buffer and fluorescence was measured over time. Fluorescence values were converted to amount of AMC and plotted against time to calculate the initial velocity of hydrolysis (V_0, nmol/min). Data were analyzed by two-way ANOVA and asterisks indicate statistically significant differences (***$P < 0.001$).

A.6 References

1. Cloutier, S. M., Kundig, C., Gygi, C. M., Jichlinski, P., Leisinger, H. J., and Deperthes, D. (2004) Profiling of proteolytic activities secreted by cancer cells using phage display substrate technology, *Tumour Biol 25*, 24-30.

2. Tannock, I. F., and Rotin, D. (1989) Acid pH in Tumors and Its Potential for Therapeutic Exploitation, *Cancer Research 49*, 4373-4384.

3. Decock, J., Paridaens, R., and Cufer, T. (2005) Proteases and metastasis: clinical relevance nowadays?, *Curr Opin Oncol 17*, 545-550.

4. Liu, C., Sun, C., Huang, H., Janda, K., and Edgington, T. (2003) Overexpression of legumain in tumors is significant for invasion/metastasis and a candidate enzymatic target for prodrug therapy, *Cancer Res. 63*, 2957-2964.

5. Chen, J. M., Dando, P. M., Rawlings, N. D., Brown, M. A., Young, N. E., Stevens, R. A., Hewitt, E., Watts, C., and Barrett, A. J. (1997) Cloning, isolation, and characterization of mammalian legumain, an asparaginyl endopeptidase, *J Biol.Chem. 272*, 8090-8098.

6. Chen, J. M., Dando, P. M., Stevens, R. A., Fortunato, M., and Barrett, A. J. (1998) Cloning and expression of mouse legumain, a lysosomal endopeptidase, *Biochem.J 335 (Pt 1)*, 111-117.

7. Halfon, S., Patel, S., Vega, F., Zurawski, S., and Zurawski, G. (1998) Autocatalytic activation of human legumain at aspartic acid residues, *FEBS Letters 438*, 114-118.